# Adipocytes Secrete Lipid-Laden Exosomes and Influence Local Macrophage Behavior

Stephen Flaherty

Submitted in partial fulfillment of the

requirements for the degree of

Doctor of Philosophy

under the Executive Committee

of the Graduate School of Arts and Sciences

COLUMBIA UNIVERSITY

2020

## ABSTRACT

To meet the body's metabolic needs, adipocytes release fatty acids and glycerol through the action of neutral lipases. Lipids are also key local regulators of immune function. During obesity, triglycerides accumulate in adipose tissue macrophages and this accumulation is associated with systemic metabolic complications including insulin resistance and atherosclerosis.

While studying the accumulation of lipid in adipose tissue macrophages, we discovered a secondary pathway of lipid release from adipocytes that occurs via exosomes and is independent of canonical lipolysis. Bone-Marrow-Derived Macrophages (BMDMs) cultured with lipase-deficient adipose tissue (as compared to WT) accumulate similar levels of neutral lipid, despite a marked decrease in free fatty acid release from these tissues. Adipocytes release exosome-sized vesicles (AdExos) that contain high levels of neutral lipid, that can be found in both adipose tissue conditioned medium and in circulation. Lean animals release ~ 1% of their adipocyte lipid content per day via exosomes; this rate more than doubles with obesity.

AdExos are taken up almost exclusively by local macrophages and are sufficient to induce the lipid-loading seen in BMDMs co-cultured with adipose tissue. AdExos and associated factors are sufficient to foster differentiation of bone marrow precursors into adipose tissue macrophage-like cells by inducing multinucleation, increased lysosomal program, increased ATM-associated gene expression, and increased lipid content. Our findings suggest both a novel pathway of local lipid release and a mechanism by which parenchymal cells can modulate tissue resident macrophage differentiation and function.

**Table of Contents**

**List of Figures**

**ACKNOWLEDGEMENTS**

I would like to thank my thesis advisor, Dr. Anthony W. Ferrante, Jr., for his support, advice, patience, and encouragement throughout my PhD. His mentorship and the environment he provides has made the work presented in this dissertation possible, and significantly aided my growth as a scientist and a person.

I would also like to thank my dissertation committee, Dr. Henry Ginsberg, Dr. Frederick Maxfield, Dr. Li Qiang, and Dr. Rebecca A. Haeusler their time and Invaluable insight that have allowed me to expand my understanding of my research.

The work in this dissertation could not have been done without the help and guidance of numerous collaborators. In particular, Ambar Grijalva, Xiaoyuan Xu, Ethan Edwin, Eleanore Ables, and Alireza Nomani were indispensable in the production of the work within this document.

I would like to thank the Institute of Human Nutrition, especially Dr. Richard Deckelbaum and Dr. Debra Wolgemuth for guiding my education. And Sara Sternglass, Leslie De Pena, Alex Sosa, and Zachary Corter for their logistical help throughout this process.

Finally, I must thank the Columbia University community, at large, my friends, and my family for building an environment of support for me that allowed for productive risk-taking and persistence towards my goals.

# CHAPTER 1:INTRODUCTION

## 1.1 Adipose Tissue

Energy is a cornerstone of life. Nearly all biological functions require energy. Having stores of energy provides flexibility in the relationship between when energy is consumed and when energy is expended, greatly increasing the ability to survive. Keeping large energy stores within cells that have other specified roles, however, would likely hamper cellular functions. The development of specialized tissue for energy storage, allows others tissues and cells to function without the burden associated with regulated storage and release of calories. In humans and other mammals, adipose tissue serves this essential function (*1*). Adipocytes are the primary storage cells of adipose tissue. As a storage depot for energy, adipose tissue must respond rapidly to any changes in the energy state of an organism. In times of energy excess, stores must expand efficiently; during periods of deficit, mobilization of energy stores must occur and be commensurate with the energy needs of tissues.

Consistent with adipocytes' essential function, much of the molecular machinery that regulates the storage of calories as lipids is conserved among invertebrates and vertebrates alike (*2-4*). Maintaining a sufficient supply of metabolic substrates during periods of negative energy balance, requires integration with signals from other tissues and a coordinated response. Over the last quarter century it has become apparent that this coordinate response to changes in energy balance includes hormonal signals from adipose tissue (*5*). In addition to leptin, which has been established as a true hormone, fat secretes more than 600 different molecules many of which have been implicated in glucose homeostasis, whole-body metabolism, appetite, and reproduction (*6-8*). While it is likely that only a small percentage of these are truly hormones, many investigators believe that many of these secreted molecules act locally to maintain adipose tissue function and lipid homeostasis (*9*). Adipose tissue also plays a role, especially in small mammals, in thermoregulation, both through uncoupling of respiration and as insulation (*10, 11*).

Impaired function of adipose tissue is implicated in many disorders. Rare mutations that affect key functions of adipocytes have profound, protean effects beyond adipose tissue. For example, mutations in *AGPAT2* which encodes a gene required for the generation of phosphatidic acid, severely limits adipocyte development leading to near absence of fat and a syndrome of congenital generalized lipodystrophy, characterized by severe hepatic steatosis and insulin resistance (*12-14*). Much more commonly, expansion of adipose tissue that occurs in obesity changes both the character and function of adipose tissue, and although the alterations are more subtle, the adverse sequela affects nearly all organ systems, increasing rates of diabetes, autoimmune disease, hepatic steatosis, more than a dozen cancers, gallbladder disease and dementia (*15-19*). Understanding the normal function of adipose tissue is required before we can fully understand these complications of altered function.

**1.2 The Obesity Epidemic**

Obesity is chronic disorder broadly defined as a state of excess body-fat mass that induces pathology. At its most basic level, obesity develops due to an imbalance of energy homeostasis: excess energy intake relative to energy expenditure. There has been an epidemic of obesity in the last several decades, starting in the industrialized nations and spreading to the developing world (*20*). Epidemiologic evidence has implicated the availability of inexpensive foods of high caloric density and decreased requirements for energy expenditure (*21*). The scope of the problem is staggering. Body Mass Index (BMI) is a easy to measure surrogate of adiposity that is especially useful in population studies. The BMI body mass divided by height-squared. In SI units normal BMI in adults for the US have been defined as between18.5 $kg/m^2$ and 25 $kg/m^2$, s with BMIs between 25 $kg/m^2$ and 30 $kg/m^2$ considered overweight, and those with a BMI > 30 $kg/m^2$ considered obese. Currently, ~70% of the adult US population has a BMI above 25 $kg/m^2$, and ~33% of the US population has a BMI above 30 $kg/m^2$ (*22*). By the year 2030, it is estimated that 50% of the US population will be obese (*23*).

A primary reason that this high and increasing rate of obesity is a health problem, is that obesity is associated with many co-morbidities. Obesity greatly increases one's risk for developing insulin resistance, Type 2 Diabetes Mellitus (T2DM), cardiovascular disease, cancer, stroke, fatty liver disease, high blood pressure, autoimmune disorders, dementia, affective disorders and infertility. Obesity and overweight together have become the second largest cause of preventable death in the US, behind only tobacco use, and the fifth largest global risk factor for death overall (*24-27*). Extreme obesity (BMI > 40 $kg/m^2$), which is also becoming more prevalent, is estimated to shorten life expectancy by as much as 14 years (*28*). In 2010, the estimated additional cost of healthcare for each patient with obesity in the US was $3500 per year, with a total aggregate cost of $315.8 billion spent on adult obese patients (*29-31*). This figure represents an increase in spending of 48.7% in a five-year period, as an estimated $212.4 billion was spent in 2005 (*32, 33*). Obesity is also known to associate with indirect costs to society related increased work absenteeism and decreased work (*34*). There are economic benefits to be had from successful obesity therapies.

Current medical treatment for obesity have had minimal effects in reducing the epidemic of obesity. Obese patients are typically advised to undertake a diet and exercise program, sometimes with intensive counseling and support. These therapies rarely provide sustained weight loss, and when initially effective, patients typically regain most of the lost weight over the subsequent 12-36 months (*35*). Incretin based therapies, including those that increase the action/signaling of GLP1 and GIP are approved and some have additional demonstrated cardiovascular benefit, but thus far have had modest overall effect to curb the tide of obesity (*36-38*). More recently and surprisingly, a new class of anti-diabetic drugs, SGLT2 inhibitors lead to modest weight loss and also reduce cardiovascular complications (*39*). However, it is not clear that these medical benefits are secondary to the small weight loss. The most effective intervention available currently is bariatric surgery. Several different surgical approaches have been shown to lead to substantial and durable weight loss in the majority of patients (*40-42*). However, even in the face of these interventions, obesity rates continue to climb at alarming rates, making it clear that new modes of therapy for the treatment of obesity are needed.

### 1.3 Lipid Storage

Obesity represents an expansion of the adipose tissue. Energy in the body can be stored as carbohydrates and protein, but the most efficient storage molecules are lipids. One gram of fatty acid produces 9 kcal of energy and does not require any water molecules for storage. By comparison, carbohydrates and proteins each produce 4 kcal per gram and must be stored with additional water molecules. In a normal weight human male, roughly 80% of the body's total energy storage is in lipids, capable of supplying the body with enough energy to last 30-40 days (*43, 44*). Beta-oxidation is the primary way in which cells use fatty acids to generate ATP and meet energy needs (*45*). The first step beta-oxidation after a fatty acid is taken up by a cell, is the formation of fatty acyl-CoA molecules in the cytoplasm. Acyl-CoA molecules are then transported across the mitochondrial membrane where oxidation occurs. Once inside the mitochondrial matrix, the fatty acyl-CoA molecule is hydrolyzed in a stepwise fashion to yield acetyl-CoA, which enter the Krebs Cycle, generating reducing equivalents that are used to produce ATP (*46*).

Unlike free fatty acids (FFAs), which have detergent-like properties, the glycerol esters of fatty acids in the form of triacylglycerides (TAGs) remain hydrophobic at all pHs (*47*). Acylglycerides are stored primarily in lipid droplets within cells. The formation of lipid droplets is not entirely understood. The leading hypothesis is that TAG accumulate in the hydrophobic environment between the two layers of phospholipid membrane of the endoplasmic reticulum. As the lipid pocket grows, the outer layer of the phospholipid bilayer eventually buds off from the endoplasmic reticulum, producing an organelle surrounded by a phospholipid monolayer and filled with a core of neutral lipid (*48, 49*). This structure can then grow further through direct diffusion of FFAs or fusion with other lipid droplets or possibly through recently identified substructures (*49*) (*50*). The membrane of the lipid droplet also accumulates and is enriched with proteins that regulate TAG and cholesteryl ester trafficking and metabolism within the cell.

The best-characterized lipid droplet-associated proteins are those of the perilipin family. The five perilipin family members (PLIN1-5) share a common overall structure and are believed to localize to the

cytoplasmic face of the lipid droplet membrane (*51, 52*). They have been implicated in regulating many different processes, including lipid metabolism, membrane stabilization and trafficking, endocytosis, exocytosis, and fusion of vesicles (*53, 54*). The expression patterns of the PLINs vary, with some being nearly ubiquitously expressed, e.g. PLIN4, while others have more limited expression, e.g. PLIN1 in adipocytes, PLIN2 in macrophages, hepatocytes. PLIN1, whose expression is largely limited to adipocytes, is the most studied and best characterized of the PLINs. One of its functions is as a negative regulator of lipolysis. In the absence of a lipolytic stimulus, it associates with another LD protein, CGI-58, preventing CGI-58 from activating LD associated lipases, including PNPLA2/ATGL (*51, 52, 55*). Lipid droplets are found in nearly all cells providing temporary storage of TAG for subsequent use to meet energy needs or to be used as substrates in the creation of various important fatty acid-derived molecules. In adipocytes, lipid droplets also make up the majority of the volume of the cell.

**1.4 Adipocytes in Energy Storage**

There are several morphologically distinguishable types of adipose tissue which serve distinct functions. White adipose tissue is the primary site of TAG storage, bone marrow adipose tissue functions in hematopoiesis and brown/beige adipose tissue is thermogenic (*56*). The adipocyte is responsible for the major energy functions of adipose tissue, including storing TAG within its cell body. In white adipose tissue, adipocytes provide metabolic substrates, FFAs and glycerol, for other tissues during periods of energy deficit. In humans, it has been estimated that adipocytes live for an average of 10 years and can change in size dramatically depending on their environment (*57*). Adipocytes in white adipose tissue typically contain one large unilocular lipid droplet. In obese subjects, this lipid droplet can be 20-fold larger in diameter than those in adipocytes of lean individuals, an increase in lipid volume of several thousand-fold (*58*). Because of the dynamic energy needs of an organism, the size of the adipocyte lipid droplet can change rapidly, especially during times of fasting when a large fraction of adipocyte TAG can be hydrolyzed.

Adipocytes provide energy substrates (FFAs and glycerol) to the rest of the body through the action of neutral lipases (*59*). During periods of negative energy balance, when caloric intake does not meet energy expenditure, hormonal (including high glucagon and norepinephrine, and low insulin concentrations) and neural signals (sympathetic activation) activate a lipolytic response in adipocytes (*55, 59, 60*). These signals act, in part, through activation of protein kinase A which, through phosphorylation of PLIN molecules, lead to activation of neutral lipases that are associated with the LD membrane (*61, 62*). Three lipases, adipocyte triglyceride lipase (PNPLA2/ATGL), hormone-sensitive lipase (LIPE/HSL) and monoacylglyeride lipase, act sequentially to hydrolyze a single fatty acid from a TAG molecule, yielding a glycerol backbone and three fatty acid residues (*57, 60*). FFAs then exit the cell, ultimately making their way into the circulation and providing energy to cells throughout the body (*60, 63, 64*).

Once in the recipient cell, a FFA can be transported to the mitochondria to undergo beta-oxidation, metabolized into other lipid species, or re-esterified into TAG for local storage. Esterification of FFAs with glycerol regenerates TAG that can once more be stored in a lipid droplet (*65, 66*). The re-esterification process reverses hydrolysis, in a stepwise fashion, requiring the action of several acyltransferases. The best studied of these enzymes, the diglyceride acyltransferases (DGAT1, DGAT2), catalyze the terminal esterification of an acyl-fatty acid to diacylglycerol. Both enzymes are capable of catalyzing the reaction, and in their absence, TAG cannot be formed in mammals (*67*). While each has distinct cellular localization and tissue expression, there also is compensatory regulation that occurs when either is mutated.

### 1.5 Delivery of Lipid and Lipoprotein Particles

While adipocytes can convert glucose, via the generation of Acetyl-CoA, into FFA, most FFA in mammals has been thought to derive from circulating TAG carried in lipoprotein particles (*68*). TAGs are primarily transported in the hydrophilic bloodstream with lipoprotein particles. Apolipoproteins and lipid combine to form a complex family of lipoprotein particles that includes chylomicrons, chylomicron remnants, very low density lipoprotein (VLDL), intermediate density lipoprotein (IDL), low density

lipoprotein (LDL), and high-density lipoprotein (HDL). These particles have cores composed of cholesteryl esters, retinol esters, and TAGs in differing proportions. In addition to varying by lipid composition, each particle has a distinct size, density, and set of apolipoproteins associated with it. The TAG-rich VLDL and chylomicrons are synthesized by hepatocytes and intestinal epithelial cells, respectively, and like all other lipoprotein particles and lipid droplets, possess a phospholipid monolayer containing proteins (*68*).

The packaging of dietary lipids into chylomicrons begins in the intestine, after orally consumed TAGs are hydrolyzed by luminal lipases which release FFAs that are in turn absorbed by enterocytes. Fatty acids and monoacylglycerides, once taken up by enterocytes, are transported to the endoplasmic reticulum (ER) (*69*). There, these substrates are converted into TAG by esterifying enzymes within the ER, including DGAT1/2. The apolipoprotein ApoB-48 is translated directly into the ER lumen and with the nascent lipoprotein particle forms a dense HDL-like pre-chylomicron, with high concentrations of phospholipids and free cholesterol. Microsomal triglyceride transfer protein then ferries and loads TAG into the pre-chylomicron particle.

Once loaded with TAG, the prechylomicron leaves the ER and moves to the Golgi. The intracellular transport of the particle remains poorly defined, but it is hypothesized to occur by enclosing the prechylomicron in a membrane-bound vesicle derived from ER membrane: the prechylomicon transport vesicle (PCTV), averaging 250nm in diameter. Once released into the cytosol, the PCTV uses SNARE proteins to be targeted to the Golgi, where it fuses with the Golgi membrane, releasing the prechylomicron into the Golgi lumen. The prechylomicrons are further processed in the Golgi into mature chylomicrons before, again, being packaged in vesicles that fuse with the baso-lateral enterocyte plasma membrane, releasing the particles into the basal extracellular space (*70, 71*). Extracellular chylomicrons are taken up by the lymph and ultimately, via a thoracic duct, reach the circulation. Once in the circulation, chylomicrons receive ApoC-II and ApoE from HDL particles and now can efficiently deliver TAG to peripheral tissues.

The enzyme lipoprotein lipase (LPL) is synthesized in the parenchymal and some immune cells of muscle, heart, and adipose tissue. After secretion, it translocates to endothelial cells where it is presented on the luminal side of capillary vessels. Via a mechanism that is incompletely understood, LPL interacts with chylomicrons and other TAG-containing particles in the circulation, and catalyzes the hydrolysis of TAG, allowing delivery of fatty acids to the underlying cells (*72*). As TAG is depleted, the particle becomes smaller and becomes known as a chylomicron remnant (*68, 73*). These remnant particles are efficiently cleared by liver. Apolipoprotein E (APOE) which is on the surface of the chylomicron is recognized by LDL-receptor and by Hepatic Lipase on the surface of the hepatocyte. The clathrin-coated pits surrounding LDL-receptor are activated upon binding, leading to the invagination of the hepatocyte membrane, taking up the remnant particle via receptor-mediated endocytosis. The intracellular vesicle fuses with acidic endocytic compartments where they undergo degradation (*74*). The delivery of TAG via chylomicrons mirrors delivery via other lipoprotein particles (*75*). VLDL particles, which contain the apolipoprotein ApoB-100, develop in a very similar manner within the hepatocyte. VLDL TAG is derived from recycled lipoprotein particles or via *de novo* lipogenesis.

**1.6 The Complexity of White Adipose Tissue**

Although adipocytes are the defining cell-type in adipose tissue, being the most histologically distinct and the site of lipid storage, adipose tissue is heterogenous and complex. The non-adipocytes within adipose tissue, often referred to as the stromal vascular cells (SVCs), include endothelial cells, stem cells, fibroblasts, immune cells and pre-adipocytes. Each appears to play important roles in maintaining lipid storage and release function of fat. SVCs are known to mediate transport of energetic materials, respond to hormonal signals, and release hormonal signals themselves (*76, 77*). Among the immune cells, the largest population is the adipose tissue macrophage (ATM).

Macrophages are professional phagocytes derived from the myeloid precursors. In most tissues there appear to be to populations of macrophages of varying proportions – one is derived from resident cells there migrated to the tissue during development and the other from circulating monocytes that are

recruited to the tissue (*78, 79*). They are best known for their role in innate immune responses. Classically, in response to a local infection sentinel immune cells and damaged parenchymal cells elaborate pro-inflammatory cytokines, chemokines, and other signals that initiate an immune response. Macrophages serve many function in immune responses: 1) As sentinels, recognizing foreign pathogens and damaged cells via pattern recognition receptors 2) Phagocytosing debris, pathogens and dead and damaged cells 3) Presenting antigens to effector T cells that mediate adaptive immunity (*80*) (*81, 82*) (*83-85*).

**1.7 Tissue Resident Macrophages and ATMs**

In addition to their role in innate immune responses, macrophages are present in tissues during normal, non-inflammatory functioning and have specialized, tissue-specific adaptive functions (*86*). For example, the tissue resident macrophages of the brain, microglia, perform synaptic stripping, a process by which microglia facilitate proper synaptic development during postnatal life (*87-89*). Another example are osteoclasts, the multinucleated tissue resident macrophage of bone, which resorb bone as part of the bone cycle required to maintain healthy bones (*90-92*). A common feature to many of the tissue-specific functions of macrophages, is that they often degrade materials within a tissue, allowing the parenchymal cell to rebuild and improve function.

The adaptive roles of adipose tissue macrophages are less well-defined. However, circumstantial evidence suggests they play a critical role in local lipid homeostasis (*93*). In the lean state, ATMs make up roughly 5-10% of the cells in white adipose tissue and contain measurable amounts of neutral lipid; in obese individuals the lipid content of ATMs increases several fold (*94, 95*). An analysis of ATMs in obese mice suggested that they play a degrative function, reminiscent of the roles played by osteoclasts and microglia (*15, 96*). Obesity increases the number of ATMs so that they constitute as much as 50% of the cells in a fat depot and also increases the lysosomal function, and specifically the release of FFA in a lysosome-dependent manner. More recently, ATMs have also been found to release lysosomes as part of a degradative process that clears apoptotic adipocytes (*97*).

Lysosomal acid lipase (LIPA) is the one known enzyme that hydrolyzes TAG and other lipid esters in lysosomes and is highly expressed in ATMs (*98, 99*). In comparison, ATMs have relatively low expression of cytosolic, neutral lipases, i.e. PNPLA2/ATGL, HSL and monoacylglycerol lipase (MGL), and thereby, they depend on lysosomal lipases to hydrolyze lipid (*100*). The importance of this gene specifically in macrophages has been revealed over the last decade. Hypomorphic or null alleles of *LIPA* manifest as cholesteryl ester storage disease (CESD) and Wolman Disease, respectively (*101, 102*). Although Wolman's Disease is more severe and leads to early mortality, typically by age 2, whereas symptoms of CESD often do not become apparent until early adulthood, both are characterized by progressive loss of fat tissue and accumulation of lipid in the liver, spleen and small intestine. This phenotype is replicated in mice deficient in LIPA. Like humans, these animals lose adipose tissue and develop massive hepatosteatosis and splenomegaly, but remarkably these defects are rescued by LIPA expression limited to macrophages, arguing for a role of macrophage lysosomal lipid catabolism being necessary to sustain adipose tissue and prevent ectopic TAG accumulation (*103*) (*99*).

**1.8 Inflammation and Obesity**

While the association of obesity with many co-morbidities including insulin resistance, dyslipidemia, more than a half dozen cancers, and dementia are well-documented, the mechanisms that underlie these associations remain poorly defined. One compelling model focuses on the longstanding observations that measures of inflammation increase with obesity and incidence of its complications (*104*). For example, in both animal models and humans, measures of inflammation in adipose tissue correlate strongly with one's risk for developing insulin resistance, a relationship that is even stronger than the relationship between insulin resistance risk and BMI (*105, 106*). A causative role for inflammation is supported by many preclinical and genetic studies in rodents, in which treatments or genetic variants that increase inflammation worsen obesity-associated insulin resistance and those that reduce inflammation improve metabolic profiles (*107, 108*). In this model, maladaptive responses to "metabolic

stresses", mediated, in part, by immune cells, activate inflammatory signaling in energetic cells, such as skeletal muscle myoblasts, to impair normal glucose and lipid metabolism.

While the data from rodent models are compelling, there are some problems with this model. Genome-wide association studies (GWAS) that identify variants associated with insulin resistance, have identified very few inflammatory or immune genes (*109, 110*). In many other disorders where inflammation and immune dysfunction are clearly causative, e.g. inflammatory bowel disease, type 1 diabetes, GWAS have identified variants in many inflammatory genes. If inflammation were central to the development of insulin resistance, one would similarly predict evidence that variants in an inflammatory gene contribute to the risk for developing the disorder. A second challenge to the model is that anti-inflammatory therapies developed to treat autoimmune disorders, and that target the same molecules implicated in rodent models of inflammation, have not been associated improved insulin sensitivity (*111*). The recently completed large CANTOS trial, which found some evidence for reduced cardiovascular disease upon treatment with an anti-Il1b molecule, did not reduce insulin resistance or the development of type 2 diabetes (*112*). Another paradox is that several mouse models have now been developed that disassociate inflammation, including adipose tissue inflammation, and insulin resistance. For example, mice fed a high-fat diet at thermoneutrality develop adipose tissue inflammation without any effect on systemic insulin signaling (*113*).

**1.9 Ectopic Lipid Deposition and Obesity**

In addition to measures of inflammation, epidemiological studies have found that complications of obesity are also strongly associated with deposition of lipids in non-adipocytes (*114*). Triglyceride storage in ectopic (non-adipose tissue) depots is a common feature of obesity and a strong predictor of the development of for T2DM, atherosclerosis, and fatty liver disease (*115*). What leads to TAG being stored in these tissues is unknown, but it seems to be tied to adipose tissue dysfunction, as it is often accompanied by stress signaling in the adipose tissue, including endoplasmic reticulum stress, unfolded protein response, and pro-inflammatory cytokine release (*116*).

The proposed mechanisms through which ectopic lipid contributes to insulin resistance in key metabolic tissues involve metabolites of TAG and other lipids activating either activating signaling pathways in a lipid species-specific fashion or via more general stress responses. Obesity does lead to the accumulation of long-chain acyl-CoA, diacylglycerol (DAG), and ceramides in tissues including skeletal and cardiac muscle, liver and pancreas (*1*). In the case of diacylglycerol, it has been proposed that DAG activates atypical protein kinase C isoforms which will phosphorylate insulin receptor substrates on serine residues that inhibit insulin signaling (*117-119*). Others have suggested that a broader of effect of lipids on cells is to induce ER stress responses that similarly activate kinases and impair insulin signaling. However, compelling data from rodent models in support of these mechanisms have not successfully translated into therapeutic strategies in people. Furthermore, GWAS studies of insulin resistance and other obesity complications have also not uncovered a set of variants consistent with signaling implicated in murine studies (*109, 110*). And like the exceptions to the association of inflammation with obesity and its complications, there are examples of dissociation of ectopic lipid accumulation with obesity complications that are not explained by the current models. For example, well trained athletes accumulate triglyceride in muscle but have increased rather than impaired insulin sensitivity (*120*).

### 1.10 ATMs and Obesity's Co-Morbidities

ATMs lie at the intersection of two leading models for the pathogenesis of obesity-associated disorders, including insulin resistance. Their contribution to adipose tissue inflammation is direct, but data also implicate ATM dysfunction in ectopic lipid deposition. Disrupting the ability of ATMs to handle lipid is associated with TAG being stored outside of the adipose tissue. As noted above loss of LIPA activity specifically in macrophages is sufficient to cause massive TAG accumulation in the liver and spleen (*99*). Additionally, macrophages can be conditionally depleted using Macrophage Fas-Induced Apoptosis (MAFIA) transgenic mouse model. When macrophages are depleted in mice being fed a high fat diet, there is a 30% reduction in adipose tissue mass, while liver and gut fat content increases, providing further evidence that ATMs are essential for maintaining adipose tissue lipid homeostasis and preventing ectopic lipid deposition (*121, 122*).

### 1.11 Exosomes

Exosomes are extracellular vesicles (EVs) that are secreted by all eukaryotic cells so far studied (*123, 124*). Like all EVs, they are particles delimited by a single phospholipid bilayer membrane and filled with an aqueous interior. The components are derived from the cell that secretes it: the membrane derived from the endocytic multivesicular bodies, and the contents derived from the cytoplasm (*125*). Exosomal biogenesis begins with the inward budding of a cell's plasma membrane. ESCRT machinery facilitates the invagination of the limiting membrane into the interior of the cell, creating an intraluminal endosomal vesicle (ILV), filled with extracellular contents (*125-127*). Through endosomal maturation an ILV is enriched with certain lipid species and membrane-associated proteins, including tetraspanins, e.g. CD63. The contents of the eventual exosome are trafficked to the ILV membrane. These contents are enveloped by the membrane as it once again invaginates and buds inward to the interior of the vesicle. This process repeats until the intraluminal vesicle matures into a multivesicular body (MVB), containing many proto-exosomes. At this point, depending on the cell's needs and environmental signally, the MVB can fuse with the lysosome to be degraded, and recycle its materials, or it can be transported to the plasma membrane for exosomal secretion (*132, 133*). MVBs that fuse directly with the cell's plasma membrane, do so through a process that requires Rab GTPases and the SNARE complex (*128*). This releases both the exosomes and the extracellular contents that were taken up during ILV formation.

Exosomes range in diameter from 50 nm to 200 nm, making their average size larger than LDL particles (22nm in diameter), but still an order of magnitude smaller than the smallest cells. There is a lack of consensus regarding the classification of extracellular vesicle subtypes into distinct groups. Some of these classifications are based on size, others on mechanisms of biogenesis, or others on differences in function. For the purposes of this work, the term "exosome" is being used as a blanket term for extracellular vesicles of ~70-200 nm in size not derived from apoptotic cells.

Almost all cell types have been shown to release exosomes, including animal, plant, and prokaryotic cells, and they are found in all body fluids (*123, 124*). It is believed that they serve a primary

function in intracellular communication. By carrying signaling molecules in their natural cytoplasmic environment, including RNAs, protein, and lipids they can have direct effects on the recipient cell once the interior of the exosome either fuses with a recipient cell or is taken up via a phagocytic process. While exosomes and other extracellular vesicles can act in a local fashion, their sturdy phospholipid bilayer enables them to travel great distances within the body for extended periods, while protecting their contents from degradation.

While exosome biogenesis is rather well-studied, the mechanisms of exosome uptake a comparatively much less understood. The mechanisms of exosome targeting and adhesion are also a topic of debate in the field. Many reports describe exosomes that are taken up by only specific types of cells, depending on the origin of the exosome. How this phenomenon is carried out is an open question (*129*). Exosomes released from immune cells have been shown to express integrins such as ICAM-1, CD18, CD29, and CD51 that are able to bind tightly to integrin receptors on recipient cells. Tetraspanins, a family of highly conserved membrane proteins that play a role in adhesion, motility, and signal transduction are expressed on all exosomes. Some of these include CD9, CD63, CD53, CD81, and CD82, although the specific tetraspanins on individual exosome populations vary. The variation in tetraspanins has been postulated to modulate both the content that is partitioned into a given exosome and alter the target cell which takes up or fuses with an exosome.

Once the exosome has arrived at the recipient cell it has several different ways of mediating its effects. Some exosomes are able to induce changes in recipient cells, through extracellular contact, interacting with receptors on the cell's surface without being taken up (*130*). Exosomes are capable of fusing directly with the plasma membrane of recipient cells, through a mechanism that is not very well studied, immediately introducing the exosomal contents into the recipient cell. This allows mRNAs, miRNAs and proteins to function directly within the target cell (*131*).

The most commonly reported means of exosome uptake occurs through the endosomal pathway. This can occur through receptor- or non-receptor-meditated mechanisms. In the former, ligands on the

exosomal surface interact with receptors in cholesterol and sphingolipid rich rafts on the surface of the recipient cell. This stimulates a clathrin-dependent endocytosis that utilizes caveolins to coat the membrane, inducing an invagination of the membrane into an intracellular vesicle (*131*). Non-receptor-meditated endocytosis, including phagocytosis and macropinocytosis are also reported to take up exosomes en mass. This process involves the outward protrusion of the plasma membrane, driven by actin filaments, that surround and endocytose extracellular fluid and particles contained within, a process dependent on PI3K and dynamin-2 (*132*). Once exosomes enter the endocytic pathway, sorting takes place by which exosomal proteins and membrane lipids can be trafficked back to the plasma membrane or to the late endosome and lysosomes (*133*). Over the last twenty five years the identification of pattern recognition receptors in endocytic compartments and nutrient sensing apparatus associated with the lysosome argues that exosomes in this pathway can trigger signaling responses that are dependent on the contents of the exosomes (*134*).

**1.12 Adipose Tissue-Derived Exosomes**

The study of adipose tissue-derived exosomes is still in its infancy, but already, they have been shown to have many important local and systemic effects, with some groups claiming that >60% of the circulating RNA is derived from adipocyte exosomes (*135*). There are multiple reports of adipose tissue-derived exosomes having systemic effects on key metabolic tissues (*136*). For example, one study found that, in mice, adipocyte-derived exosomes traffic to the liver where they are taken up by hepatocytes. In the hepatocytes, exosomal microRNAs directly inhibit FGF21 expression and improve glucose homeostasis in obese mice (*135*). More recently, exosomes from endothelial cells in adipose tissue have been shown to transfer functional caveolin 1 protein to adipocytes, thereby regulating adipocyte function (*137*). Several groups have suggested that ATM-derived exosomes act to modulate systemic metabolism either by locally regulating adipocytes to alter adipokine secretion or by direct inflammatory effects on key metabolic tissues, including the liver and pancreas (*138*). Although many of these studies await replication and confirmation, it seems clear that adipose tissue plays a large role in exosomal signaling at large, and that once the biology of exosomes is more clearly elucidated, adipose tissue derived exosomes may provide an avenue for therapy in metabolic disorders.

### 1.13 References


1. M. Bosma, S. Kersten, M. K. Hesselink, P. Schrauwen, Re-evaluating lipotoxic triggers in skeletal muscle: relating intramyocellular lipid metabolism to insulin sensitivity. *Prog Lipid Res* **51**, 36-49 (2012).
2. E. Ottaviani, D. Malagoli, C. Franceschi, The evolution of the adipose tissue: a neglected enigma. *Gen Comp Endocrinol* **174**, 1-4 (2011).
3. S. Gesta, Y. H. Tseng, C. R. Kahn, Developmental origin of fat: tracking obesity to its source. *Cell* **131**, 242-256 (2007).
4. R. M. McKay, J. P. McKay, L. Avery, J. M. Graff, C elegans: a model for exploring the genetics of fat storage. *Dev Cell* **4**, 131-142 (2003).
5. J. Conde *et al.*, Adipokines: biofactors from white adipose tissue. A complex hub among inflammation, metabolism, and immunity. *Biofactors* **37**, 413-420 (2011).
6. S. Lehr, S. Hartwig, H. Sell, Adipokines: a treasure trove for the discovery of biomarkers for metabolic disorders. *Proteomics Clin Appl* **6**, 91-101 (2012).
7. O. A. MacDougald, C. F. Burant, The rapidly expanding family of adipokines. *Cell Metab* **6**, 159-161 (2007).
8. P. E. Scherer, Adipose tissue: from lipid storage compartment to endocrine organ. *Diabetes* **55**, 1537-1545 (2006).
9. J. H. Stern, J. M. Rutkowski, P. E. Scherer, Adiponectin, Leptin, and Fatty Acids in the Maintenance of Metabolic Homeostasis through Adipose Tissue Crosstalk. *Cell Metab* **23**, 770-784 (2016).
10. A. Fedorenko, P. V. Lishko, Y. Kirichok, Mechanism of fatty-acid-dependent UCP1 uncoupling in brown fat mitochondria. *Cell* **151**, 400-413 (2012).
11. P. Trayhurn, Origins and early development of the concept that brown adipose tissue thermogenesis is linked to energy balance and obesity. *Biochimie* **134**, 62-70 (2017).
12. M. Lightbourne, R. J. Brown, Genetics of Lipodystrophy. *Endocrinol Metab Clin North Am* **46**, 539-554 (2017).
13. A. K. Agarwal *et al.*, AGPAT2 is mutated in congenital generalized lipodystrophy linked to chromosome 9q34. *Nat Genet* **31**, 21-23 (2002).
14. S. K. Mathur *et al.*, Genetics of Lipodystrophy: Can It Help in Understanding the Pathophysiology of Metabolic Syndrome? *Biomolecules* **8**, (2018).
15. U. J. Jung, M. S. Choi, Obesity and its metabolic complications: the role of adipokines and the relationship between obesity, inflammation, insulin resistance, dyslipidemia and nonalcoholic fatty liver disease. *Int J Mol Sci* **15**, 6184-6223 (2014).
16. B. B. Kahn, J. S. Flier, Obesity and insulin resistance. *J Clin Invest* **106**, 473-481 (2000).
17. E. Fabbrini, S. Sullivan, S. Klein, Obesity and nonalcoholic fatty liver disease: biochemical, metabolic, and clinical implications. *Hepatology* **51**, 679-689 (2010).
18. T. Pischon, K. Nimptsch, Obesity and Risk of Cancer: An Introductory Overview. *Recent Results Cancer Res* **208**, 1-15 (2016).
19. I. Anjum, M. Fayyaz, A. Wajid, W. Sohail, A. Ali, Does Obesity Increase the Risk of Dementia: A Literature Review. *Cureus* **10**, e2660 (2018).
20. J. O. Hill, V. Catenacci, H. R. Wyatt, Obesity: overview of an epidemic. *Psychiatr Clin North Am* **28**, 1-23, vii (2005).
21. K. D. Hall, Did the Food Environment Cause the Obesity Epidemic? *Obesity (Silver Spring)* **26**, 11-13 (2018).
22. L. Zamosky, Obesity's growing threat. While the adult obesity rate went up again in 2013, associated health problems could explode in the next 10 years unless patients and physicians take action. *Med Econ* **91**, 36, 38-41 (2014).
23. E. A. Finkelstein *et al.*, Obesity and severe obesity forecasts through 2030. *Am J Prev Med* **42**, 563-570 (2012).
24. R. F. Kushner, Medical management of obesity. *Semin Gastrointest Dis* **13**, 123-132 (2002).
25. J. Logue, Obesity is an independent risk factor for death from CHD. *Practitioner* **255**, 5 (2011).
26. F. X. Pi-Sunyer, Medical hazards of obesity. *Ann Intern Med* **119**, 655-660 (1993).
27. H. J. Schneider, H. U. Wittchen, H. Wallaschofski, Obesity and risk of death. *N Engl J Med* **360**, 1043; author reply 1043-1044 (2009).

28. C. Printz, Extreme obesity may shorten life expectancy up to 14 years. *Cancer* **120**, 3591 (2014).
29. A. Biener, J. Cawley, C. Meyerhoefer, The High and Rising Costs of Obesity to the US Health Care System. *J Gen Intern Med* **32**, 6-8 (2017).
30. A. Biener, J. Cawley, C. Meyerhoefer, The Impact of Obesity on Medical Care Costs and Labor Market Outcomes in the US. *Clin Chem* **64**, 108-117 (2018).
31. D. D. Kim, A. Basu, Estimating the Medical Care Costs of Obesity in the United States: Systematic Review, Meta-Analysis, and Empirical Analysis. *Value Health* **19**, 602-613 (2016).
32. J. Cawley, C. Meyerhoefer, The medical care costs of obesity: an instrumental variables approach. *J Health Econ* **31**, 219-230 (2012).
33. S. Kuriyama, Impact of overweight and obesity on medical care costs, all-cause mortality, and the risk of cancer in Japan. *J Epidemiol* **16**, 139-144 (2006).
34. J. Cawley, J. A. Rizzo, K. Haas, Occupation-specific absenteeism costs associated with obesity and morbid obesity. *J Occup Environ Med* **49**, 1317-1324 (2007).
35. S. D. Moore, A. C. King, M. Kiernan, C. D. Gardner, Outcome expectations and realizations as predictors of weight regain among dieters. *Eat Behav* **12**, 60-63 (2011).
36. Long-term pharmacotherapy in the management of obesity. National Task Force on the Prevention and Treatment of Obesity. *JAMA* **276**, 1907-1915 (1996).
37. E. Brown, D. J. Cuthbertson, J. P. Wilding, Newer GLP-1 receptor agonists and obesity-diabetes. *Peptides* **100**, 61-67 (2018).
38. Y. Seino, M. Fukushima, D. Yabe, GIP and GLP-1, the two incretin hormones: Similarities and differences. *J Diabetes Investig* **1**, 8-23 (2010).
39. M. J. Pereira, J. W. Eriksson, Emerging Role of SGLT-2 Inhibitors for the Treatment of Obesity. *Drugs* **79**, 219-230 (2019).
40. K. Dumon, G. Savulionyte, Bariatric surgery produces greater weight loss and improvements in medical conditions than non-surgical treatment of obesity. *Evid Based Med* **19**, 138 (2014).
41. H. J. Kissler, U. Settmacher, Bariatric surgery to treat obesity. *Semin Nephrol* **33**, 75-89 (2013).
42. B. M. Wolfe, E. Kvach, R. H. Eckel, Treatment of Obesity: Weight Loss and Bariatric Surgery. *Circ Res* **118**, 1844-1855 (2016).
43. W. K. Stewart, L. W. Fleming, Features of a successful therapeutic fast of 382 days' duration. *Postgrad Med J* **49**, 203-209 (1973).
44. G. F. Cahill, Jr., Survival in starvation. *Am J Clin Nutr* **68**, 1-2 (1998).
45. S. M. Houten, R. J. Wanders, A general introduction to the biochemistry of mitochondrial fatty acid beta-oxidation. *J Inherit Metab Dis* **33**, 469-477 (2010).
46. S. Eaton, K. Bartlett, M. Pourfarzam, Mammalian mitochondrial beta-oxidation. *Biochem J* **320 ( Pt 2)**, 345-357 (1996).
47. P. Cohen, B. M. Spiegelman, Cell biology of fat storage. *Mol Biol Cell* **27**, 2523-2527 (2016).
48. S. Martin, R. G. Parton, Lipid droplets: a unified view of a dynamic organelle. *Nat Rev Mol Cell Biol* **7**, 373-378 (2006).
49. T. C. Walther, J. Chung, R. V. Farese, Jr., Lipid Droplet Biogenesis. *Annu Rev Cell Dev Biol* **33**, 491-510 (2017).
50. J. A. Olzmann, P. Carvalho, Dynamics and functions of lipid droplets. *Nat Rev Mol Cell Biol* **20**, 137-155 (2019).
51. H. Itabe, T. Yamaguchi, S. Nimura, N. Sasabe, Perilipins: a diversity of intracellular lipid droplet proteins. *Lipids Health Dis* **16**, 83 (2017).
52. A. S. Greenberg *et al.*, Perilipin, a major hormonally regulated adipocyte-specific phosphoprotein associated with the periphery of lipid storage droplets. *J Biol Chem* **266**, 11341-11346 (1991).
53. T. C. Walther, R. V. Farese, Jr., Lipid droplets and cellular lipid metabolism. *Annu Rev Biochem* **81**, 687-714 (2012).
54. S. Xu, X. Zhang, P. Liu, Lipid droplet proteins and metabolic diseases. *Biochim Biophys Acta Mol Basis Dis* **1864**, 1968-1983 (2018).
55. J. Laurencikiene *et al.*, Regulation of lipolysis in small and large fat cells of the same subject. *J Clin Endocrinol Metab* **96**, E2045-2049 (2011).
56. B. Bjorndal, L. Burri, V. Staalesen, J. Skorve, R. K. Berge, Different adipose depots: their role in the development of metabolic syndrome and mitochondrial response to hypolipidemic agents. *J Obes* **2011**, 490650 (2011).

57. P. Arner *et al.*, Dynamics of human adipose lipid turnover in health and metabolic disease. *Nature* **478**, 110-113 (2011).
58. J. Jo *et al.*, Hypertrophy and/or Hyperplasia: Dynamics of Adipose Tissue Growth. *PLoS Comput Biol* **5**, e1000324 (2009).
59. P. Arner, Human fat cell lipolysis: biochemistry, regulation and clinical role. *Best Pract Res Clin Endocrinol Metab* **19**, 471-482 (2005).
60. R. E. Duncan, M. Ahmadian, K. Jaworski, E. Sarkadi-Nagy, H. S. Sul, Regulation of lipolysis in adipocytes. *Annu Rev Nutr* **27**, 79-101 (2007).
61. A. R. Kimmel, C. Sztalryd, The Perilipins: Major Cytosolic Lipid Droplet-Associated Proteins and Their Roles in Cellular Lipid Storage, Mobilization, and Systemic Homeostasis. *Annu Rev Nutr* **36**, 471-509 (2016).
62. H. Li *et al.*, Identification of lipid droplet-associated proteins in the formation of macrophage-derived foam cells using microarrays. *Int J Mol Med* **26**, 231-239 (2010).
63. R. Zechner, P. C. Kienesberger, G. Haemmerle, R. Zimmermann, A. Lass, Adipose triglyceride lipase and the lipolytic catabolism of cellular fat stores. *J Lipid Res* **50**, 3-21 (2009).
64. R. Zechner, J. G. Strauss, G. Haemmerle, A. Lass, R. Zimmermann, Lipolysis: pathway under construction. *Curr Opin Lipidol* **16**, 333-340 (2005).
65. N. K. Edens, R. L. Leibel, J. Hirsch, Mechanism of free fatty acid re-esterification in human adipocytes in vitro. *J Lipid Res* **31**, 1423-1431 (1990).
66. A. R. Nawrocki, P. E. Scherer, The delicate balance between fat and muscle: adipokines in metabolic disease and musculoskeletal inflammation. *Curr Opin Pharmacol* **4**, 281-289 (2004).
67. N. D. Roe, M. K. Handzlik, T. Li, R. Tian, The Role of Diacylglycerol Acyltransferase (DGAT) 1 and 2 in Cardiac Metabolism and Function. *Sci Rep* **8**, 4983 (2018).
68. K. R. Feingold, C. Grunfeld, in *Endotext,* K. R. Feingold *et al.*, Eds. (South Dartmouth (MA), 2000).
69. M. M. Hussain, A proposed model for the assembly of chylomicrons. *Atherosclerosis* **148**, 1-15 (2000).
70. T. El Arnaout, T. Soulimane, Targeting Lipoprotein Biogenesis: Considerations towards Antimicrobials. *Trends Biochem Sci* **44**, 701-715 (2019).
71. D. A. Widdick *et al.*, Dissecting the complete lipoprotein biogenesis pathway in Streptomyces scabies. *Mol Microbiol* **80**, 1395-1412 (2011).
72. J. R. Mead, S. A. Irvine, D. P. Ramji, Lipoprotein lipase: structure, function, regulation, and role in disease. *J Mol Med (Berl)* **80**, 753-769 (2002).
73. A. D. Cooper, Hepatic uptake of chylomicron remnants. *J Lipid Res* **38**, 2173-2192 (1997).
74. S. E. Crawford, J. Borensztajn, Plasma clearance and liver uptake of chylomicron remnants generated by hepatic lipase lipolysis: evidence for a lactoferrin-sensitive and apolipoprotein E-independent pathway. *J Lipid Res* **40**, 797-805 (1999).
75. S. Tiwari, S. A. Siddiqi, Intracellular trafficking and secretion of VLDL. *Arterioscler Thromb Vasc Biol* **32**, 1079-1086 (2012).
76. S. Han, H. M. Sun, K. C. Hwang, S. W. Kim, Adipose-Derived Stromal Vascular Fraction Cells: Update on Clinical Utility and Efficacy. *Crit Rev Eukaryot Gene Expr* **25**, 145-152 (2015).
77. G. J. Hausman, M. V. Dodson, Stromal Vascular Cells and Adipogenesis: Cells within Adipose Depots Regulate Adipogenesis. *J Genomics* **1**, 56-66 (2013).
78. J. M. Cavaillon, Cytokines and macrophages. *Biomed Pharmacother* **48**, 445-453 (1994).
79. Y. Lavin, A. Mortha, A. Rahman, M. Merad, Regulation of macrophage development and function in peripheral tissues. *Nat Rev Immunol* **15**, 731-744 (2015).
80. L. Peiser, S. Gordon, The function of scavenger receptors expressed by macrophages and their role in the regulation of inflammation. *Microbes Infect* **3**, 149-159 (2001).
81. G. Arango Duque, A. Descoteaux, Macrophage cytokines: involvement in immunity and infectious diseases. *Front Immunol* **5**, 491 (2014).
82. E. R. Unanue, Antigen-presenting function of the macrophage. *Annu Rev Immunol* **2**, 395-428 (1984).
83. J. Cole, J. Aberdein, J. Jubrail, D. H. Dockrell, The role of macrophages in the innate immune response to Streptococcus pneumoniae and Staphylococcus aureus: mechanisms and contrasts. *Adv Microb Physiol* **65**, 125-202 (2014).

84. D. Hirayama, T. Iida, H. Nakase, The Phagocytic Function of Macrophage-Enforcing Innate Immunity and Tissue Homeostasis. *Int J Mol Sci* **19**, (2017).
85. C. Rosales, E. Uribe-Querol, Phagocytosis: A Fundamental Process in Immunity. *Biomed Res Int* **2017**, 9042851 (2017).
86. C. Varol, A. Mildner, S. Jung, Macrophages: development and tissue specialization. *Annu Rev Immunol* **33**, 643-675 (2015).
87. H. Kettenmann, F. Kirchhoff, A. Verkhratsky, Microglia: new roles for the synaptic stripper. *Neuron* **77**, 10-18 (2013).
88. V. H. Perry, V. O'Connor, The role of microglia in synaptic stripping and synaptic degeneration: a revised perspective. *ASN Neuro* **2**, e00047 (2010).
89. B. D. Trapp *et al.*, Evidence for synaptic stripping by cortical microglia. *Glia* **55**, 360-368 (2007).
90. B. F. Boyce, L. Xing, Functions of RANKL/RANK/OPG in bone modeling and remodeling. *Arch Biochem Biophys* **473**, 139-146 (2008).
91. W. J. Boyle, W. S. Simonet, D. L. Lacey, Osteoclast differentiation and activation. *Nature* **423**, 337-342 (2003).
92. S. L. Teitelbaum, Bone resorption by osteoclasts. *Science* **289**, 1504-1508 (2000).
93. A. W. Ferrante, Jr., Macrophages, fat, and the emergence of immunometabolism. *J Clin Invest* **123**, 4992-4993 (2013).
94. A. W. Ferrante, Jr., The immune cells in adipose tissue. *Diabetes Obes Metab* **15 Suppl 3**, 34-38 (2013).
95. H. Shapiro *et al.*, Adipose tissue foam cells are present in human obesity. *J Clin Endocrinol Metab* **98**, 1173-1181 (2013).
96. X. Xu *et al.*, Obesity activates a program of lysosomal-dependent lipid metabolism in adipose tissue macrophages independently of classic activation. *Cell Metab* **18**, 816-830 (2013).
97. S. Cinti *et al.*, Adipocyte death defines macrophage localization and function in adipose tissue of obese mice and humans. *J Lipid Res* **46**, 2347-2355 (2005).
98. H. Du, G. A. Grabowski, Lysosomal acid lipase and atherosclerosis. *Curr Opin Lipidol* **15**, 539-544 (2004).
99. C. Yan *et al.*, Macrophage-specific expression of human lysosomal acid lipase corrects inflammation and pathogenic phenotypes in lal-/- mice. *Am J Pathol* **169**, 916-926 (2006).
100. F. Li, H. Zhang, Lysosomal Acid Lipase in Lipid Metabolism and Beyond. *Arterioscler Thromb Vasc Biol* **39**, 850-856 (2019).
101. Z. Reiner *et al.*, Lysosomal acid lipase deficiency--an under-recognized cause of dyslipidaemia and liver dysfunction. *Atherosclerosis* **235**, 21-30 (2014).
102. A. Tylki-Szymanska, A. Jurecka, Lysosomal acid lipase deficiency: wolman disease and cholesteryl ester storage disease. *Pril (Makedon Akad Nauk Umet Odd Med Nauki)* **35**, 99-106 (2014).
103. H. Du *et al.*, Lysosomal acid lipase-deficient mice: depletion of white and brown fat, severe hepatosplenomegaly, and shortened life span. *J Lipid Res* **42**, 489-500 (2001).
104. S. P. Weisberg *et al.*, Obesity is associated with macrophage accumulation in adipose tissue. *J Clin Invest* **112**, 1796-1808 (2003).
105. M. Bluher, Adipose tissue inflammation: a cause or consequence of obesity-related insulin resistance? *Clin Sci (Lond)* **130**, 1603-1614 (2016).
106. J. M. Olefsky, C. K. Glass, Macrophages, inflammation, and insulin resistance. *Annu Rev Physiol* **72**, 219-246 (2010).
107. M. C. Arkan *et al.*, IKK-beta links inflammation to obesity-induced insulin resistance. *Nat Med* **11**, 191-198 (2005).
108. B. R. Coats *et al.*, Metabolically Activated Adipose Tissue Macrophages Perform Detrimental and Beneficial Functions during Diet-Induced Obesity. *Cell Rep* **20**, 3149-3161 (2017).
109. A. Xue *et al.*, Genome-wide association analyses identify 143 risk variants and putative regulatory mechanisms for type 2 diabetes. *Nat Commun* **9**, 2941 (2018).
110. I. M. Heid, T. W. Winkler, A multitrait GWAS sheds light on insulin resistance. *Nat Genet* **49**, 7-8 (2016).
111. Z. G. Gao, J. P. Ye, Why do anti-inflammatory therapies fail to improve insulin sensitivity? *Acta Pharmacol Sin* **33**, 182-188 (2012).

112. P. M. Ridker *et al.*, Antiinflammatory Therapy with Canakinumab for Atherosclerotic Disease. *N Engl J Med* **377**, 1119-1131 (2017).
113. X. Y. Tian *et al.*, Thermoneutral Housing Accelerates Metabolic Inflammation to Potentiate Atherosclerosis but Not Insulin Resistance. *Cell Metab* **23**, 165-178 (2016).
114. J. Boren, M. R. Taskinen, S. O. Olofsson, M. Levin, Ectopic lipid storage and insulin resistance: a harmful relationship. *J Intern Med* **274**, 25-40 (2013).
115. G. I. Shulman, Ectopic fat in insulin resistance, dyslipidemia, and cardiometabolic disease. *N Engl J Med* **371**, 2237-2238 (2014).
116. M. Snel *et al.*, Ectopic fat and insulin resistance: pathophysiology and effect of diet and lifestyle interventions. *Int J Endocrinol* **2012**, 983814 (2012).
117. J. E. Schaffer, Lipotoxicity: when tissues overeat. *Curr Opin Lipidol* **14**, 281-287 (2003).
118. T. Scherer *et al.*, Brain insulin controls adipose tissue lipolysis and lipogenesis. *Cell Metab* **13**, 183-194 (2011).
119. A. C. Sletten, L. R. Peterson, J. E. Schaffer, Manifestations and mechanisms of myocardial lipotoxicity in obesity. *J Intern Med* **284**, 478-491 (2018).
120. X. Li *et al.*, Skeletal Muscle Lipid Droplets and the Athlete's Paradox. *Cells* **8**, (2019).
121. C. L. Wu *et al.*, Conditional Macrophage Depletion Increases Inflammation and Does Not Inhibit the Development of Osteoarthritis in Obese Macrophage Fas-Induced Apoptosis-Transgenic Mice. *Arthritis Rheumatol* **69**, 1772-1783 (2017).
122. S. H. Burnett *et al.*, Conditional macrophage ablation in transgenic mice expressing a Fas-based suicide gene. *J Leukoc Biol* **75**, 612-623 (2004).
123. R. Spaull *et al.*, Exosomes populate the cerebrospinal fluid of preterm infants with post-haemorrhagic hydrocephalus. *Int J Dev Neurosci* **73**, 59-65 (2019).
124. E. van der Pol, A. N. Boing, P. Harrison, A. Sturk, R. Nieuwland, Classification, functions, and clinical relevance of extracellular vesicles. *Pharmacol Rev* **64**, 676-705 (2012).
125. M. Frydrychowicz, A. Kolecka-Bednarczyk, M. Madejczyk, S. Yasar, G. Dworacki, Exosomes - structure, biogenesis and biological role in non-small-cell lung cancer. *Scand J Immunol* **81**, 2-10 (2015).
126. N. P. Hessvik, A. Llorente, Current knowledge on exosome biogenesis and release. *Cell Mol Life Sci* **75**, 193-208 (2018).
127. D. M. Pegtel, S. J. Gould, Exosomes. *Annu Rev Biochem* **88**, 487-514 (2019).
128. M. Ostrowski *et al.*, Rab27a and Rab27b control different steps of the exosome secretion pathway. *Nat Cell Biol* **12**, 19-30; sup pp 11-13 (2010).
129. P. Puzar Dominkus *et al.*, PKH26 labeling of extracellular vesicles: Characterization and cellular internalization of contaminating PKH26 nanoparticles. *Biochim Biophys Acta Biomembr* **1860**, 1350-1361 (2018).
130. L. Muller *et al.*, Human tumor-derived exosomes (TEX) regulate Treg functions via cell surface signaling rather than uptake mechanisms. *Oncoimmunology* **6**, e1261243 (2017).
131. K. J. McKelvey, K. L. Powell, A. W. Ashton, J. M. Morris, S. A. McCracken, Exosomes: Mechanisms of Uptake. *J Circ Biomark* **4**, 7 (2015).
132. D. Feng *et al.*, Cellular internalization of exosomes occurs through phagocytosis. *Traffic* **11**, 675-687 (2010).
133. T. Tian *et al.*, Exosome uptake through clathrin-mediated endocytosis and macropinocytosis and mediating miR-21 delivery. *J Biol Chem* **289**, 22258-22267 (2014).
134. M. Laplante, D. M. Sabatini, mTOR signaling at a glance. *J Cell Sci* **122**, 3589-3594 (2009).
135. T. Thomou *et al.*, Adipose-derived circulating miRNAs regulate gene expression in other tissues. *Nature* **542**, 450-455 (2017).
136. S. Kita, N. Maeda, I. Shimomura, Interorgan communication by exosomes, adipose tissue, and adiponectin in metabolic syndrome. *J Clin Invest* **129**, 4041-4049 (2019).
137. C. Crewe *et al.*, An Endothelial-to-Adipocyte Extracellular Vesicle Axis Governed by Metabolic State. *Cell* **175**, 695-708 e613 (2018).
138. W. Ying *et al.*, Adipose Tissue Macrophage-Derived Exosomal miRNAs Can Modulate In Vivo and In Vitro Insulin Sensitivity. *Cell* **171**, 372-384 e312 (2017).

# CHAPTER 2:CHARACTERIZING ADIPOSE TISSUE-DERIVED EXOSOMES

## 2.1 Results

Adipose tissue contains many cell types including adipocytes, endothelial, mesenchymal, stem, and immune cells. All have distinct roles, some of which are clear, while others are still emerging. In white adipose tissue, adipocytes contain large unilocular lipid droplets composed of triacylglycerides (TAGs) and other neutral lipids. These TAGs serve as the major long-term energy reserves for the body in mammals (*1*). During times of negative energy balance, starvation signals are sent to the adipose tissue to mobilize these energy reserves. Our current understanding is that this occurs through the activation of cytoplasmic lipases in the adipocyte, including adipose tissue triglyceride lipase (ATGL/PNPLA2), hormone sensitive lipase HSL, and monoglyceride lipase (MGL) (*2, 3*). These enzymes sequentially hydrolyze triglyceride within lipid droplets, cleaving the ester bonds of the glycerol backbone and releasing three free fatty acids per TG molecule (*4*). The free fatty acids are released from the cell, in a process that still remains poorly defined, and enter the circulation where they can be taken up by the cells as metabolic substrates (*5*).

Adipose tissue macrophages (ATMs) are present in the adipose tissue and contain amounts of neutral lipid visible by light microscopy (*6, 7*). Both ATM number and lipid content increase in obese animals and individuals (*8, 9*). It had been assumed that ATM lipid stores originate from adipocyte-released free fatty acid (FFA). The accepted model postulated that FFAs are taken up by the macrophage, re-esterified by diglyceride acyltransferases (DGAT1 & DGAT2), and stored in intracellular lipid droplets (Figure 2.1). This model explained that the increased lipid content of ATMs that is observed in obesity results from increased fatty acid release, caused by increased lipolytic activity of adipocytes (*10, 11*).

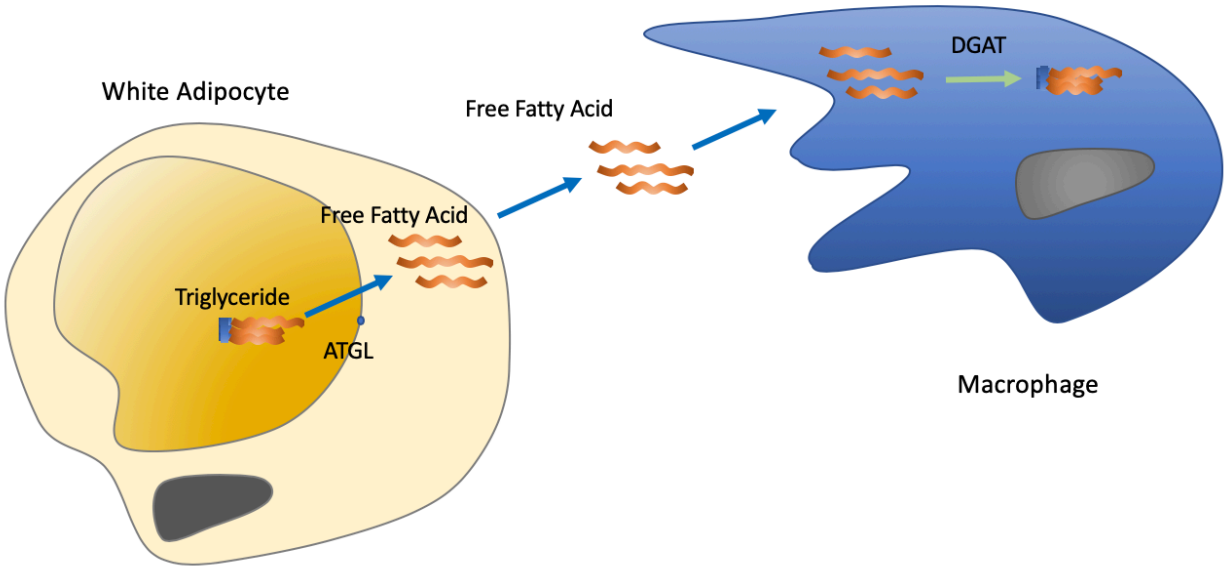


**Figure 2.1. Prevailing model of neutral lipid accumulation in adipose tissue macrophages.**

Aggregates of neutral lipid within cells are typically stored in lipid droplets, organelles whose perimeter is defined by a phospholipid monolayer, and that serves as the transition barrier between the hydrophobic lipid core and the hydrophilic cytoplasm (*12, 13*). This lipid droplet monolayer contains proteins required for droplet formation, lipid flux into and out of the droplet, and signaling (*14, 15*). Over the last decade, studies also revealed that lipid droplets, or portions of lipid droplets, can undergo autophagy, providing a mechanism to deliver lipid to the lysosome for hydrolysis by acid lipase(s) (*2, 16, 17*). Unexpectedly, previous studies had revealed that lipid in ATMs underwent lysosomal hydrolysis by a mechanism independent of classical macroautophagy (*18*). This suggested that visible, aggregated neutral lipid in ATMs might not be contained within lipid droplets.

Among the most abundant lipid droplet-associated proteins are the perilipin (PLIN) family proteins, a family of molecules that in cell-specific fashions are key regulators of lipase activity (*19-21*). They are commonly used as immunohistochemical markers of lipid droplets, and the predominant PLIN-protein in macrophages is perilipin-2 (PLIN2)(*20, 22*). To further characterize the neutral lipid storage within ATMs we used confocal microscopy of whole adipose tissue. Adipose tissue from obese mice was used to increase our ability to visualize lipid in ATMs. The tissue was stained with 1) BODIPY, a

fluorescent dye used to visualize neutral lipid, 2) DAPI, a fluorescent dye used to stain nucleic acids and to mark nuclei, and antibodies against 3) F4/80, a marker found in macrophage plasma membrane, and 4) PLIN2, a protein on classical macrophage lipid droplet membranes. Despite many examples of PLIN2+/BODIPY+ lipid droplets within the ATMs, the majority of BODIPY staining within F4/80+ cells was not associated with PLIN2 (Figure 2.2), indicating that neutral lipid within ATMs is either not stored in lipid droplets, or that a subpopulation of lipid droplets in ATMs lack PLIN2.

In order to investigate the lipid content in ATMs and its delivery from adipocytes, we moved to an *in vitro* system. Previously, it had been shown that culturing bone marrow derived myeloid precursor cells with colony stimulating factor-1 (CSF1/MCSF) in the presence of adipose tissue, leads to the differentiation of precursors into macrophage cells that accumulate lipid and are ATM-like (*18, 23*). The technique we used to generate ATM-like cells employed bone marrow from femurs of young mice that were co-cultured with perigonadal adipose tissue (PGAT) from adult mice. We have dubbed these cells bone marrow adipose tissue macrophages (BM-ATMs) to distinguish them from bone marrow cells differentiated solely in the presence of CSF1 (BMDMs). This process induces the cells to assume many of the characteristics of primary ATMs, including neutral lipid accumulation, multinuclear formation, a transcriptional profile typical of ATMs, lysosome biogenesis, and lipid catabolism, as described previously (*18, 23*).

Because BM-ATMs grow in a monolayer, we used transmission electron microscopy to study their cellular ultrastructure. As a positive control, we used foam cells generated in vitro. Briefly, treating BMDMs with acetylated-LDL leads to formation of in vitro foam cells – similar to macrophages seen in atherosclerotic plaques. It has previously been shown that lipid in in vitro foam cells is stored in lipid droplets (monolayer membrane) and undergoes hydrolysis, in part, via lipophagy (Figure 2.3, right [Ambar Grijalva]). In contrast, in BM-ATMs we could detect some lipid droplets (monolayer membrane), but most of the lipid seemed to be stored in distinct lipid vesicles surrounded by a bilayer membrane (Figure 2.3, left [Ambar Grijalva]). Autophagosomes, the hallmark of autophagy, were abundant in foam cells but not within BM-ATMs.

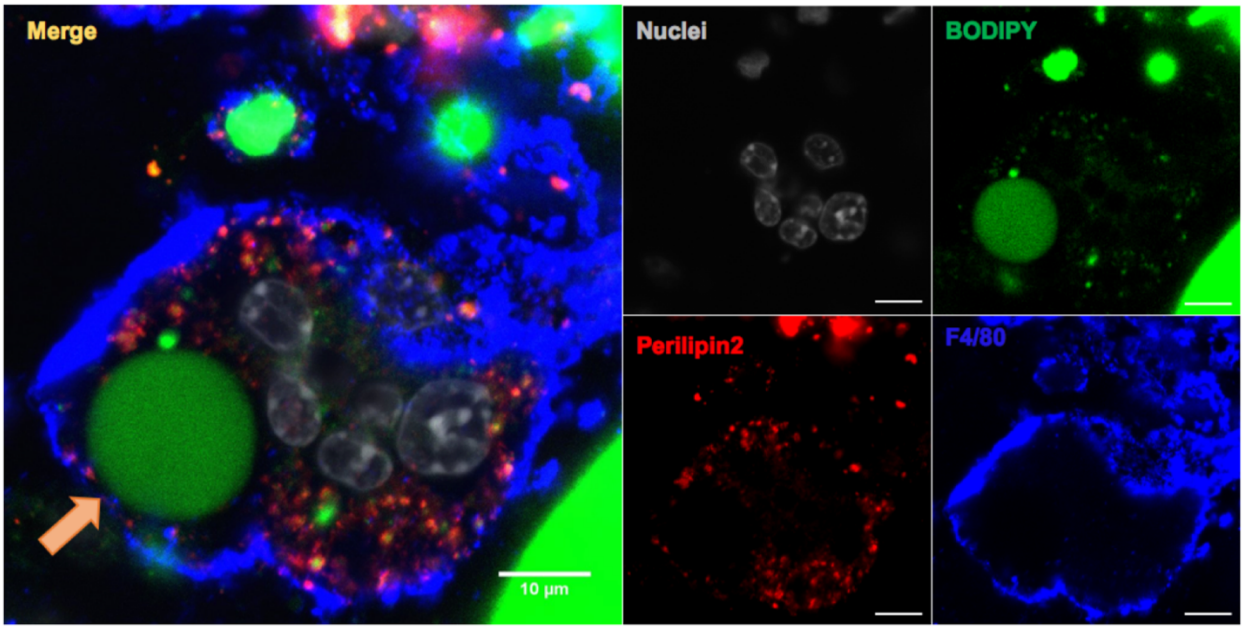


**Figure 2.2. ATM lipid stores not associated with lipid droplet proteins.** Confocal microscopy images of whole PGAT from *Lep*$^{ob/ob}$ mice, immunostained with antibodies against perilipin 2 (red) and F4/80 (blue) and incubated with DNA fluorescent stain 4′,6-diamidino-2-phenylindole (DAPI) (white) and neutral lipid fluorescent stain boron-dipyrromethene (BODIPY) (green). Orange arrow highlights lipid accumulation within ATM. Scale bars, 10 mm.

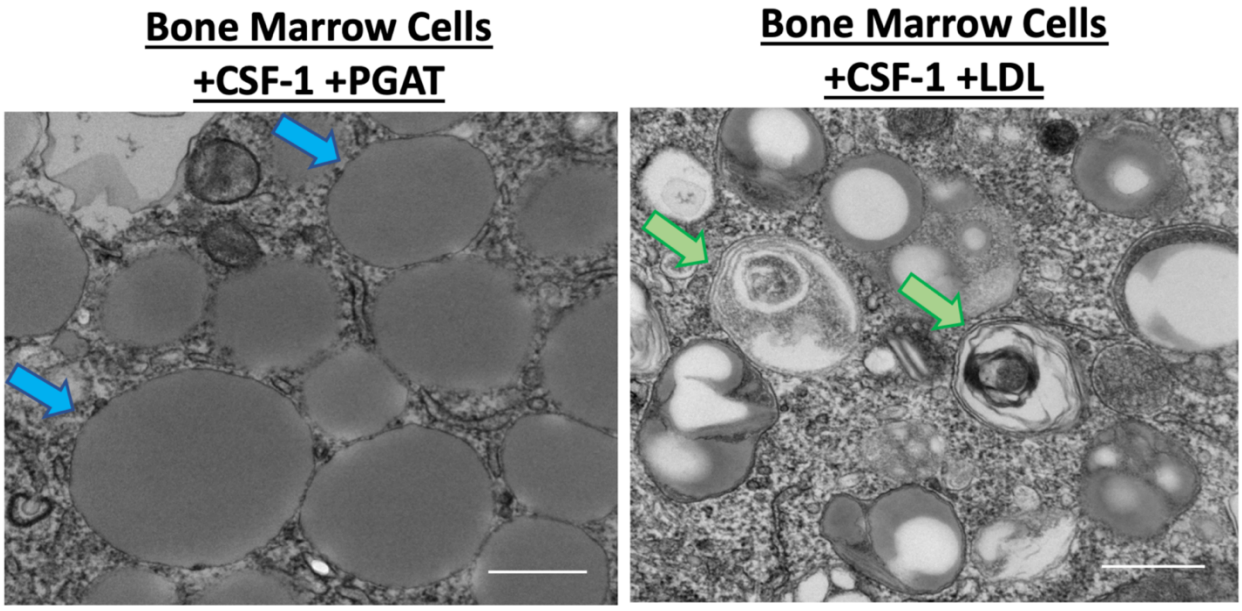


**Figure 2.3. BM-ATM lipid stored in intracellular vesicles.** Electron microscopy images of BM-ATMs (left) and bone marrow–derived foam cells (right). Arrows highlight lipid vesicles and lipid-rich autophagosomes(blue and green, respectively). Scale bars, 200 nm. LDL, low-density lipoprotein.

Lipid droplets are formed through the esterification of FFA, but given the distinct structures in which lipid resides in BM-ATMs, we were prompted to determine whether lipid released by adipocytes requires lipolysis of TG or is distributed through an alternative mechanism. Adipocyte-specific ATGL/PNPLA2 deficient animals do not tolerate fasting but tend to have large amounts of lipid in ATMs (*24*). To determine the relative contribution of lipolytic free fatty acid to ATM lipid accumulation, WT BMDMs were co-cultured with WT PGAT or with PGAT from adipocyte-specific ATGL/PNPLA2 deficient mice. Using confocal microscopy, we saw that BMDMs co-cultured with WT PGAT had the expected accumulation of neutral lipid (Figure 2.4, middle [Ambar Grijalva]). Surprisingly, however, PGAT from adipocyte-specific ATGL/PNPLA2 deficient mice was just as effective at inducing BMDM lipid accumulation as WT PGAT (Figure 2.4, bottom [Ambar Grijalva]).

The existence of an alternative mechanism was confirmed using pharmacological inhibitors of lipolysis. Atglistatin, an ATGL/PNPLA2 inhibitor, was able to effectively decrease the amount of free fatty acid (FFA) released from WT PGAT explants (Figure 2.5). But whether conditioned medium from these explants or control-treated explants were added to WT BMDM cultures, macrophages accumulated equivalent amounts of TG (Figure 2.6). The same phenomenon can be seen when treating explants with lipolytic inhibitors known to affect hormone sensitive lipase, as well (Figure 2.7). This demonstrates that the ability of adipose tissue to release FFA is dissociated from its ability to transfer lipid to BMDMs.

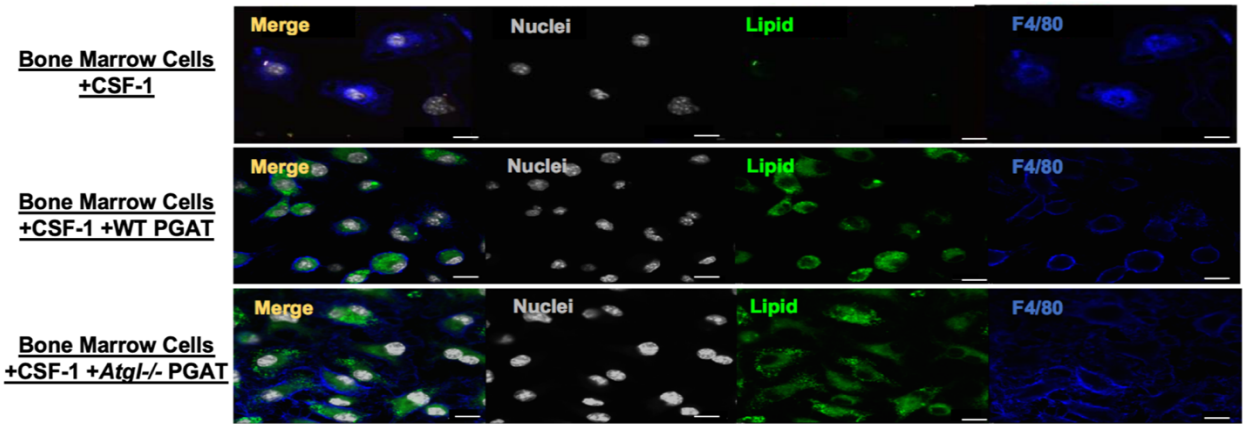


**Figure 2.4. PGAT from ATGL deficient animals transfers lipid to BMDMs when co-cultured.** Confocal microscopy images of BMDMs (top), BM-ATMs differentiated in the presence of adipose tissue (middle), and BM-ATMs differentiated in the presence of Atgl/Pnpla2-deficient adipose tissue (bottom), immunostained with antibodies against F4/80 (blue), as well as DNA fluorescent stain DAPI (white) and neutral lipid fluorescent stain BODIPY (green). Scale bars, 10 mm.

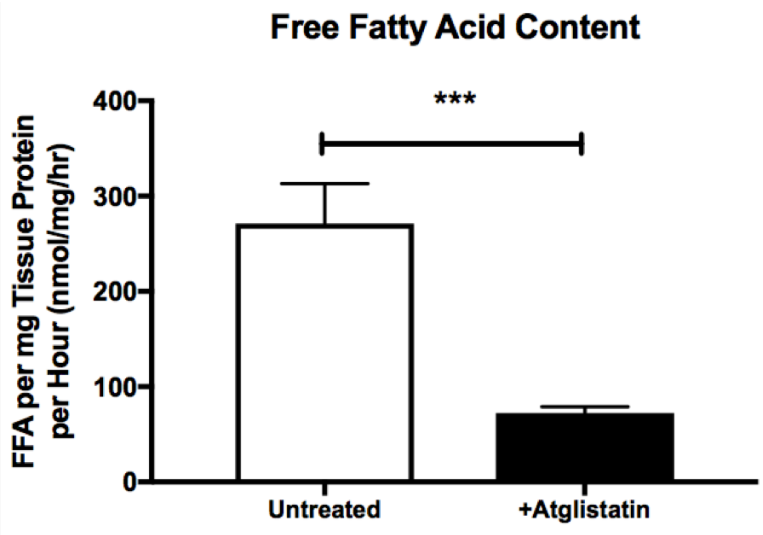


**Figure 2.5. Atglistatin treatment decreases FFA release from PGAT explants**. Free fatty acid content of PGAT conditioned medium cultured with or without Atglistatin for 16 hours per gram per hour. Unpaired two-tailed t test; n = 6; ***, P < 0.001.

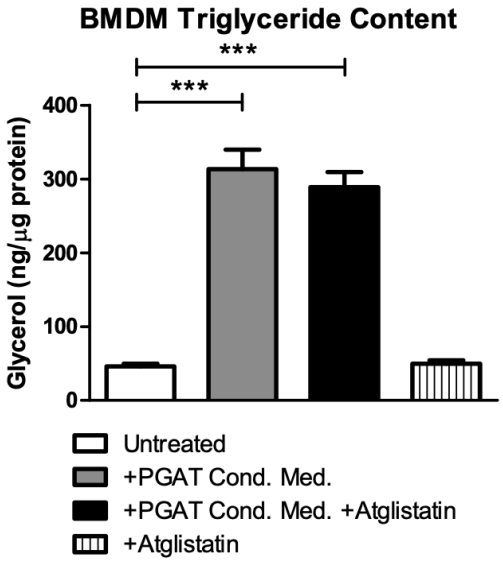


**Figure 2.6. Atglistatin treatment does not reduce neutral lipid transfer to BMDMs.** Triglyceride content of BMDMs (untreated) or treated with medium-containing 50μM Atglistatin, BM-ATM differentiated with conditioned medium of wild-type (WT) PGAT or with conditioned medium WT PGAT treated with 50 μM Atglistatin. One-way analysis of variance (ANOVA); n = 6; ***P < 0.001. Error bars represent standard deviation (SD).

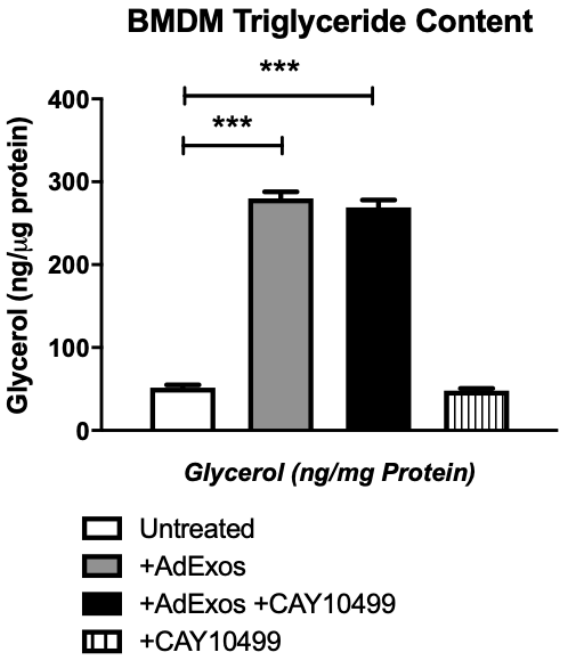


**Figure 2.7. HSL inhibition does not reduce neutral lipid transfer to BMDMs.** Triglyceride content of BMDMs (untreated) or treated with medium-containing 5μM CAY10499, BM-ATM differentiated with conditioned medium of wild-type (WT) PGAT or with conditioned medium WT PGAT treated with 5 μM CAY. One-way analysis of variance (ANOVA); n = 6; ***P < 0.001. Error bars represent SD.

In search of this alternative mode of lipid release from adipocytes we examined the interior structure of primary mouse adipocytes using electron microscopy. These micorgraphs reveal the expected large unilocular lipid droplet in each cell and a thin rim of cytoplasm. However, they also revealed smaller, invaginated, lipid-filled bodies in the cytoplasm (Figure 2.8). The position and structure of these bodies were consistent with smaller lipid droplets either fusing with or budding off of the central lipid droplet. Also visible were nearby structures consistent with multivesicular endosomes (*25-27*). A major function of multivesicular endosomes is as an intermediary step in the release of extracellular vesicles, including exosomes(*28-30*).

Exosomes are small cellular-derived vesicles ranging in diameter from 50nm to 200nm (*31*). Exosomes are released by most cell types and can function in intercellular communication (*32, 33*). These vesicles are bound by phospholipid bilayers and contain protein, mRNA, miRNA, and lipid species from their cellular parent (*30, 34-38*). Given these observations, we hypothesized that lipid transfer from adipocytes to BMDMs occurs, in part, via exosomes. To begin to test this, we examined conditioned media from mouse PGAT explants, cultured without serum with electron microscopy. These micrographs revealed a high concentration of extracellular vesicular particles ranging in diameter from 50 to 100 nm, consistent with the size of exosomes and related vesicles (Figure 2.9 [Ambar Grijalva]).

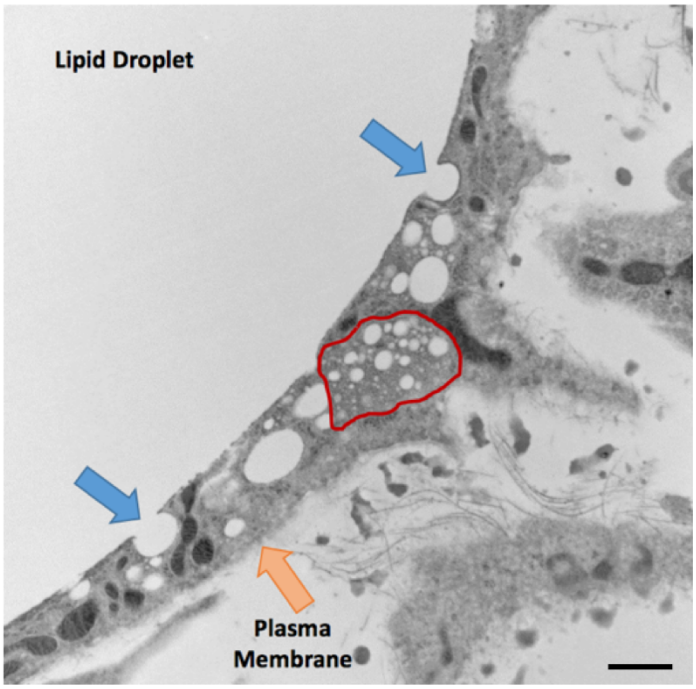


**Figure 2.8. Adipocytes contain small, invaginated lipid structures in their cytoplasm.** Electron microscopy image of whole, fixed adipose tissue. Arrows highlight the adipocyte plasma membrane and the budding- like structures of the central lipid droplet (orange and blue arrows, respectively), and the red outline indicates a multivesicular endosome-like structure. Scale bar, 200 nm.

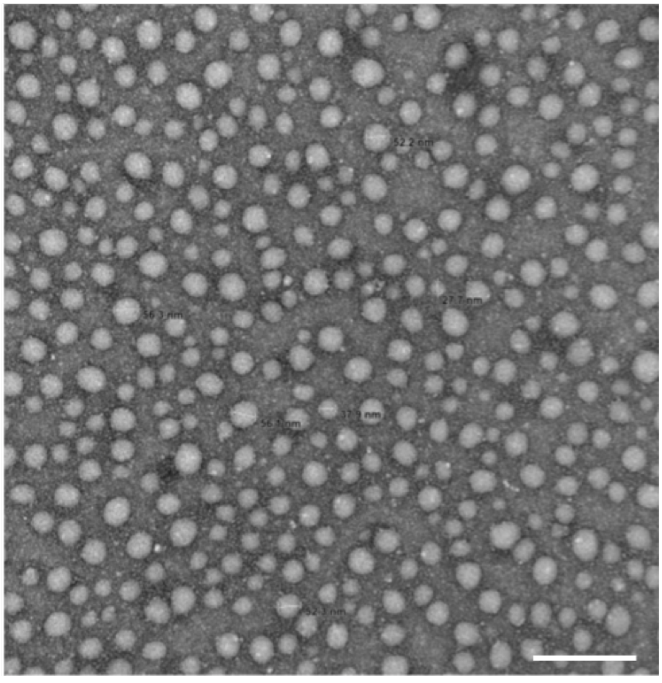

**Figure 2.9. PGAT conditioned medium contains extracellular vesicles in the size range of exosomes.** Electron microscopy image of vesicles collected from adipose tissue–conditioned medium. Scale bar, 200 nm.

Because these adipose tissue-derived exosomes (AdExos), were expected to contain large amounts of neutral lipid, this presented a new challenge as the gold standard for exosome purification is separating extracellular materials by density using ultracentrifugation. As the high lipid content of AdExos would likely affect their density, such that they would no longer be found at expected exosomal densities, we set out to isolate these exosomes using a different technique. Using a series of gel fractionation columns and filtration, we were able to achieve a high level of purity in our exosome samples, as determined by Nanoparticle Tracking Analysis (NTA), separating extracellular materials strictly by size and not by density (Figure 2.10).

As a secondary method of verification for the protocol, we took advantage of the structure of the exosome, namely its phospholipid bilayer membrane, which allowed for labeling using fluorescent dyes, like PKH26 and PKH67 which intercalate within lipid bilayers (*39, 40*). AdExos were incubated with PKH26 and then isolated using the size-exclusion method. Fractions were collected as they came off of the final column. Each fraction's PKH26 fluorescence was measured and each fraction was analyzed using NTA. The fractions that contained particles consistent with exosomes were the same fractions that contained the PKH26 label (Figure 2.10). This is in contrast to exosomes that were incubated with bovine serum albumin (BSA) before being labeled, as the BSA-bound PKH26 came off of the column in later fractions, and did not contain any exosomes (Figure 2.11).

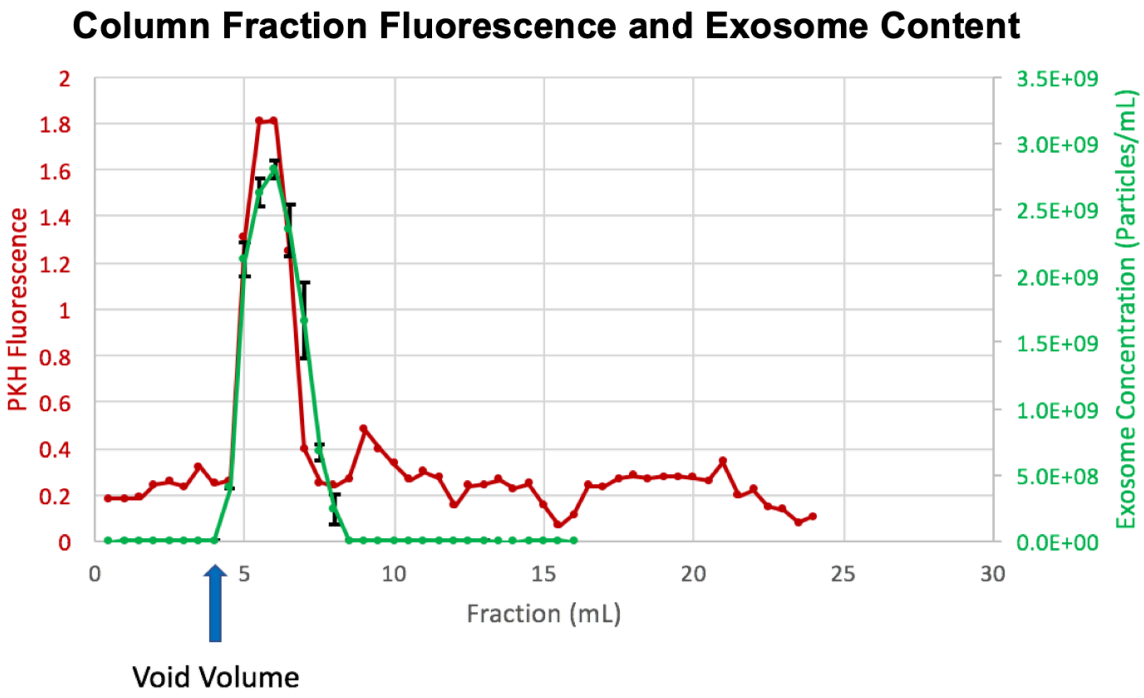


**Figure 2.10. Exosomes elute with fluorescent label.** PKH26 fluorescence (left y-axis) and exosome concentration, as determined by Nanoparticle Tracking Analysis (right y-axis), of gel filtration column fractions (n = 3).

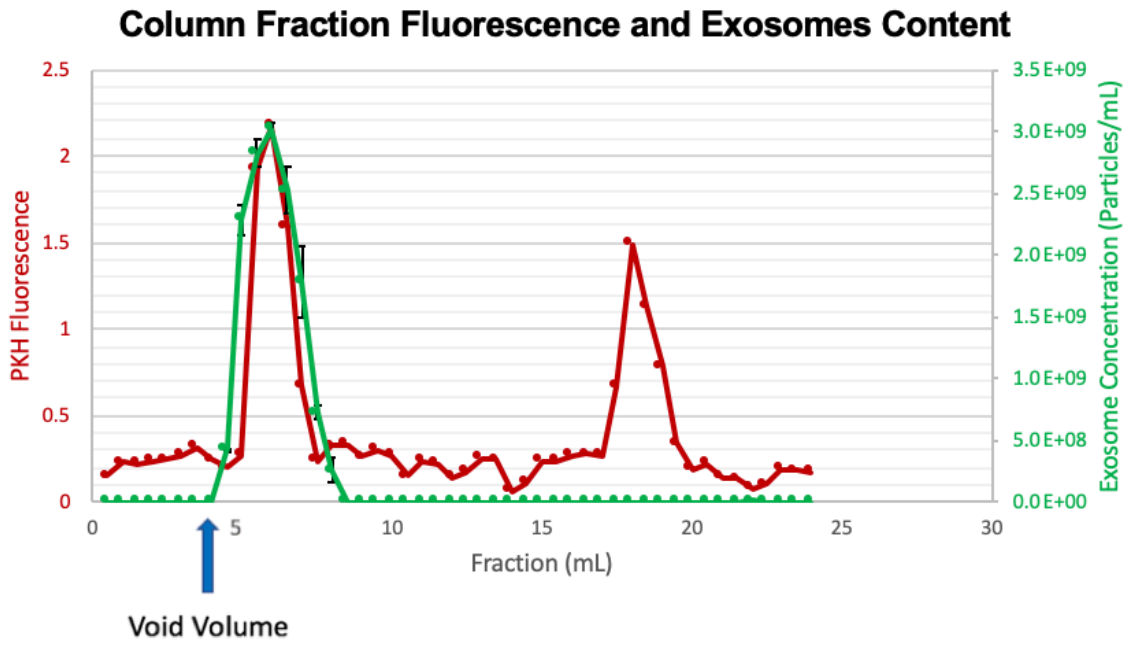


**Figure 2.11. Exosomes do not elute with BSA.** Exosomes were co-labeled with BSA before being added to gel filtration column. PKH26 fluorescence (left y-axis) and exosome concentration, as determined by Nanoparticle Tracking Analysis (right y-axis), of gel filtration column fractions (n = 3).

After establishing a suitable protocol for purifying AdExos, we set out to characterize them. The AdExos were found to range in diameter from 50nm – 200nm as determined using NTA on two different instruments: the Nanosight (Supplemental Figure 1.1, Supplemental Figure 1.2) and the Viewsizer 3000 (Supplemental Figure 1.3, Supplemental Figure 1.4). The measurement of size, distribution and number of AdExos obtained by the two systems were very similar. (Figure 2.12, Figure 2.13). We found that PGAT from lean 10-week-old mice released ~$1.3x10^{11}$ particles per gram of tissue each hour (Figure 2.14). In addition, the rate of AdExo release was stable from hour to hour within a 12-hour culture period (Figure 2.15). The exosome release rate from PGAT is relatively high when compared to rates reported for other tissues that have been studied using the same technique (*41-43*).

Exosomes, as a class of extracellular vesicle, contain proteins that have been implicated in their biogenesis and function, including CD63, HSP70 and CD9 (*32, 37*). Using antibodies against these proteins, we were able to confirm their presence in our AdExo samples via western blot (Figure 2.16). Our hypothesis argues that AdExos also contain proteins typically found in adipocytes. Among the proteins most abundant in and relatively specific to adipocytes are caveolin 1 (CAV1), fatty acid binding protein 4 (FABP4), and adipocyte lipid droplet membrane-associated proteins, including ATGL/PNPLA2 and PLIN1. Indeed, each of these are detectable by western blot in AdExos (Figure 2.17, Figure 2.18). Notably, AdExos do not contain cytochrome c oxidase subunit 4 (COXIV) or lamin b1 (LAMINB1), consistent with these exosomes not containing mitochondrial or nuclear debris (Figure 2.17). PGAT from adipocyte-specific ATGL/PNPLA2 deficient animals still secrete AdExos and these AdExos still contain the same proteins, except that ATGL/PNPLA2 can no longer be found in the exosomes, indicating that the ATGL in AdExos is adipocyte-derived (Figure 2.19).

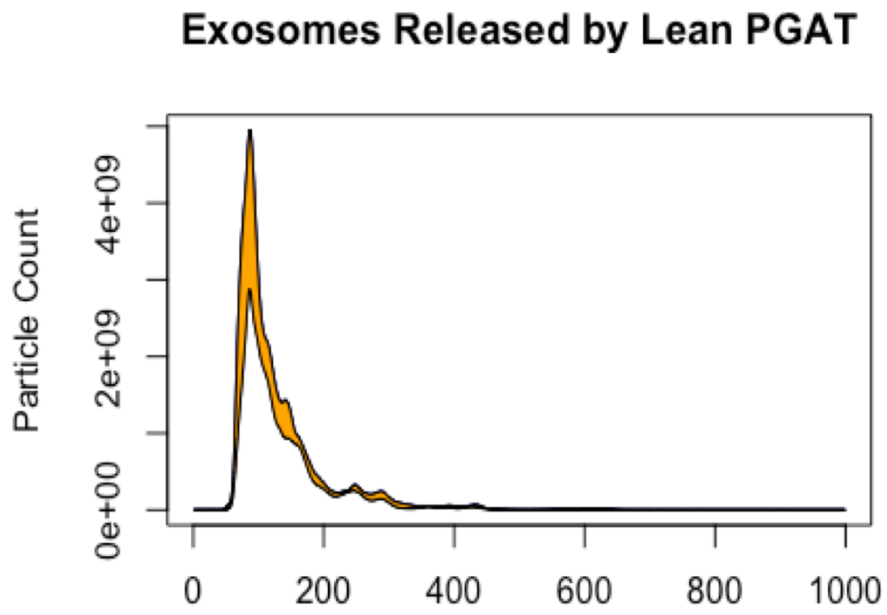


**Figure 2.12. Majority of AdExos in 50nm – 200nm diameter range.** Nanosight Nanoparticle Tracking Analysis histogram of purified adipose tissue-derived exosomes, depicting particle diameter and the number of particles at each diameter released by 1 g of lean adipose tissue per hour.

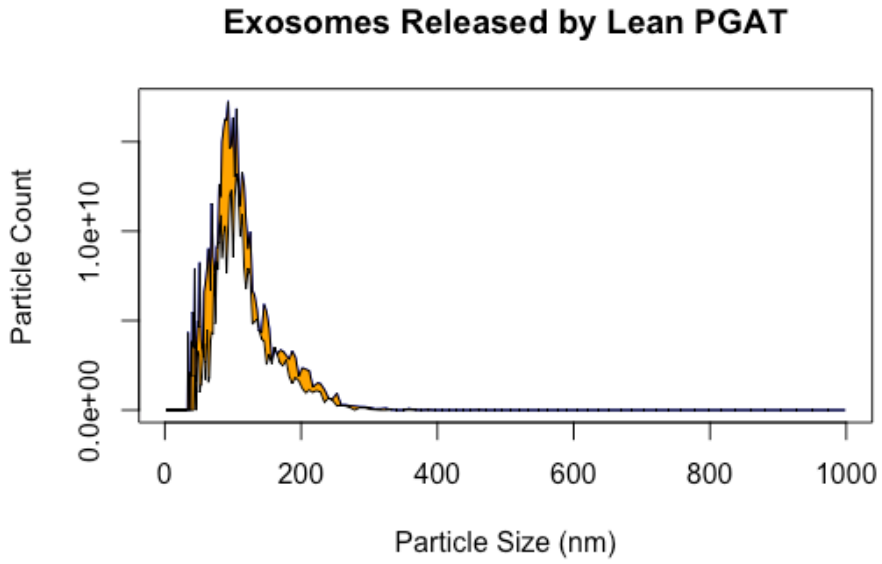


**Figure 2.13. Majority of AdExos in 50nm – 200nm diameter range.** Viewsizer 3000 Nanoparticle Tracking Analysis histogram of purified adipose tissue-derived exosomes, depicting particle diameter and the number of particles at each diameter released by 1 g of lean adipose tissue per hour.

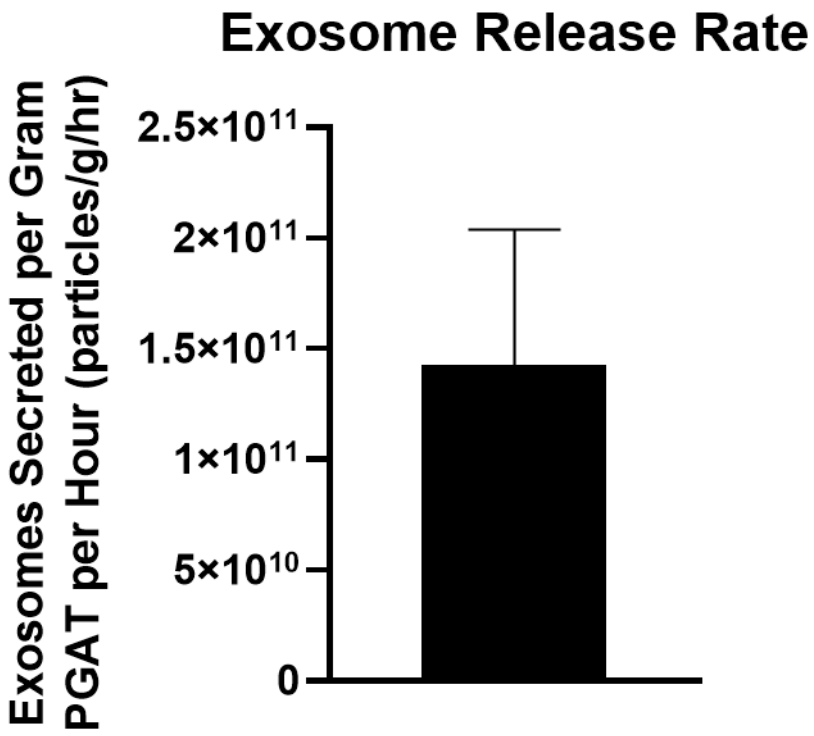


**Figure 2.14. PGAT releases ~1.3x10$^{11}$ AdExos per gram of tissue per hour.** Quantification of exosome released by adipose tissue per gram per hour from adipose tissue from lean mice. n = 8; Error bars represent SD.

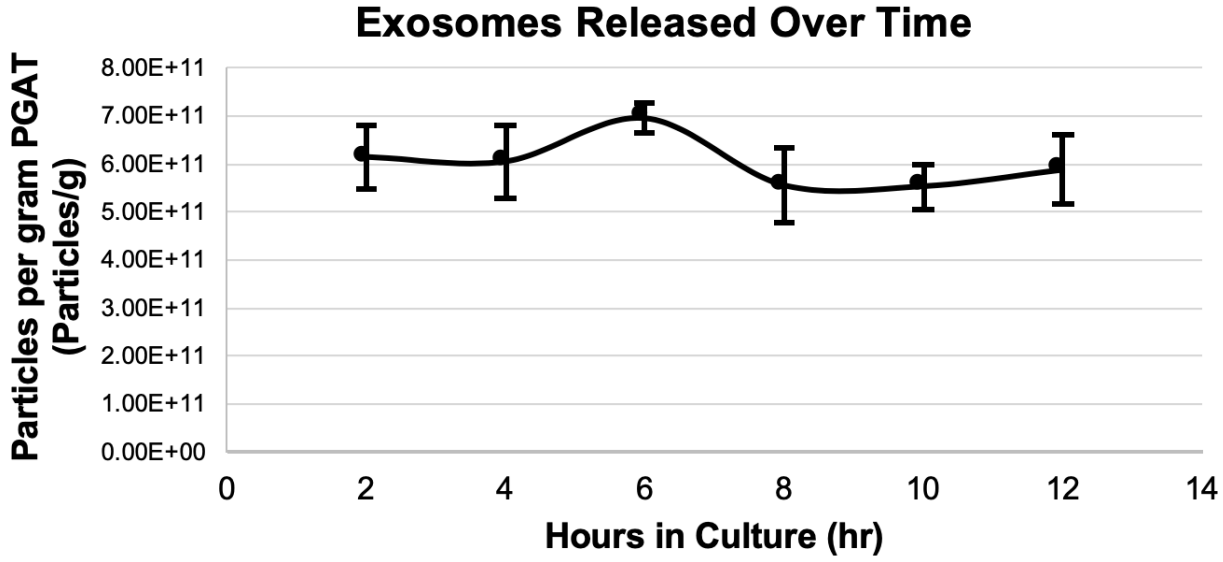


**Figure 2.15. AdExo release rate is stable over a 12-hour period.** Exosome release from obese PGAT expressed per gram of tissue, as measured by Nanoparticle Tracking Analysis. Conditioned medium was taken and exosome content measured every 2 hours over a 12-hour time period (n = 4).

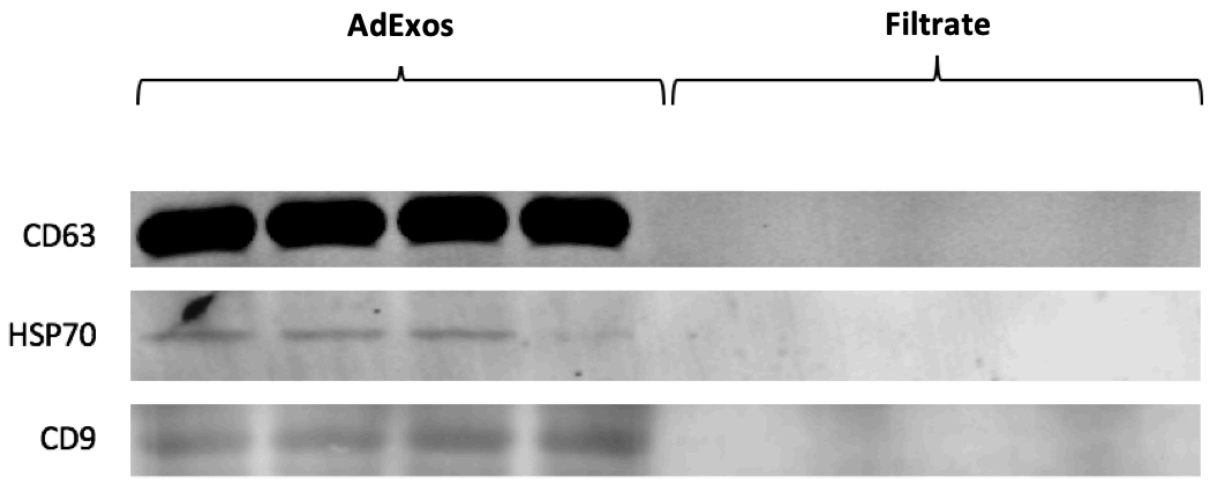


**Figure 2.16. AdExos contain canonical exosome proteins.** Western blots of exosomal protein isolated from adipose tissue-conditioned media (AdExos) and conditioned media content smaller than 100 kD (filtrate). Blots were probed using antibodies against CD63, HSP70, and CD9.

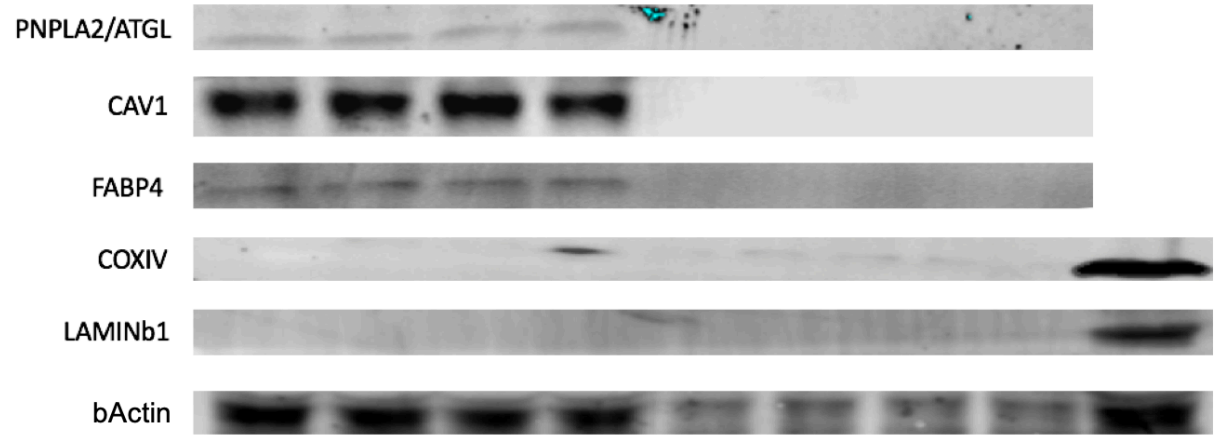


**Figure 2.17. AdExos contain adipocyte proteins.** Western blots of exosomal protein isolated from adipose tissue–conditioned media (AdExos), conditioned media content smaller than 100 kD (Filtrate), and whole PGAT. Blots were probed using antibodies against ATGL, CAV1, FABP4, COX4, LMNB1, and bACTIN.

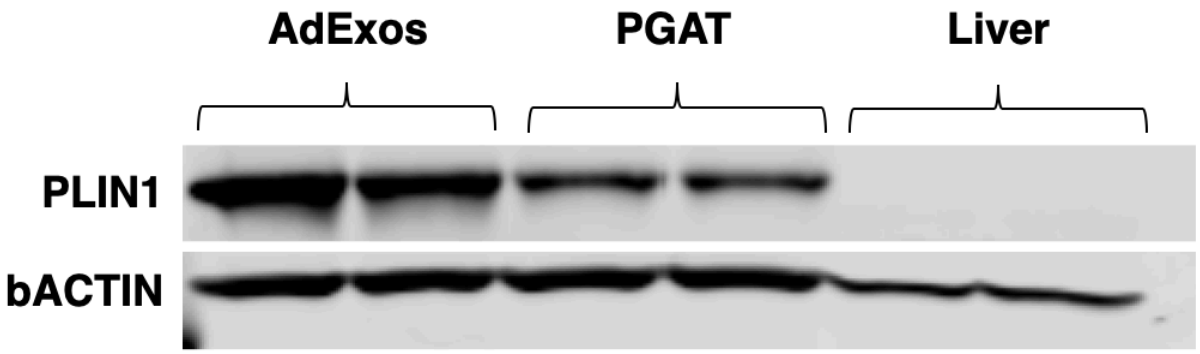


**Figure 2.18. AdExos contain adipocyte lipid droplet-associated protein PLIN1.** Western blots of exosomal protein isolated from adipose tissue conditioned media (AdExos), whole perigonadal adipose tissue (PGAT), and whole liver lysate (Liver). Blots were probed using antibodies against PLIN1 and bActin.

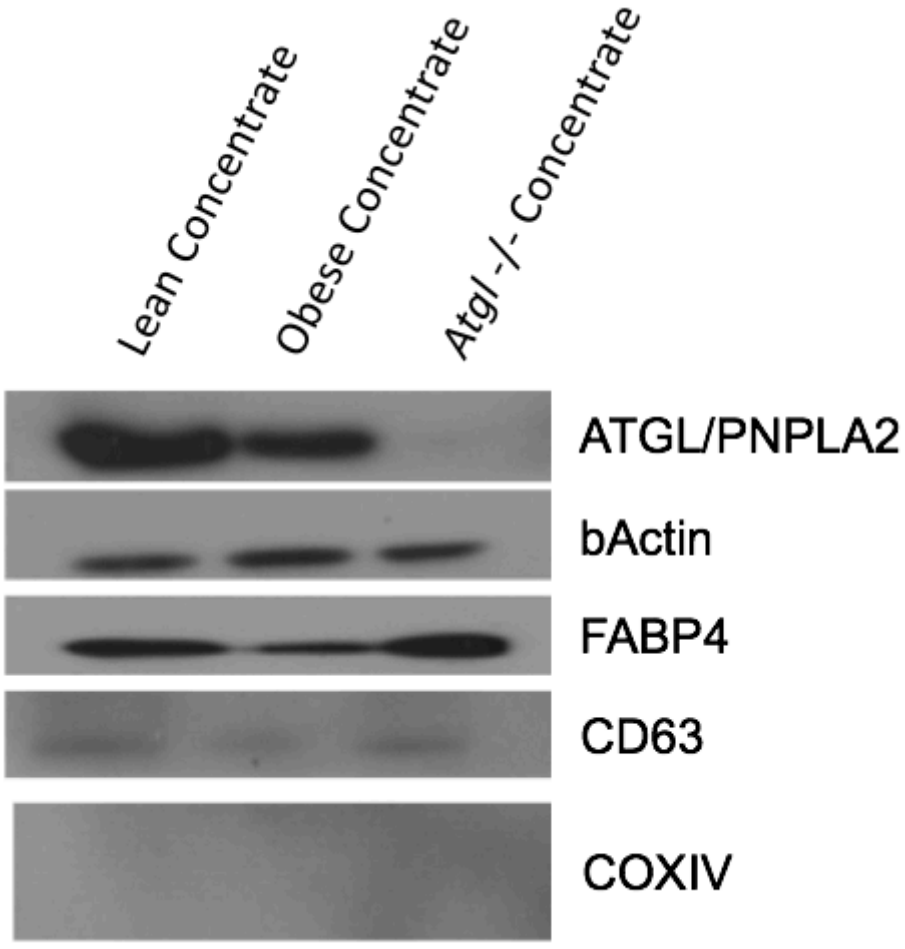


**Figure 2.19. AdExos from adipocyte-specific ATGL deficient animals do not contain ATGL.** Western blots of AdExo protein isolated from lean, obese (*Lep*$^{ob/ob}$), and adipocyte-specific ATGL-deficient mice. Blots were probed using antibodies against ATGL/PNPLA2, bActin, FABP4, CD63, and COXIV.

The electron micrographs of adipose tissue (Figure 2.8) and presence of lipid droplet-associated proteins suggest that the AdExos have an unusual structure and may maintain an intact lipid droplet membrane surrounded by a plasma/endosomal membrane derived bilayer. If so, the topology would predict that CD63 would be found on the exterior surface of the AdExo bilayer while lipid droplet-associated proteins would be contained within the AdExos and not exposed to the exterior (Figure 2.20). To determine whether these proteins were localized as expected, purified AdExos were exposed to a very low concentration of proteinase K, an enzyme that hydrolyses amid peptide bonds, but cannot cross lipid bilayers. When AdExos are exposed to proteinase K, western blot with antibodies against ATGL/PNPLA2 and the extracellular domain of CD63 revealed that CD63 is rapidly degraded while the ATGL/PNPLA2 is stable (Figure 2.21). However, if the AdExos are first exposed to a non-ionic detergent (Triton X-100), which disrupts membrane structures before proteinase treatment, both ATGL/PNPLA2 and CD63 are degraded (Figure 2.21). These experiments confirm that CD63 localizes to the exterior plasma membrane of the exosome, while ATGL/PNPLA2 is contained on the interior of the AdExo.

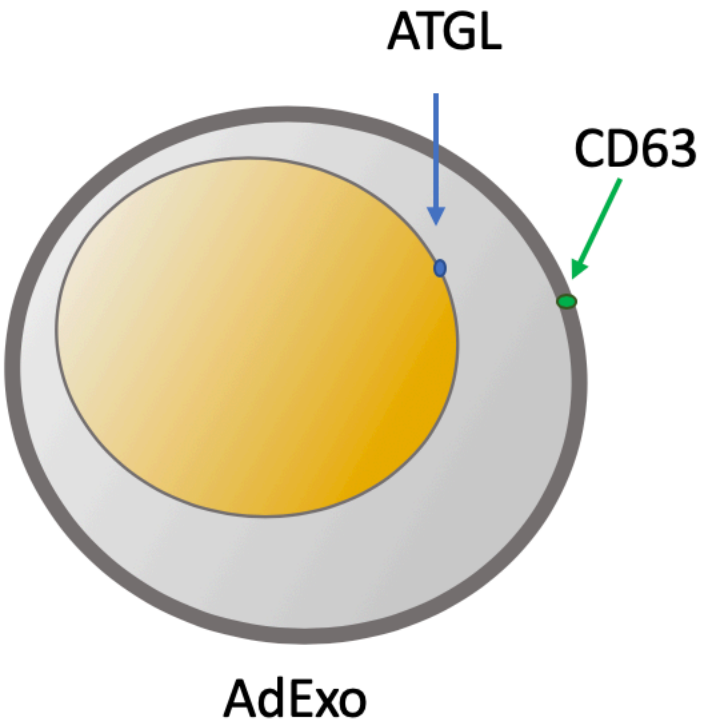


**Figure 2.20. Hypothesized localization of AdExo proteins.**

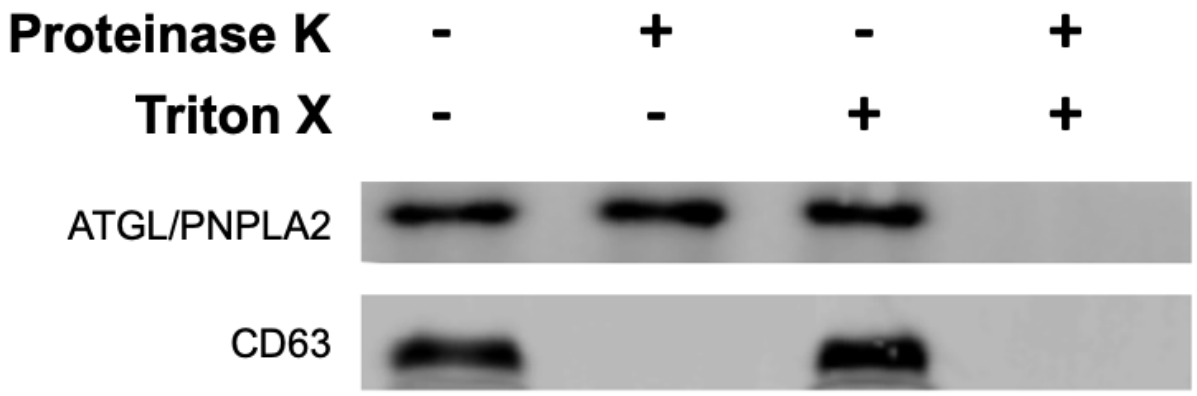


**Figure 2.21. AdExo ATGL is protected from Proteinase K degradation.** Western blots of protein extracted from purified exosomes that were untreated, treated with 100 mg/ml proteinase K, treated with 0.5% Triton X-100, or both. Blots were probed with antibodies against CD63 and ATGL.

AdExos were released in high rate and contained exosomal and adipocyte lipid droplet proteins. We next tested whether they contained lipid and were possibly the vehicle for lipid transfer to BMDMs. Using enzymatic assay on PGAT conditioned medium and AdExo fractions purified from that conditioned medium, we found that AdExos contain very little FFA as compared to the total FFA released from the tissue (Figure 2.22). However, AdExos contain high concentrations of acylglyceride and a high fraction of the total amount of acylglyceride released from the tissue (Figure 2.23). Lean PGAT releases nearly one µmol of acylglyceride per gram of tissue in AdExos every hour. This is 0.04% of the total acylglyceride content of the tissue being released in exosomes every hour (Figure 2.24). Although these rates are dwarfed by the release of lipid during maximally activated lipolysis, a steady release rate implies the complete turnover of lipid within adipocytes by exosomes, every 104 days in lean animals(*44-47*). As discussed previously, treating PGAT explants with inhibitors of lipolysis is able to acutely reduce FFA release from the tissue (Figure 2.6). This treatment, however, has no effect on exosome release rate and the lipid content of the AdExos (Figure 2.25, Figure 2.26).

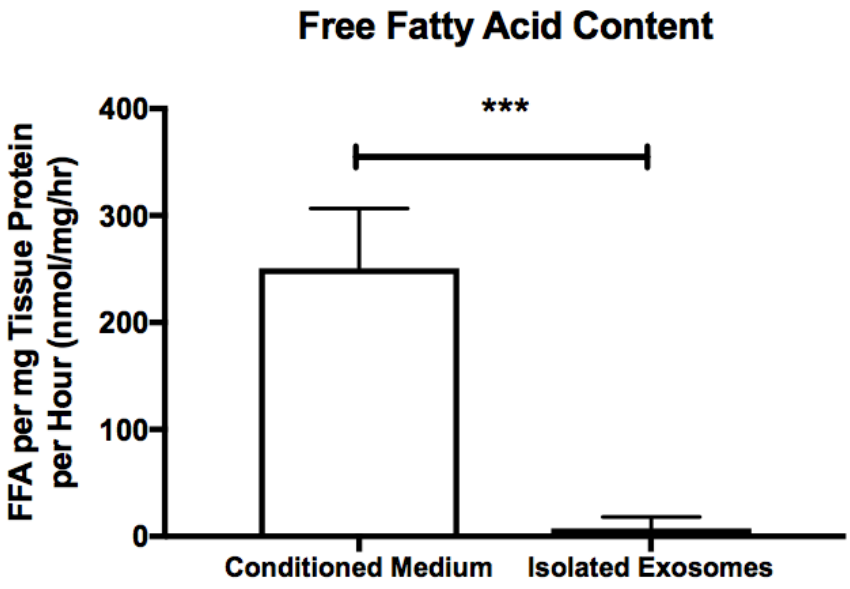


**Figure 2.22. AdExos contain little free fatty acid.** Free fatty acid content of PGAT conditioned medium and exosomes isolated from that medium after a 16-hour culture, expressed per mg of tissue per hour Unpaired two-tailed t test; n = 4; ***P < 0.001. Error bars represent SD.

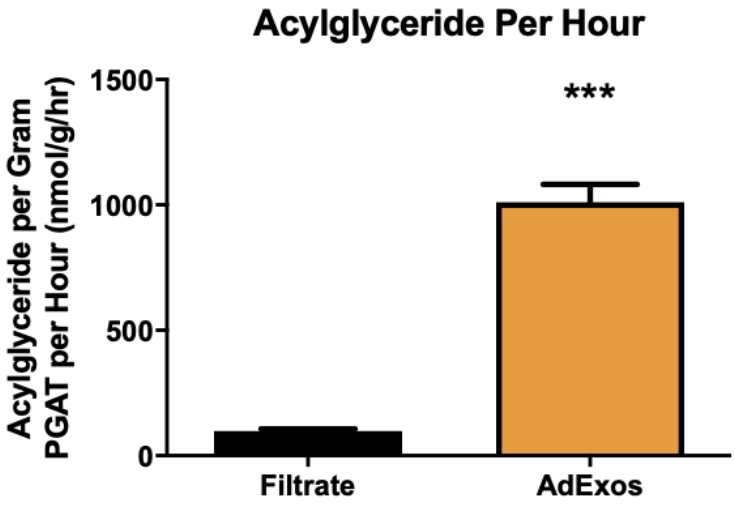


**Figure 2.23. AdExos contain high levels of acylglyceride.** Acylglyceride content of PGAT conditioned medium depleted of AdExos and exosomes isolated from that medium after a 16-hour culture, expressed per mg of tissue per hour. Unpaired two-tailed t test; n = 8; ***P < 0.001. Error bars represent SD.

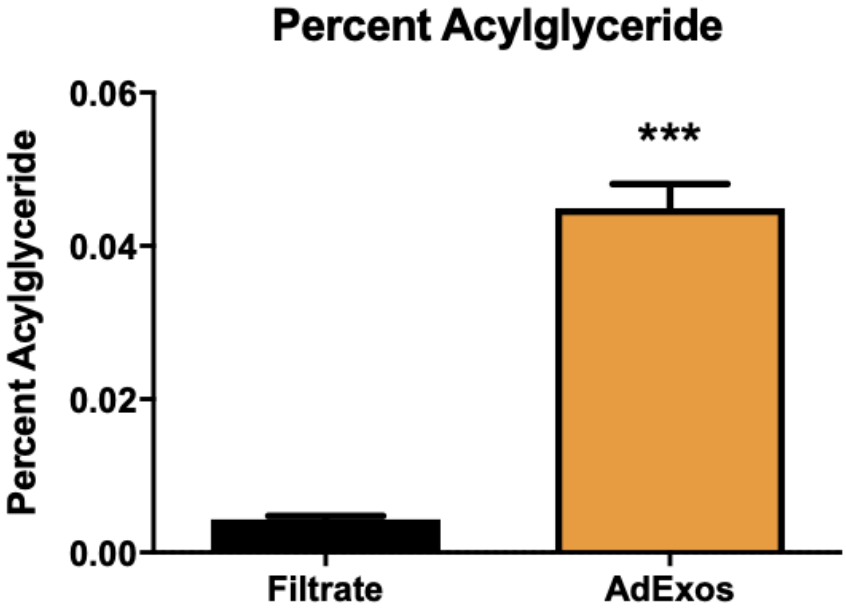


**Figure 2.24. AdExo acylglyceride content by percent.** Acylglyceride content of conditioned medium depleted of AdExos and purified adipocyte-derived exosomes, expressed as a percentage of the acylglyceride content of the tissue itself. Unpaired two-tailed t test; n = 8; ***P < 0.001. Error bars represent SD.

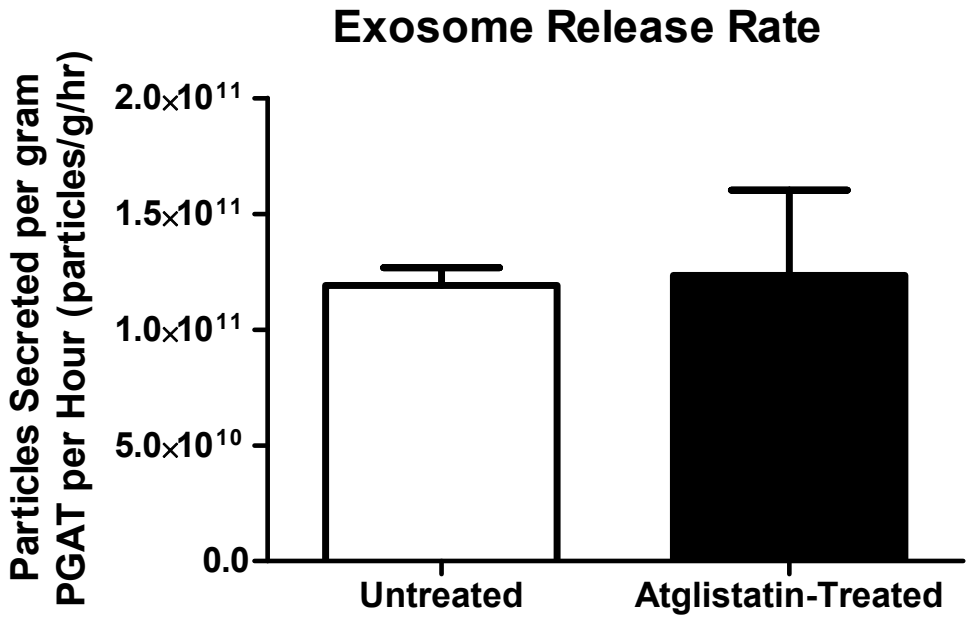


**Figure 2.25. Atglistatin treatment does not affect AdExo release rate.** Quantification of total particle count via NTA released by PGAT, treated with or without Atglistatin for 16 hours per gram per hour (n = 6).

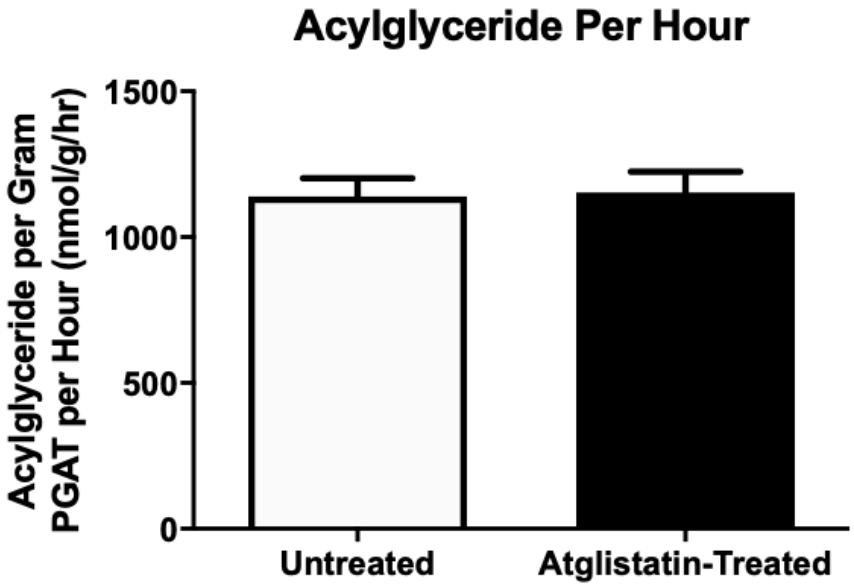


**Figure 2.26. Atglistatin treatment does not affect the amount of acylglyceride released within AdExos.** The rate of release of acylglyceride associated with AdExos isolated from adipose tissue conditioned medium after 16 hours of culture with or without Atglistatin (n = 9).

To further characterize the lipid content of these vesicles, we performed targeted lipidomics via mass spectroscopy on purified AdExos. Given the AdExos' size and that they likely contain both a phospholipid bilayer and a phospholipid monolayer, we expected that on a molar ratio, membrane-associated lipids would be the dominant lipid species. Indeed, this turned out to be the case, with phospholipids and free cholesterol making up the majority of the lipid contained within the vesicles (Figure 2.27). The exosomes also contained stoichiometrically large amounts of acylglyceride, that were roughly evenly distributed between triacylglycerides (TAGs) and monoacylglycerides (MAGs) (Figure 2.27). On the basis of physical chemical properties and the concentration of TAGs and MAGs, we would predict a volume of $2.6 \times 10^{-21}$ $m^3$ of acylglyceride per exosome. This is roughly consistent with the predicted internal volume of AdExos (derived from the measured exosome diameter) of between $1.5 \times 10^{-21}$ $m^3$ and $7.2 \times 10^{-21}$ $m^3$.

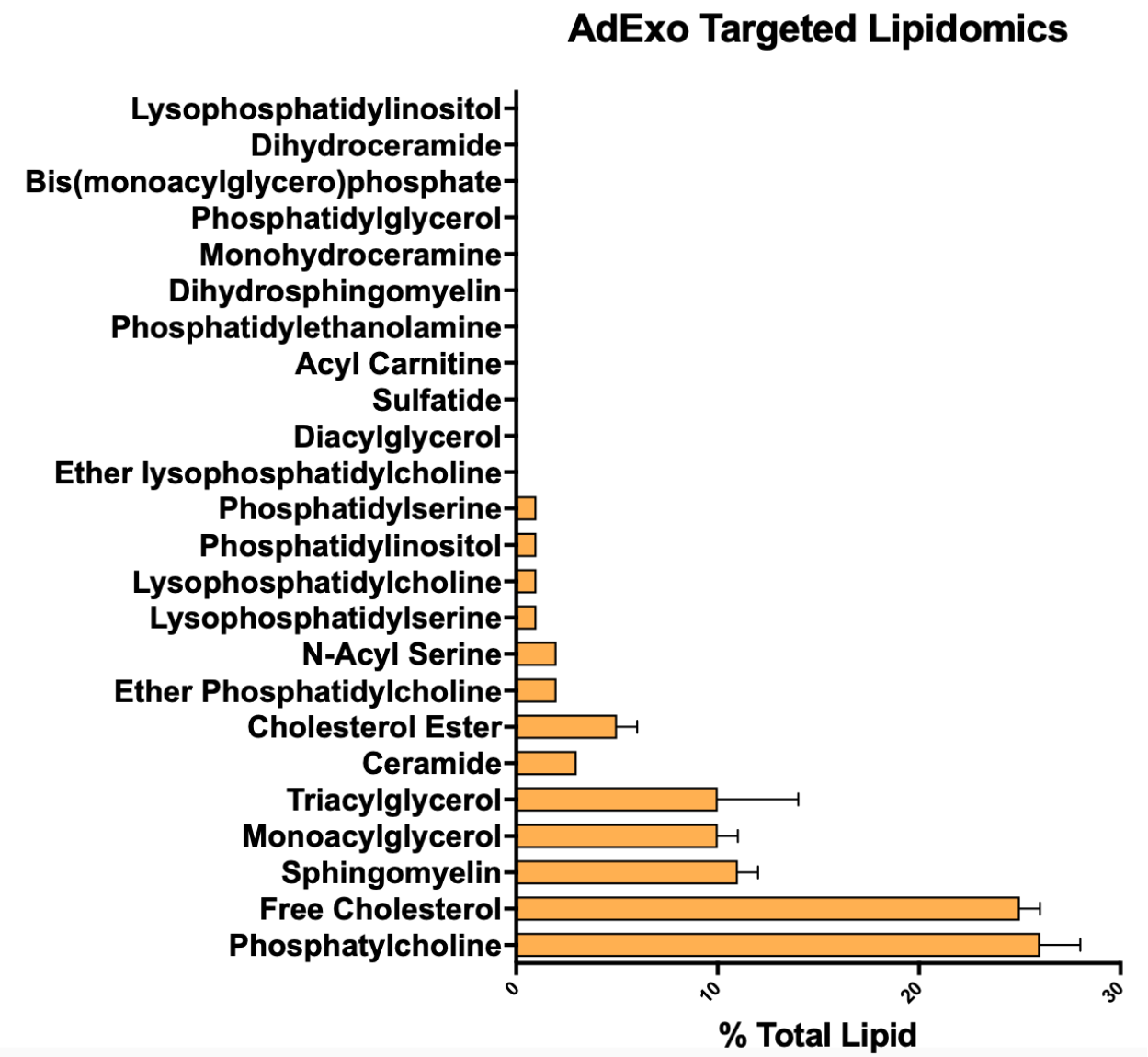


**Figure 2.27. AdExo targeted lipidomics.** Targeted lipidomics of adipocyte-derived exosomes isolated from lean mouse PGAT; n = 3.

Based on these data, a model of AdExo structure emerged in which they range in diameter from 50nm – 200nm. These data are also consistent with AdExos being surrounded by a phospholipid bilayer membrane derived from the invagination of the adipocyte plasma membrane. This membrane contains adipocyte membrane proteins, such as CAV1, and exosome-associated proteins, such as CD63. Within the AdExos we predicted there would be what is the equivalent of a miniature adipocyte lipid droplet. This structure has a core of neutral lipid, made up of TAGs and MAGs, and a significant amount of cholesteryl esters. The neutral acylglyceride core is surrounded by a phospholipid monolayer, rich in phosphatidylcholines and free cholesterol. Associated with this monolayer are adipocyte lipid droplet membrane-associated proteins, including ATGL/PNPLA2 and PLIN1 (Figure 2.28).

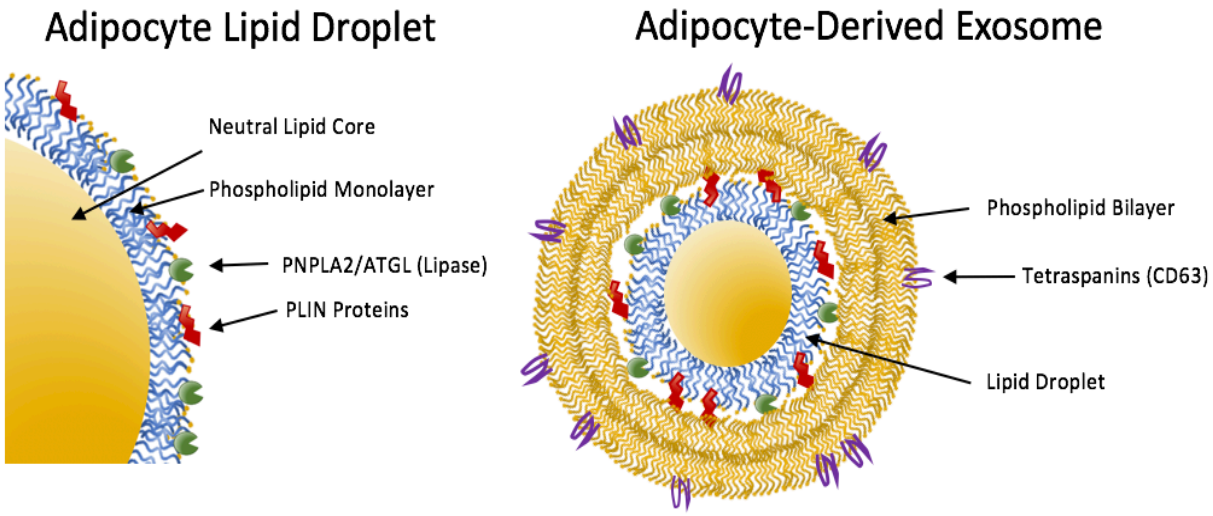


**Figure 2.28. Graphical representation of adipocyte lipid droplet structure (left) and hypothesized structure of adipocyte-derived exosome (right).**

## 2.2 References


1. P. E. Scherer, Adipose tissue: from lipid storage compartment to endocrine organ. *Diabetes* **55**, 1537-1545 (2006).
2. R. Zechner, F. Madeo, D. Kratky, Cytosolic lipolysis and lipophagy: two sides of the same coin. *Nat Rev Mol Cell Biol* **18**, 671-684 (2017).
3. R. Zechner, J. G. Strauss, G. Haemmerle, A. Lass, R. Zimmermann, Lipolysis: pathway under construction. *Curr Opin Lipidol* **16**, 333-340 (2005).
4. R. Zechner, P. C. Kienesberger, G. Haemmerle, R. Zimmermann, A. Lass, Adipose triglyceride lipase and the lipolytic catabolism of cellular fat stores. *J Lipid Res* **50**, 3-21 (2009).
5. K. N. Frayn, F. Karpe, B. A. Fielding, I. A. Macdonald, S. W. Coppack, Integrative physiology of human adipose tissue. *Int J Obes Relat Metab Disord* **27**, 875-888 (2003).
6. A. W. Ferrante, Jr., Macrophages, fat, and the emergence of immunometabolism. *J Clin Invest* **123**, 4992-4993 (2013).
7. A. W. Ferrante, Jr., The immune cells in adipose tissue. *Diabetes Obes Metab* **15 Suppl 3**, 34-38 (2013).
8. C. N. Lumeng, S. M. Deyoung, J. L. Bodzin, A. R. Saltiel, Increased inflammatory properties of adipose tissue macrophages recruited during diet-induced obesity. *Diabetes* **56**, 16-23 (2007).
9. L. Russo, C. N. Lumeng, Properties and functions of adipose tissue macrophages in obesity. *Immunology* **155**, 407-417 (2018).
10. P. Morigny, M. Houssier, E. Mouisel, D. Langin, Adipocyte lipolysis and insulin resistance. *Biochimie* **125**, 259-266 (2016).
11. K. Verboven *et al.*, Abdominal subcutaneous and visceral adipocyte size, lipolysis and inflammation relate to insulin resistance in male obese humans. *Sci Rep* **8**, 4677 (2018).
12. S. Martin, R. G. Parton, Lipid droplets: a unified view of a dynamic organelle. *Nat Rev Mol Cell Biol* **7**, 373-378 (2006).
13. T. C. Walther, R. V. Farese, Jr., Lipid droplets and cellular lipid metabolism. *Annu Rev Biochem* **81**, 687-714 (2012).
14. S. Xu, X. Zhang, P. Liu, Lipid droplet proteins and metabolic diseases. *Biochim Biophys Acta Mol Basis Dis* **1864**, 1968-1983 (2018).
15. L. Yang *et al.*, The proteomics of lipid droplets: structure, dynamics, and functions of the organelle conserved from bacteria to humans. *J Lipid Res* **53**, 1245-1253 (2012).
16. K. Kounakis, M. Chaniotakis, M. Markaki, N. Tavernarakis, Emerging Roles of Lipophagy in Health and Disease. *Front Cell Dev Biol* **7**, 185 (2019).
17. R. J. Schulze, A. Sathyanarayan, D. G. Mashek, Breaking fat: The regulation and mechanisms of lipophagy. *Biochim Biophys Acta Mol Cell Biol Lipids* **1862**, 1178-1187 (2017).
18. A. Grijalva, X. Xu, A. W. Ferrante, Jr., Autophagy Is Dispensable for Macrophage-Mediated Lipid Homeostasis in Adipose Tissue. *Diabetes* **65**, 967-980 (2016).
19. P. E. Bickel, J. T. Tansey, M. A. Welte, PAT proteins, an ancient family of lipid droplet proteins that regulate cellular lipid stores. *Biochim Biophys Acta* **1791**, 419-440 (2009).
20. H. Itabe, T. Yamaguchi, S. Nimura, N. Sasabe, Perilipins: a diversity of intracellular lipid droplet proteins. *Lipids Health Dis* **16**, 83 (2017).
21. A. R. Kimmel, C. Sztalryd, The Perilipins: Major Cytosolic Lipid Droplet-Associated Proteins and Their Roles in Cellular Lipid Storage, Mobilization, and Systemic Homeostasis. *Annu Rev Nutr* **36**, 471-509 (2016).
22. J. Persson, E. Degerman, J. Nilsson, M. W. Lindholm, Perilipin and adipophilin expression in lipid loaded macrophages. *Biochem Biophys Res Commun* **363**, 1020-1026 (2007).
23. X. Xu *et al.*, Obesity activates a program of lysosomal-dependent lipid metabolism in adipose tissue macrophages independently of classic activation. *Cell Metab* **18**, 816-830 (2013).
24. G. Schoiswohl *et al.*, Impact of Reduced ATGL-Mediated Adipocyte Lipolysis on Obesity-Associated Insulin Resistance and Inflammation in Male Mice. *Endocrinology* **156**, 3610-3624 (2015).
25. M. Gireud-Goss *et al.*, Distinct mechanisms enable inward or outward budding from late endosomes/multivesicular bodies. *Exp Cell Res* **372**, 1-15 (2018).
26. H. Shapiro *et al.*, Adipose tissue foam cells are present in human obesity. *J Clin Endocrinol Metab* **98**, 1173-1181 (2013).

27. P. D. Stahl, M. A. Barbieri, Multivesicular bodies and multivesicular endosomes: the "ins and outs" of endosomal traffic. *Sci STKE* **2002**, pe32 (2002).
28. K. Denzer, M. J. Kleijmeer, H. F. Heijnen, W. Stoorvogel, H. J. Geuze, Exosome: from internal vesicle of the multivesicular body to intercellular signaling device. *J Cell Sci* **113 Pt 19**, 3365-3374 (2000).
29. N. P. Hessvik, A. Llorente, Current knowledge on exosome biogenesis and release. *Cell Mol Life Sci* **75**, 193-208 (2018).
30. M. E. Kranendonk *et al.*, Extracellular vesicle markers in relation to obesity and metabolic complications in patients with manifest cardiovascular disease. *Cardiovasc Diabetol* **13**, 37 (2014).
31. D. M. Pegtel, S. J. Gould, Exosomes. *Annu Rev Biochem* **88**, 487-514 (2019).
32. G. Raposo, W. Stoorvogel, Extracellular vesicles: exosomes, microvesicles, and friends. *J Cell Biol* **200**, 373-383 (2013).
33. B. Wang, D. Xing, Y. Zhu, S. Dong, B. Zhao, The State of Exosomes Research: A Global Visualized Analysis. *Biomed Res Int* **2019**, 1495130 (2019).
34. M. Frydrychowicz, A. Kolecka-Bednarczyk, M. Madejczyk, S. Yasar, G. Dworacki, Exosomes - structure, biogenesis and biological role in non-small-cell lung cancer. *Scand J Immunol* **81**, 2-10 (2015).
35. H. Valadi *et al.*, Exosome-mediated transfer of mRNAs and microRNAs is a novel mechanism of genetic exchange between cells. *Nat Cell Biol* **9**, 654-659 (2007).
36. Y. Zhang, M. Yu, W. Tian, Physiological and pathological impact of exosomes of adipose tissue. *Cell Prolif* **49**, 3-13 (2016).
37. J. Kowal *et al.*, Proteomic comparison defines novel markers to characterize heterogeneous populations of extracellular vesicle subtypes. *Proc Natl Acad Sci U S A* **113**, E968-977 (2016).
38. T. Skotland, N. P. Hessvik, K. Sandvig, A. Llorente, Exosomal lipid composition and the role of ether lipids and phosphoinositides in exosome biology. *J Lipid Res* **60**, 9-18 (2019).
39. W. D. Gray, A. J. Mitchell, C. D. Searles, An accurate, precise method for general labeling of extracellular vesicles. *MethodsX* **2**, 360-367 (2015).
40. P. Puzar Dominkus *et al.*, PKH26 labeling of extracellular vesicles: Characterization and cellular internalization of contaminating PKH26 nanoparticles. *Biochim Biophys Acta Biomembr* **1860**, 1350-1361 (2018).
41. A. Riches, E. Campbell, E. Borger, S. Powis, Regulation of exosome release from mammary epithelial and breast cancer cells - a new regulatory pathway. *Eur J Cancer* **50**, 1025-1034 (2014).
42. F. J. Verweij *et al.*, Quantifying exosome secretion from single cells reveals a modulatory role for GPCR signaling. *J Cell Biol* **217**, 1129-1142 (2018).
43. D. van de Vlekkert *et al.*, Excessive exosome release is the pathogenic pathway linking a lysosomal deficiency to generalized fibrosis. *Sci Adv* **5**, eaav3270 (2019).
44. P. Arner, Human fat cell lipolysis: biochemistry, regulation and clinical role. *Best Pract Res Clin Endocrinol Metab* **19**, 471-482 (2005).
45. J. Laurencikiene *et al.*, Regulation of lipolysis in small and large fat cells of the same subject. *J Clin Endocrinol Metab* **96**, E2045-2049 (2011).
46. C. E. Dugan, R. T. Kennedy, Measurement of lipolysis products secreted by 3T3-L1 adipocytes using microfluidics. *Methods Enzymol* **538**, 195-209 (2014).
47. M. Schweiger *et al.*, Measurement of lipolysis. *Methods Enzymol* **538**, 171-193 (2014).
48. M. Komatsu *et al.*, Impairment of starvation-induced and constitutive autophagy in Atg7-deficient mice. *The Journal of cell biology* **169**, 425-434 (2005).

# CHAPTER 3:INVESTIGATING THE EFFECTS OF ADIPOSE TISSUE-DERIVED EXOSOMES ON THE LOCAL IMMUNE POPULATION

## 3.1 Results

Macrophages are key mediators of the innate immune response. Myeloid in origin, they act as sentinels recognizing damage to tissue and foreign pathogens via pattern recognition receptors. In response, they expand their numbers, orchestrate the response of other immune cells and clear debris and pathogens via phagocytosis. They expand their numbers locally either by expansion of tissue resident cells or by differentiation of recruited monocytes into macrophages (*1, 2*). In a pathogen or injury-specific manner, macrophages elaborate cytokines, chemokines, and bioactive lipids to recruit and activate other immune cells. A successful immune response typically requires the coordinated action of multiple immune cells, that in a classic bacterial infection includes the initial recruitment of neutrophils, followed by a wave of macrophages and dendritic cells, that then can present antigen to T-cells. Throughout the immune response, macrophages clear debris, apoptotic or damaged cells and pathogens through phagocytosis (*4-6*). Macrophages are fit with the tools of professional phagocytes, capable of invaginating their cell membranes to envelop and degrade large amounts of material via phagocytosis (*7-9*).

In the absence of infection or tissue damage, most organs contain a population of resident macrophages that exist in a non-inflammatory state (*10*). For many of these tissue resident macrophages investigators have identified tissue-specific adaptive functions (*11*). For example, the microglia are the tissue resident macrophage of the brain and these cells are capable of performing synaptic stripping (*12-15*), and the osteoclasts, multinucleated macrophages of the bone, are specialized in mineralized bone resorption (*16, 17*). Both these processes are required to maintain healthy tissue.

Adipose tissue has its own tissue resident macrophage population, dubbed adipose tissue macrophages (ATMs). ATMs contain varying amounts of neutral lipid but can be so lipid-laden that they float in aqueous buffers and resist sedimentation when centrifuged. They also possess distinct transcriptional profiles and proteins that distinguish them from other tissue resident macrophage

populations (*18-22*). The efforts that led to the identification of AdExos described in the previous chapter were originally focused on the lipid handling by ATMs. We discovered that they accounted for the majority of TAG in the conditioned medium from adipose tissue and are therefore, a potential source of lipid found in ATMs. In this chapter we sought to determine whether macrophages do take up AdExos and whether they alter the lipid content and profile of cells that do.

**AdExos are taken up by ATMs**

As discussed in the previous chapter AdExos are surrounded by a phospholipid bilayer that is derived from the adipocyte plasma membrane. Because of this membrane, dyes such as PKH26 and PKH67 which intercalate into phospholipid bilayers can be used to label AdExos, allowing for tracing studies. To test whether ATMs in vivo take up AdExos, isolated AdExos were labeled with PKH26 and injected into PGAT. Using whole tissue confocal microscopy, we could follow the fate of the AdExos and identify which cells take them up. From whole-mount images it is clear that the PKH26 signal concentrates in cells that are not adipocytes (Supplemental Figure 3.1). If this tissue is counterstained with an antibody against F4/80, a macrophage marker, it becomes clear that the PKH26 exosome uptake signal and the F4/80 signal co-localize, indicating that the exosomes are being taken up by ATMs in the PGAT (Figure 3.1).

To further investigate the target cells within the PGAT, the injected tissue was treated with a collagenase allowing separation of adipocyte and non-adipocyte, stromal vascular cell (SVC) fractions. The cells in each fraction were lysed and measured for PKH26 fluorescence using a fluorescence spectrophotometer. Cells from PGAT which was injected with PBS instead of PKH26-labeled AdExos provided a background fluorescence signal. Consistent with our microscopy, in the PGAT injected with labeled AdExos, adipocytes were not fluorescent above background (Figure 3.2). In fact, almost all of the PKH26 signal in the injected PGAT was in the SVC fraction (Figure 3.2). This indicated that AdExos were being taken up by non-adipocytes in the PGAT. The SVC fraction was further characterized using FACS. SVCs were labeled with fluorescence-conjugated antibodies against CD45 (an immune cell marker),

CD11b (a myeloid cell marker), and F4/80 (a macrophage marker) and then sorted by a flow cytometer. Analysis revealed that >85% of the cells that contained PKH26 fluorescence were CD45+, CD11b+, and F4/80+ (Figure 3.3) consistent with the vast majority of the cells that take up AdExos being ATMs (Figure 3.4).

Exosomes are well known for their signaling capabilities, and these particular AdExos have also been shown to contain large amounts of lipid. To elucidate the effects these vesicles might have on the macrophages that take them up, we moved to an *in vitro* system. Bone marrow-derived macrophages (BMDMs) provide a plentiful source that can be used to investigate the cellular behavior of primary macrophages. Bone marrow cells are taken from young mice and differentiated into mature macrophages, in culture, using colony-stimulating factor 1 (CSF-1) and associated factors. Previous work in our laboratory demonstrated that co-culture of bone marrow cells with adipose tissue (or conditioned medium from adipose tissue) and CSF-1 induces the differentiation of ATM-like cells.

Naïve BMDMs were cultured with PKH-26-labeled AdExos to investigate their effects on macrophage cell biology. Using confocal microscopy, it was clear that the BMDMs were taking up AdExos, as their F4/80+ cell bodies were labeled with PKH-26 (Figure 3.5). AdExo treatment was also sufficient to induce significant lipid accumulation within the BMDMs as evidenced by BODIPY staining within the macrophages (Figure 3.5). Of note, only PKH26+ BMDMs displayed the increased BODIPY staining. These AdExo-treated BMDMs were examined using targeted lipidomics to determine how AdExos altered the lipid make up of macrophages. Mass spectrometry revealed that BMDMs treated with AdExos had the same relative molar amounts of lipid species as untreated BMDMs, except for a large increase in the amount of TAG (Figure 3.6). AdExo-treated BMDMs contained roughly eight-fold more TAG than the untreated control.

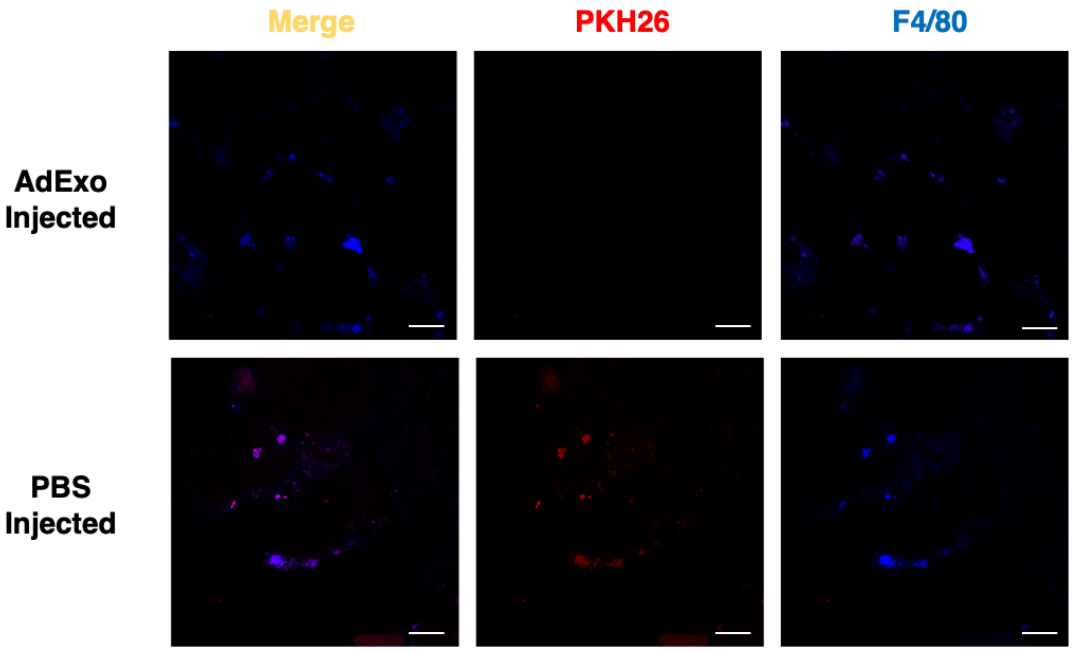


**Figure 3.1. AdExos Taken up by F4/80+ Cells in PGAT.** Confocal microscopy images of whole PGAT mounts. *Lep*$^{ob/ob}$ PGAT was injected with PKH26-labeled AdExos and stained with fluorescently-conjugated antibody against F4/80. Scale bars represent 20μm.

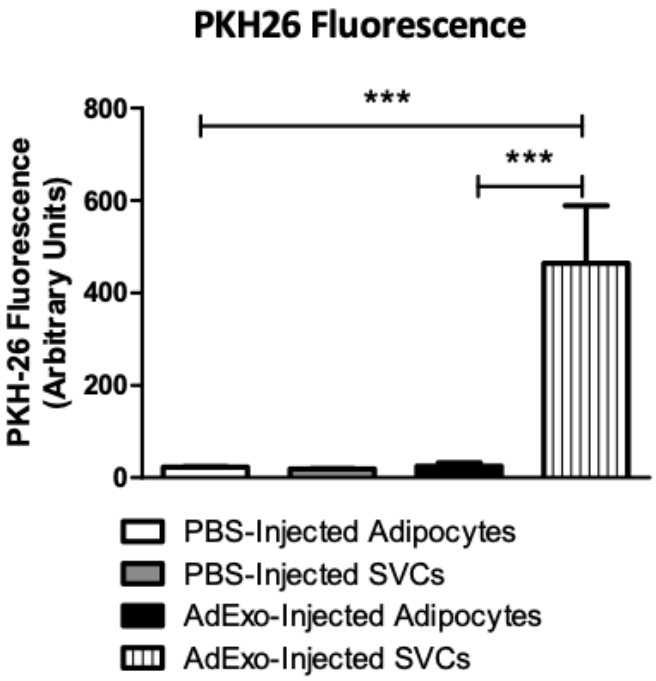


**Figure 3.2. In Adipose Tissue AdExos are Taken Up by Non-adipocytes.** PKH26 Fluorescence of adipocyte and SVC lysates from PGAT injected with phosphate-buffered saline (PBS) (left) or PKH26-labeled AdExos (right). One-way ANOVA; n = 4; ***P < 0.001.

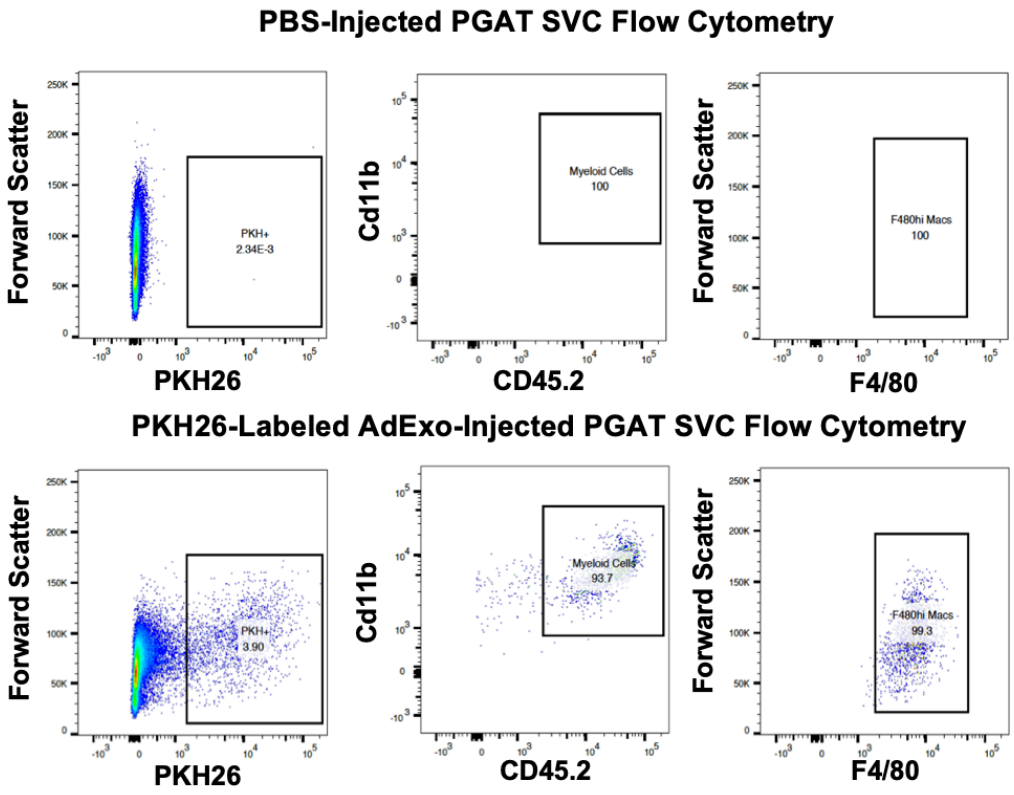


**Figure 3.3. AdExo-Injected SVC FACS.** Representative Flow Cytometry gating of SVCs from PGAT injected with PBS (top) or PKH26-labeled AdExos (bottom).

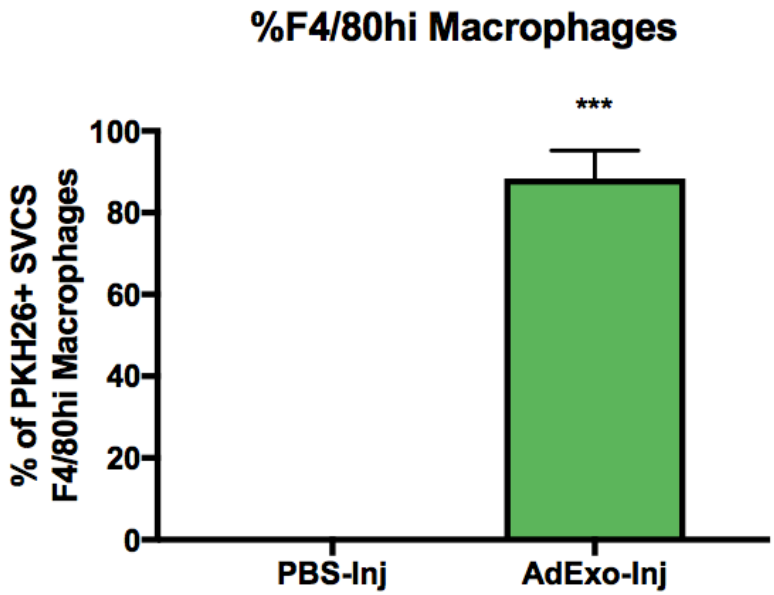


**Figure 3.4. AdExos are Taken up by Macrophages in PGAT.** Percent PKH26+ SVCs that are CD45.2+ CD11b+ F4/80hi macrophages is quantified for PBS-Inj and AdExo-Inj groups (Inj, injected), as determined by flow cytometry. Unpaired two-tailed t test; n = 4; ***P < 0.001.

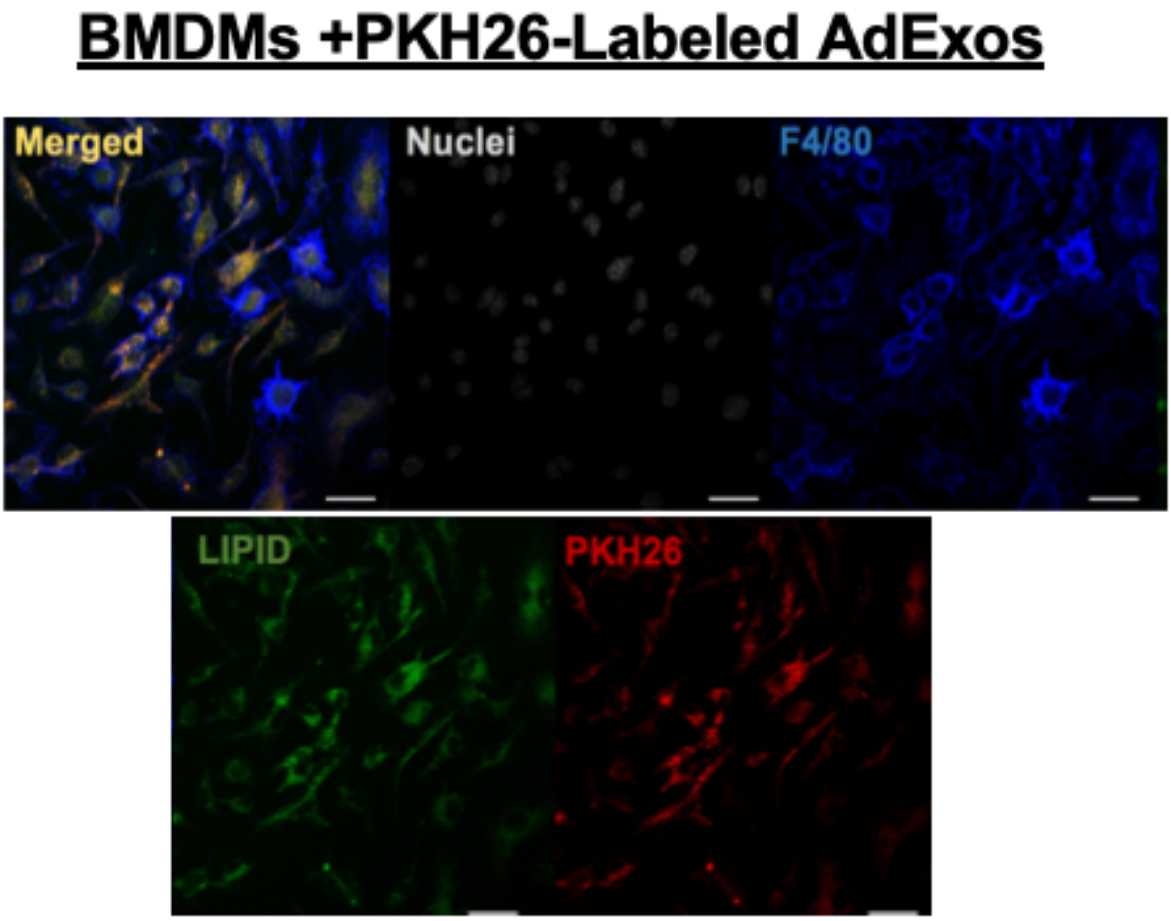


**Figure 3.5. AdExos Induce Neutral Lipid Accumulation in BMDMs.** Confocal microscopy images of in vitro-generated BMDMs cultured with PKH26-labeled AdExos and immunostained with antibodies against F4/80 (blue), as well as DNA fluorescent stain DAPI (white) and neutral lipid fluorescent stain BODIPY (green). Scale bars, 10 mm.

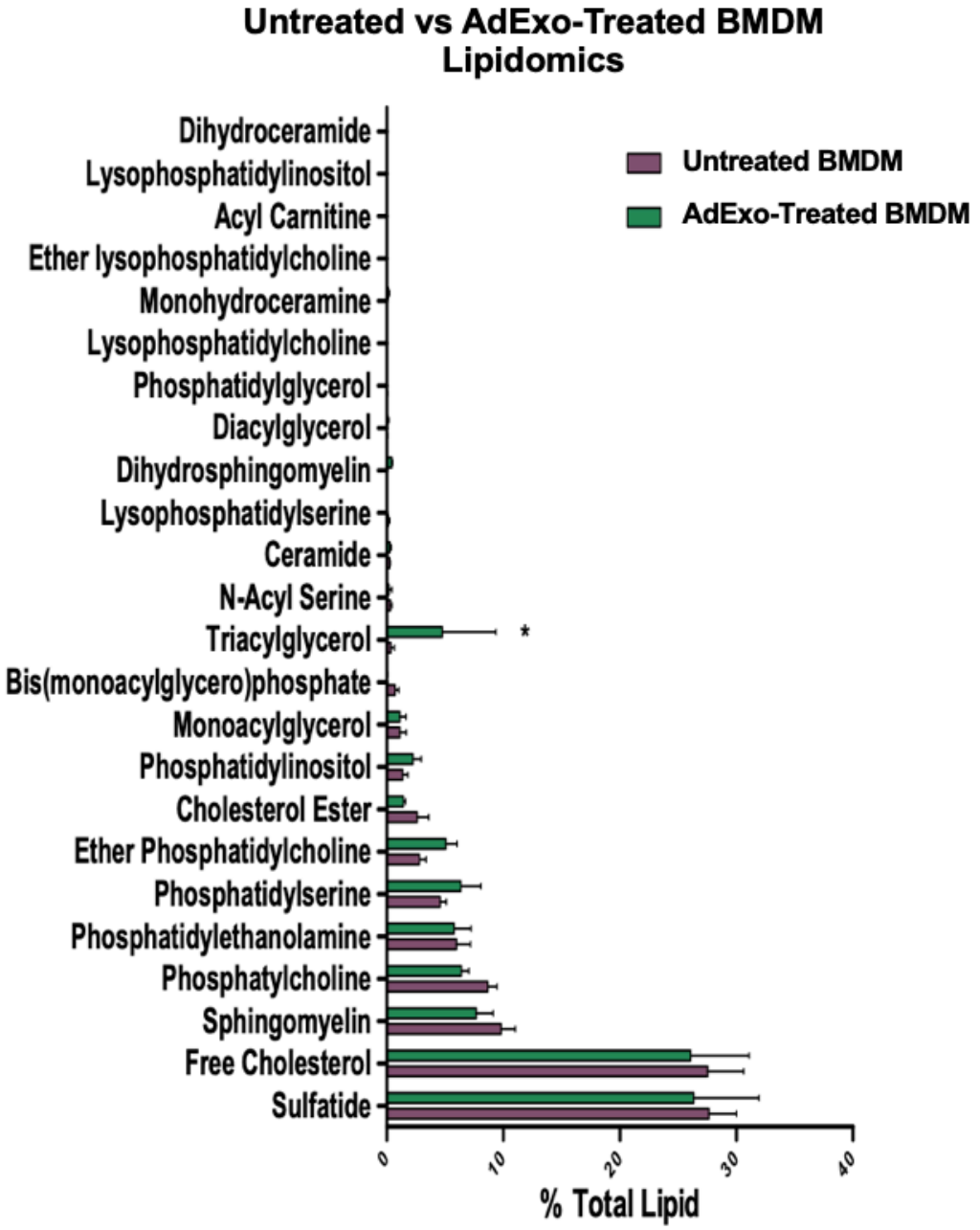


**Figure 3.6. AdExo-Treated BMDM Lipidomics.** Targeted lipidomics of Untreated or AdExo-treated BMDMs. Unpaired two-tailed t test; n = 3; *P < 0.05.

As discussed earlier, the typical pathway of TAG accumulation in cells occurs through the re-esterification of free fatty acids (FFAs) (*23*). FFAs are taken up by cells and attached to glycerol backbones through the action of diglyceride acyltransferases, DGAT1 and DGAT2 (*24, 25*). AdExos contain relatively little FFA (Figure 2.22) but high concentrations of TAG (Figure 2.23). However, to formally confirm that TAG accumulation occurred through uptake of intake AdExo TAG and not through a hydrolysis and re-esterification process or re-esterification of FFAs associated with AdExos, BMDMs were pre-treated with inhibitors of DGAT1 and DGAT2, before being incubated with AdExos. Using confocal microscopy, we saw that F4/80+ BMDMs still accumulated large amounts of neutral lipid (Figure 3.7). This finding was confirmed using enzymatic assays, where DGAT inhibitors had no measurable effect on the acylglyceride content of AdExo-treated BMDMs (Figure 3.8). This is a particularly interesting finding considering that treating BMDMs with FFA is able to induce TAG accumulation in BMDMs (Figure 3.9). Incidentally, direct FFA treatment induced a significant amount of BMDM death, a finding that was not reproduced when treating BMDM with AdExos. Overall, these data indicate that while macrophages are capable of accumulating TAG via esterification of FFAs, TAG accumulation in BMDMs by AdExos occurs independent of DGAT activity.

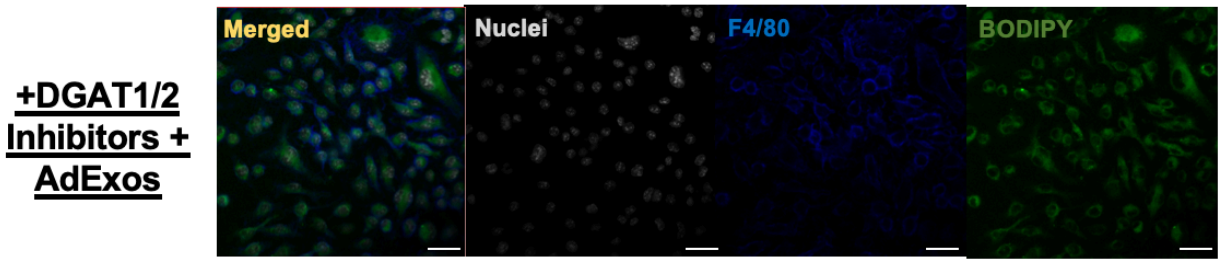


**Figure 3.7. AdExos Lead to Neutral Lipid Accumulation in BMDMs Independent of DGAT Activity.** Confocal microscopy images of in vitro-generated BMDMs pre-treated with inhibitors against DGAT1 and DGAT2 activity, before being cultured with AdExos and immunostained with antibodies against F4/80 (blue), as well as DNA fluorescent stain DAPI (white) and neutral lipid fluorescent stain BODIPY (green). Scale bars, 10 mm.

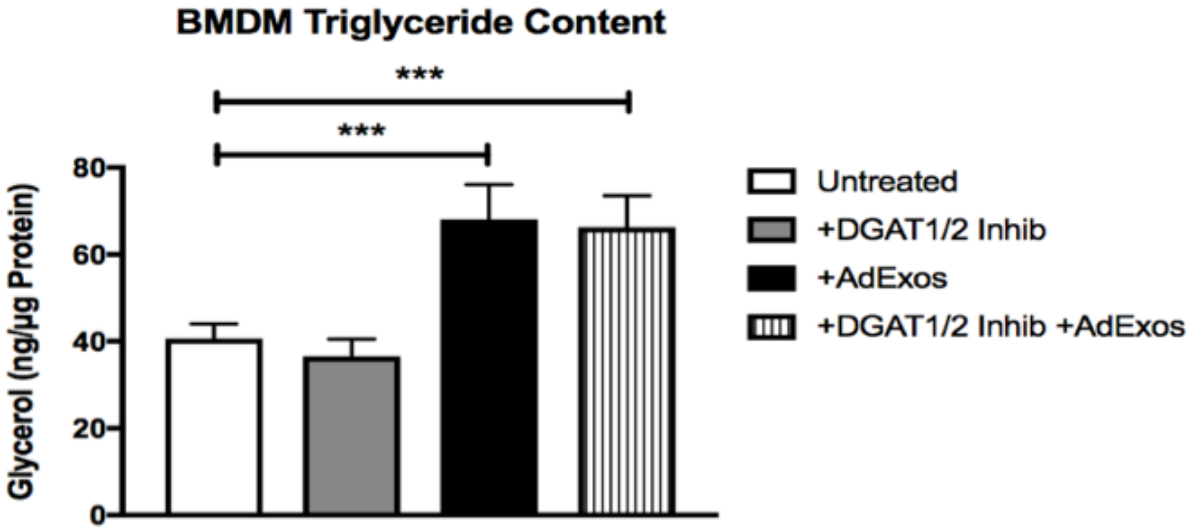


**Figure 3.8. AdExos Transfer Acylglyceride to BMDMs Independently of DGAT Activity.** Triglyceride levels of BMDMs cultured alone, with DGAT1/2 Inhibitors, with AdExos, or with both DGAT1/2 Inhibitors and AdExos for 24 hours, measured enzymatically. One-way ANOVA; n = 6; *** p-value < 0.001.

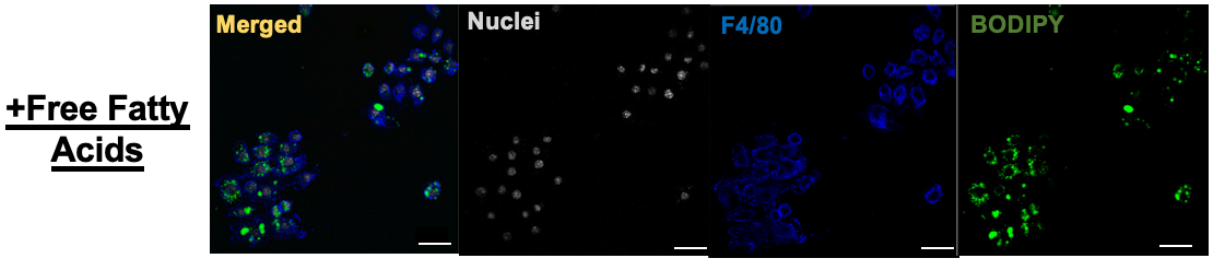


**Figure 3.9. FFA Treatment Induces TAG Accumulation in BMDMs.** Confocal microscopy images of in vitro-generated BMDMs treated with FFA and immunostained with antibodies against F4/80 (blue), as well as DNA fluorescent stain DAPI (white) and neutral lipid fluorescent stain BODIPY (green). Scale bars, 10 mm.

Exosome uptake can occur through several different pathways that include direct fusion with the recipient cell's plasma membrane, receptor-mediated lipid raft endocytosis, or non-receptor-mediated endocytosis mechanisms, including phagocytosis or macropinocytosis (*26*). Macrophages are professional phagocytes characterized by their proclivity to take up pathogens and extracellular material through actin-driven protrusions (*8*). It is therefore possible that AdExos are being taken up via phagocytosis or macropinocytosis, processes that are dependent upon PI3K activity (*9, 27*). To test this hypothesis, BMDMs were pre-treated with a PI3K inhibitor before AdExo treatment. The acylglyceride content of the BMDMs was determined using enzymatic assays. The macropinocytosis inhibitor had no effect on the TAG content of untreated BMDMs. However, AdExo-treated BMDMs had significantly reduced TAG content when the cells were pre-treated with the inhibitor (Figure 3.10). These data indicate that the ability for macrophages to macropinocytose is necessary to induce the lipid accumulation that occurs upon AdExo treatment.

Some interesting observations were made in AdExo-treated BMDMs when investigating the lipid accumulation. The first is that BMDMs that were treated with AdExos often contained more than one nucleus, as determined by DAPI staining and confocal microscopy (Figure 3.11). This phenomenon of multinucleation is commonly seen in primary ATMs. Additionally, AdExos appeared to be sufficient to induce increased lysosomal content in BMDMs, as evidenced by increased acidic compartment content of BMDMs (Figure 3.12) and by increased levels of lysosome-associated protein (Figure 3.13).

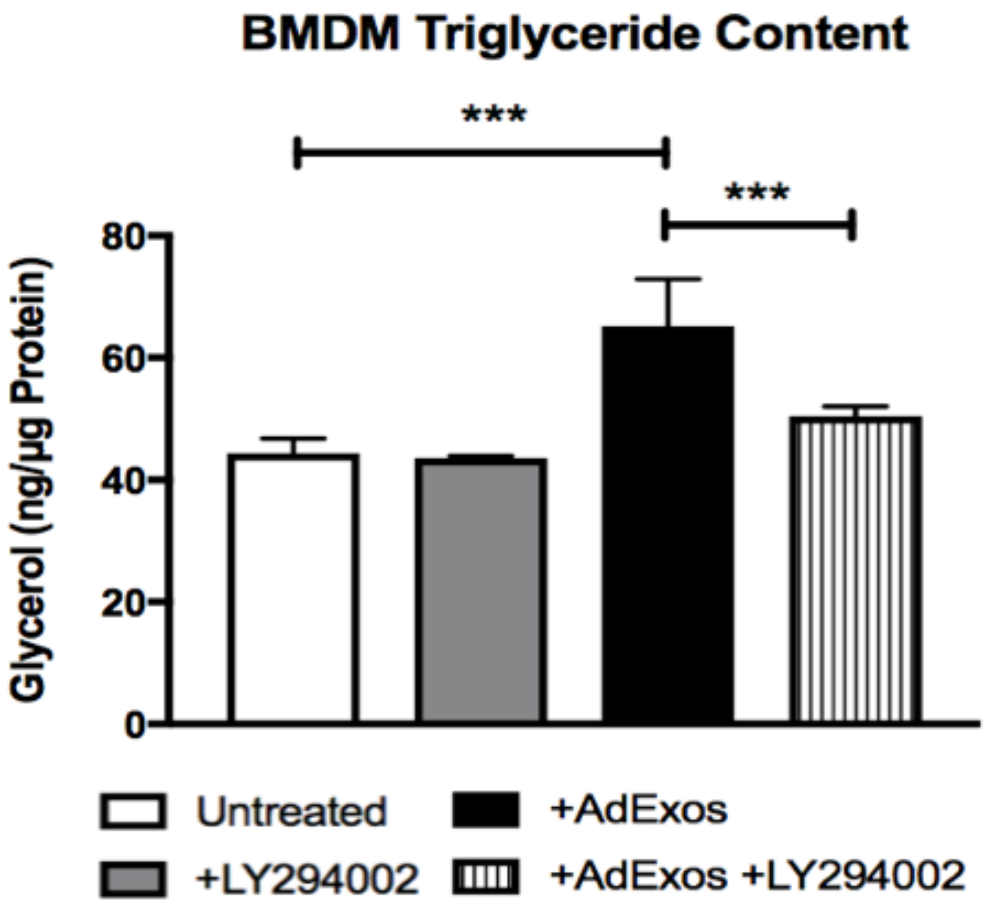


**Figure 3.10. Macropinocytosis is Necessary for AdExo-Induced Acylglyceride Accumulation in BMDMs.** Triglyceride levels of BMDMs cultured alone, with 100 mM LY294002, with AdExos, or with both 100 mM LY294002 and AdExos for 24 hours, measured enzymatically. One-way ANOVA; n = 6; ***P < 0.001.

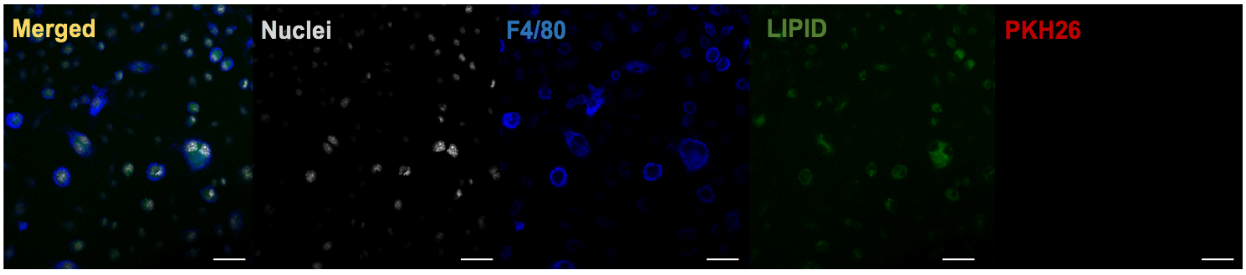


**Figure 3.11. AdExos Induce Multinucleation in BMDMs.** Confocal microscopy images of in vitro-generated BMDMs cultured with AdExos and immunostained with antibodies against F4/80 (blue), as well as DNA fluorescent stain DAPI (white) and neutral lipid fluorescent stain BODIPY (green). Scale bars, 10 mm.

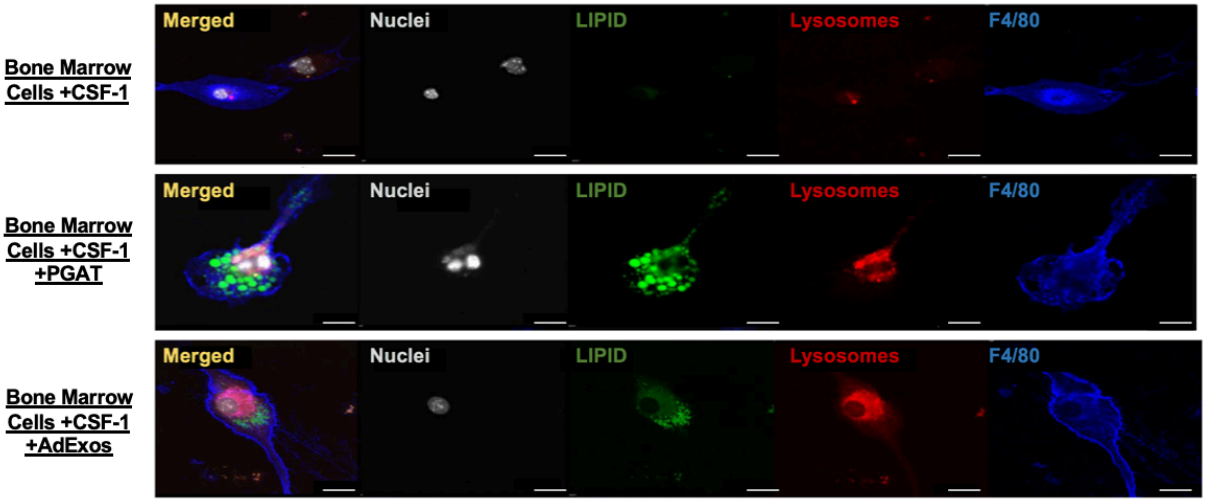


**Figure 3.12. AdExos Increase Acidic Compartment Content of BMDMs.** Confocal microscopy images of in vitro–generated BMDMs either cultured alone (top), with WT PGAT (middle), or with AdExos (bottom) for 3 days, immunostained with antibodies against F4/80 (blue), as well as DNA fluorescent stain DAPI (white), neutral lipid fluorescent stain BODIPY (green), and acidic organelle stain LysoTracker (red). Scale bars, 10 mm.

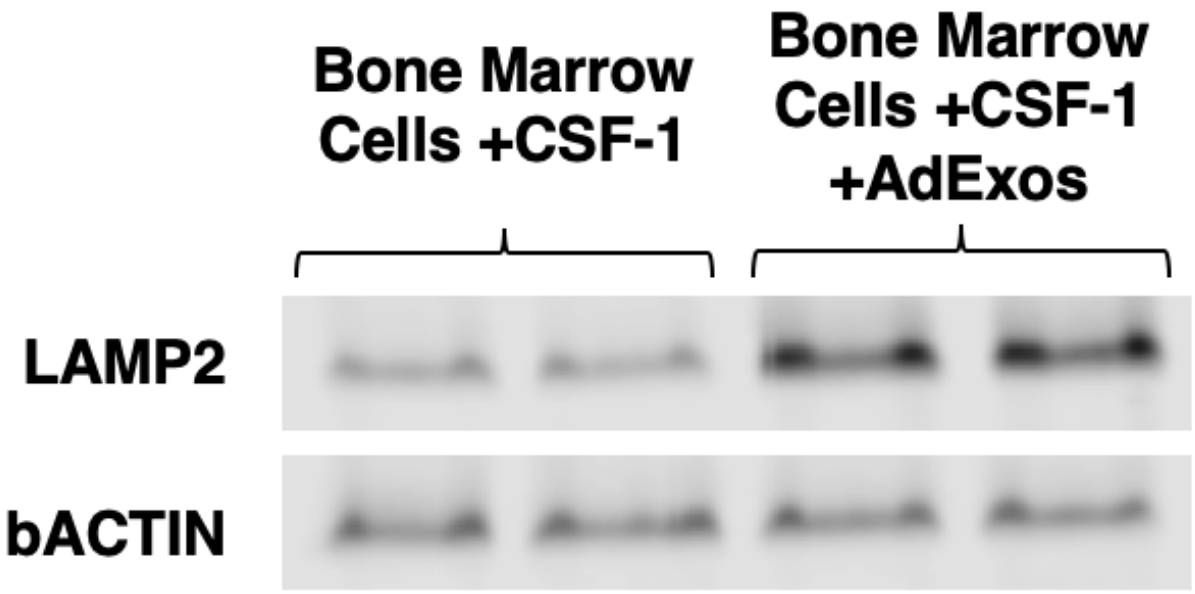


**Figure 3.13. AdExos Increase Lysosomal Protein Content of BMDMs.** Western blots of protein isolated from untreated BMDMs (left) or AdExo-treated BMDMs (right). Blots were probed using antibodies against LAMP2 and bActin.

Increased lysosomal content, multinucleation, and increased TAG content are all hallmarks of primary ATMs, suggesting that AdExos when added to CSF-1-treated bone marrow cells could induce differentiation towards an ATM-like cell. To investigate the effects on the transcription profile of AdExo-treated BMDMs, naïve BMDMs were either untreated, co-cultured with PGAT, treated with AdExos, treated with PGAT conditioned medium depleted of AdExos, or treated with exosomes from primary osteoblast cultures for six days (Figure 3.14). RNA was taken from the cells and analyzed using quantitative PCR.

The first set of genes we studied were “ATM Genes”. Several RNAseq studies have been done on macrophage populations from various murine tissues in an effort to understand the differences between the populations and identify markers that distinguish macrophage populations (*28-30*). “ATM Genes” are a selection of genes that have been found to be highly expressed in ATMs, when compared to other macrophage populations (*31-33*). We tested whether ATM genes are induced in BMDMs by co-culture with PGAT and found that compared to BMDMs without exposure to PGAT explants, adipose tissue did induce these genes (Figure 3.15). We next treated BMDMs with AdExos during differentiation and found AdExos contained the factors that induced ATM gene expression, but that these genes do not increase when BMDMs are treated with filtrate (PGAT conditioned medium that has been depleted of AdExos) or with exosomes isolated from irrelevant cells: primary osteoblast cultures (OsbExos). This indicates that the adipose tissue-induced ATM-like differentiation is mediated by AdExos.

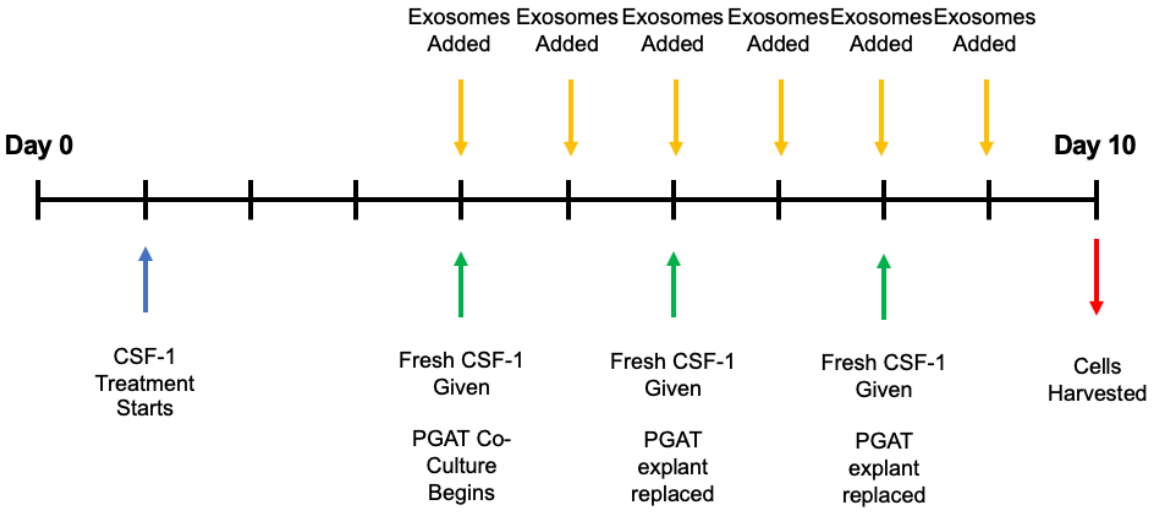


**Figure 3.14. BMDM Treatment Protocol.**

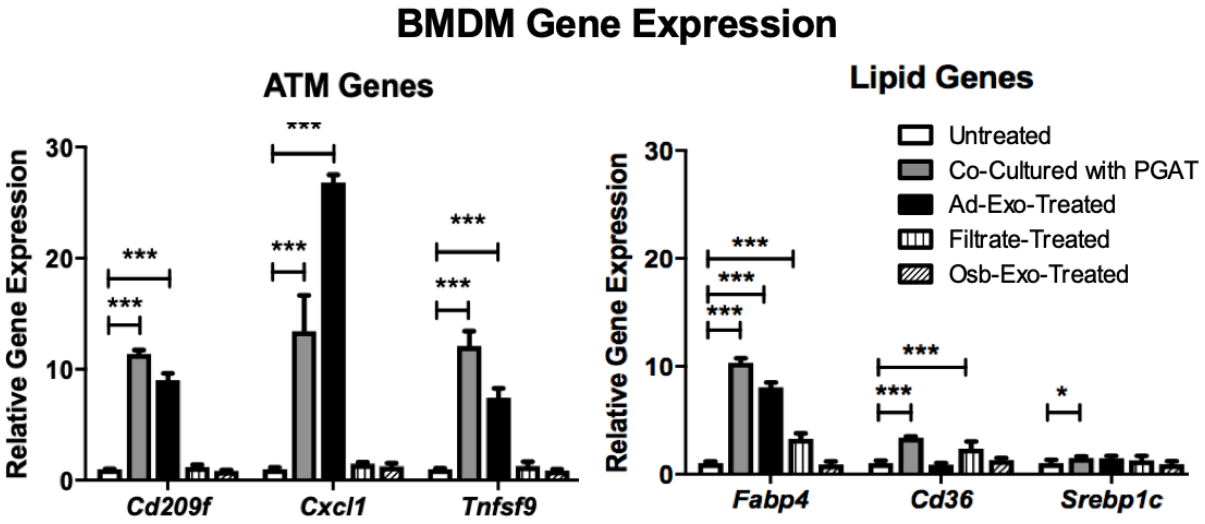


**Figure 3.15. AdExos Induce Upregulation of ATM Genes in BMDMs.** Quantitative polymerase chain reaction for BMDMs cultured alone, with WT PGAT, with AdExos, with filtrate from PGAT-conditioned medium (AdExos removed), or with exosomes secreted from primary osteoblasts (OsbExos) for 6 days. One-way ANOVA; n = 3 to 5; *P < 0.05; **P < 0.01; ***P < 0.001. Error bars represent SD.

Next, we looked at how AdExos altered the expression of genes whose products are involved in lipid binding, transport, metabolism, and action (Figure 3.15). *Fatty acid binding protein 4* (*Fabp4*) is elevated in ATMs and thought to be important in intracellular lipid trafficking and to be upregulated as the lipid content of a cell increases. BMDMs upregulate this gene in response to PGAT co-culture, AdExo treatment, and to the FFA-containing filtrate treatment. *Cd36* is a fatty acid receptor on the exterior of macrophages that facilitates transport of FFA across the plasma membrane. *Cd36* expression is upregulated in response to PGAT co-culture and filtrate treatment, but expression is not increased in response to AdExo treatment. This supports the hypothesis that AdExo-induced TAG accumulation is not acting through FFA uptake. *Srebp1c*, a gene that encodes a transcriptional regulator of TAG is modestly increased in BMDMs cultured in the presence of adipose tissue, but not by AdExos (Figure 3.15). The BMDM response to AdExos does not seem to be a generalized “tissue resident-like” polarization, as they do not induce changes in expression of “Kupffer Cell Genes” (Figure 3.16). The last thing to note here is that this response to AdExos does not seem to be a general response to any exosomes, as OsbExos do not induce the same expression patterns in BMDMs.

As a short aside, OsbExos have a wider distribution of particle diameter than AdExos (Figure 3.17, Supplemental Figure 3.2). Treatment of BMDMs with OsbExos did not induce TAG accumulation in F4/80+ cells (Figure 3.18). We also examined “Osteoclast Genes” in our qPCR experiment, to investigate whether OsbExos were capable of inducing gene expression profiles consistent with primary osteoclasts, the tissue resident macrophages of the bone. The results from this section of the experiment were difficult to interpret. Certain “Osteoclast Genes” were upregulated in response to OsbExo treatment, whereas others were not (Figure 3.19). In addition, some genes that were induced by OsbExos, were also induced by AdExos, indicating that the response was not specific to OsbExo treatment.

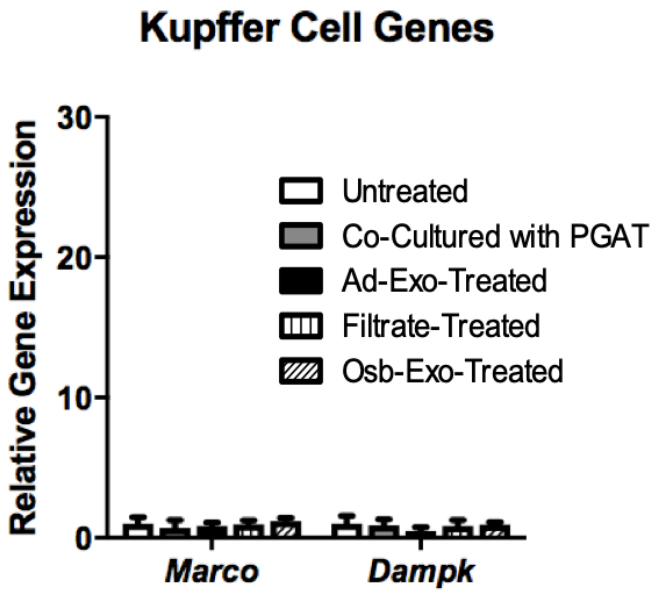


**Figure 3.16. AdExos Do Not Induce Kupffer Cell Gene Expression in BMDMs.** Quantitative polymerase chain reaction for BMDMs cultured alone, with WT PGAT, with AdExos, with filtrate from PGAT-conditioned medium (AdExos removed), or with exosomes secreted from primary osteoblasts (OsbExos) for 6 days. One-way ANOVA; n = 3 to 5; Error bars represent SD.

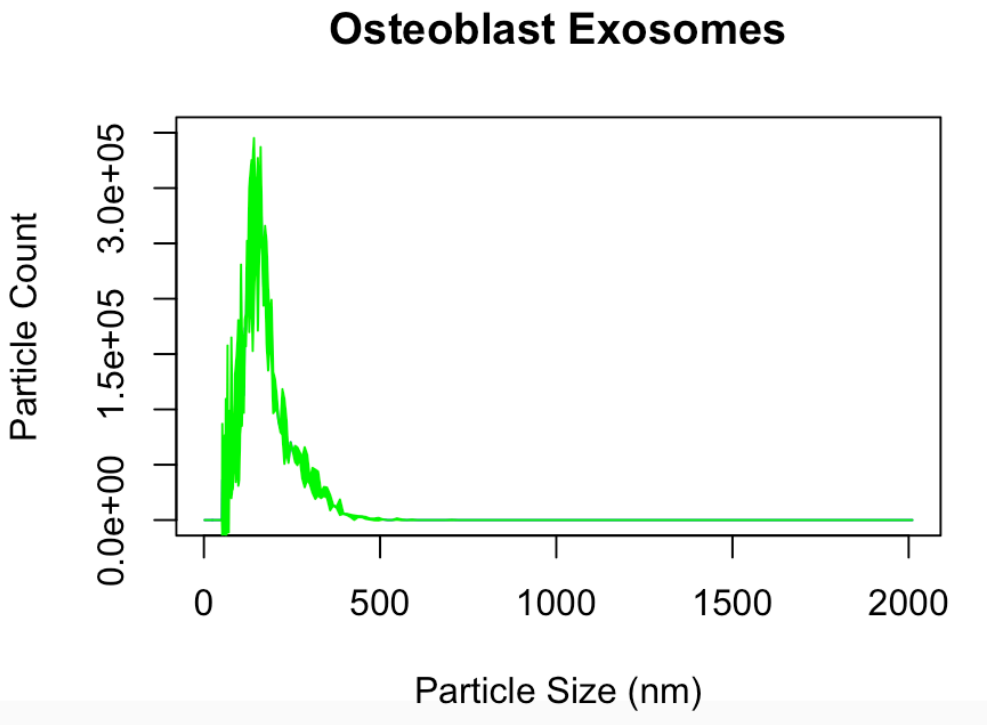


**Figure 3.17. Osteoblast-Derived Exosome Size Distribution.** Viewsizer 3000 Nanoparticle Tracking Analysis histogram of exosomes purified from primary osteoblast conditioned medium, depicting particle diameter and the number of particles at each diameter released by 1 g of lean adipose tissue per hour.

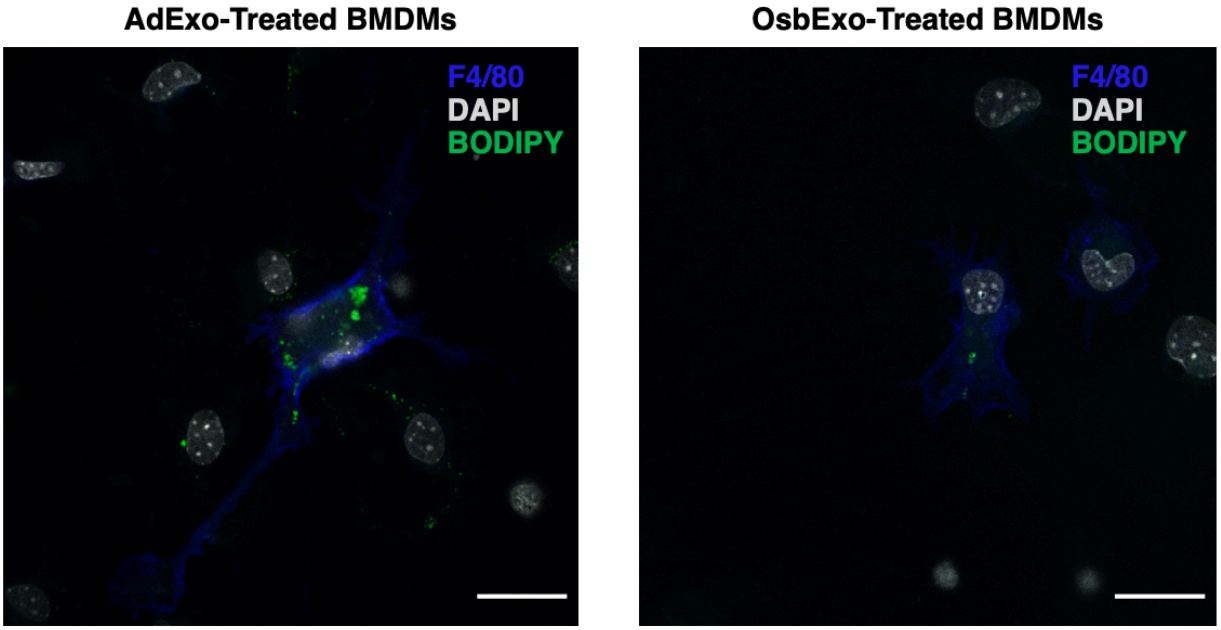


**Figure 3.18. OsbExos Do Not Induce Neutral Lipid Accumulation in BMDMs.** Confocal microscopy images of AdExo-treated or OsbExo-treated BMDMs. Cells were immunostained with antibodies against F4/80 (blue), as well as DNA fluorescent stain DAPI (white) and neutral lipid fluorescent stain BODIPY (green). Scale bars, 10 mm.

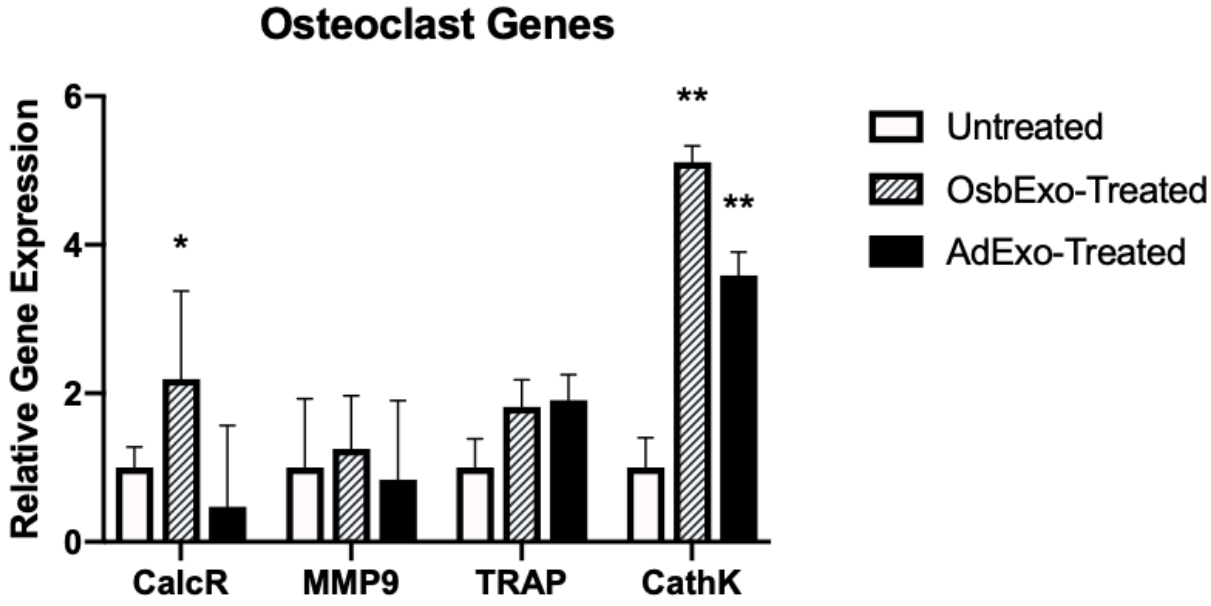


**Figure 3.19. OsbExos Do Not Induce Osteoclast-Like Gene Expression Profile.** Quantitative polymerase chain reaction for BMDMs cultured alone, with AdExos, or with exosomes secreted from primary osteoblasts (OsbExos) for 6 days. One-way ANOVA; n = 3 to 5; *P < 0.05; **P < 0.01. Error bars represent SD.

To delve further into ATM-like differentiation in response to AdExos, RNAseq experiments were performed on BMDMs that were either differentiated only with CSF-1, differentiated with CSF-1 in the presence of PGAT, or differentiated with CSF-1 and AdExos. Density plots of the sequencing data revealed a similar distribution of reads per base, indicating that the sample could be compared (Figure 3.20). Principal Component Analyses (PCA) were performed to assess whether two component analysis of transcripts distinguished BMDMs from AdExo and PGAT conditioned medium treated BMDMs (Figure 3.21). Untreated BMDM samples clustered together tightly and clearly separated themselves from the AdExo-treated and PGAT co-cultured BMDMs which clustered quite closely to one another.

Co-culturing with PGAT upregulated 1344 genes with a nominal p-value < 0.001 compared to untreated BMDMs. Of these 1334 genes, 1032 of them were also upregulated in BMDMs treated with AdExos, representing 77% of upregulated genes. 1077 genes were downregulated by PGAT co-culture and of these 881 were also downregulated by AdExo treatment, representing 82%. Magnitude of expression abundance was plotted with heat maps for genes significantly upregulated by PGAT co-culture (Figure 3.22) and genes significantly downregulated (Figure 3.23). Consistent with the small selection of genes we assessed by qPCR previously treatment with AdExo and PGAT conditioned medium, the signaling from AdExos dominate the gene expression response to PGAT in BMDMs.

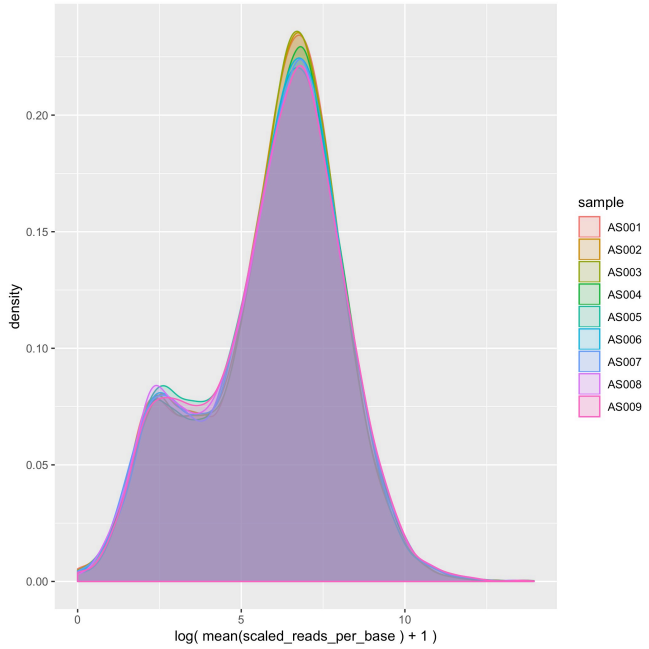


**Figure 3.20. BMDM RNAseq Density Plots.** Reads per base count density plots for RNA from Untreated (AS001, AS002, AS003), PGAT-co-cultured (AS004, AS005, AS006), and AdExo-treated (AS007, AS008, AS009) BDMDMs.

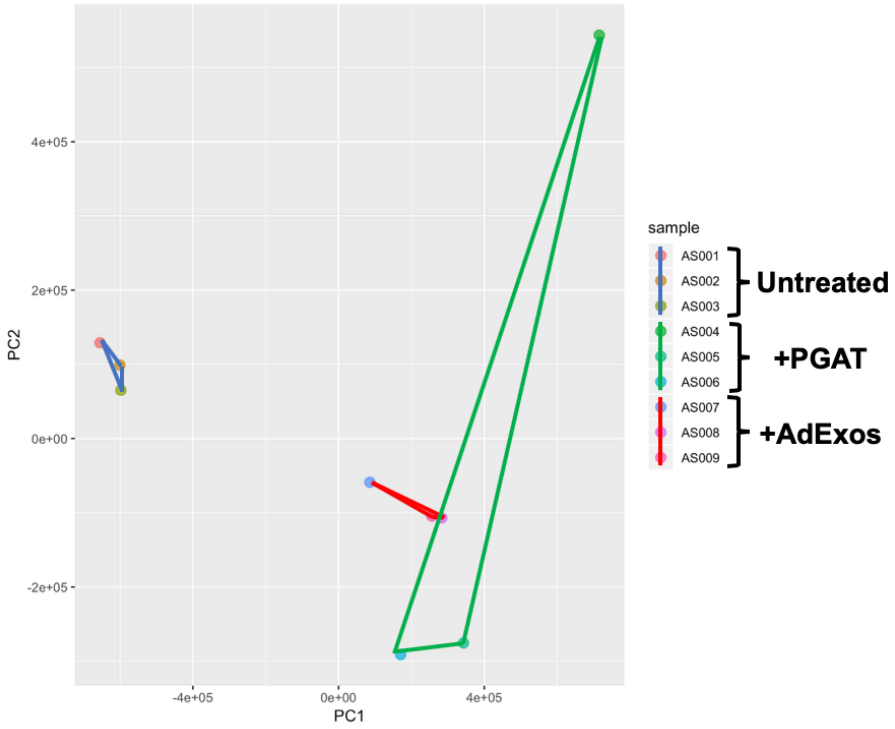


**Figure 3.21. BMDMs Treated with AdExos Cluster with BMDMs Co-Culture with PGAT.** Projection of samples onto two dimensions of principal components for untreated (blue lines), PGAT-co-cultured (green lines) and AdExo-treated (red lines) BMDMs.

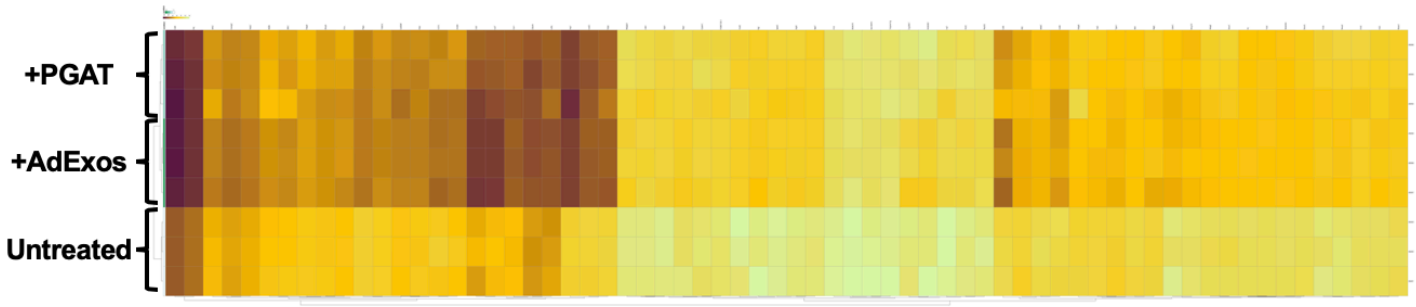


**Figure 3.22. RNA Abundance Heat Map for Genes Upregulated by PGAT Co-Culture.** Heatmap of genes upregulated in BMDMs by PGAT co-culture with a p-value < 0.001. Darker shades indicate increasing upregulation.

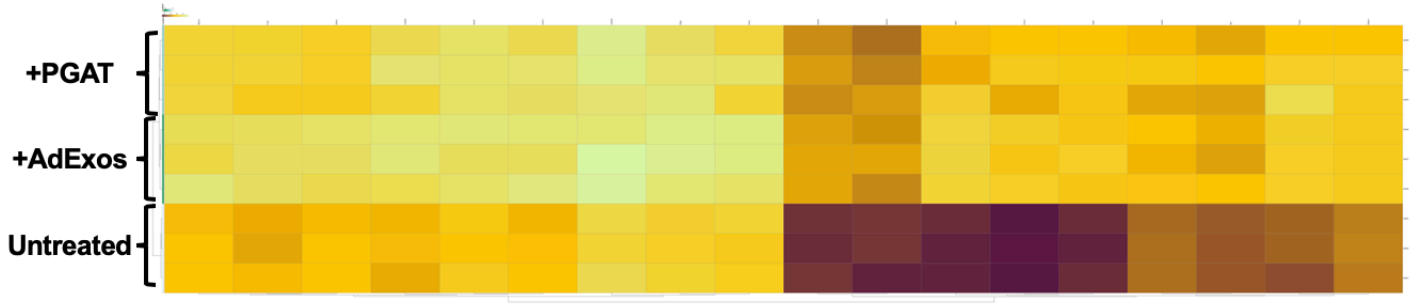


**Figure 3.23. RNA Abundance Heat Map for Genes Downregulated by PGAT Co-Culture.** Heatmap of genes downregulated in BMDMs by PGAT co-culture with a p-value < 0.001. Darker shades indicate increasing upregulation.

The 1000 genes with the lowest nominal p-values when comparing expression between BMDMs and BMDMs differentiated in the presence of AdExos were analyzed using Enrichr to determine whether the expression of genes in functional pathways were overrepresented (Figure 3.24). The two most enriched pathways both involve response to cholesterol. There are several gene pathways that involve changes to immune signaling, and there are also several pathways that are heavily involved in adipose tissue, including leptin and insulin signaling and white fat cell differentiation pathways. Genes altered by AdExo treatment are most associated with blood, not surprising as BMDMs are bone marrow-derived, and adipose tissue (Figure 3.25). And lastly, as far as subcellular components are concerned, these genes are most associated with lysosomes and vesicle membranes, consistent with the increase in lysosomes seen by microscopy (Figure 3.26). These transcriptional signatures are consistent AdExo-treated BMDMs activating programs for the uptake and lysosomal degradation of lipid-laden exosomes.

To better understand the relationship of BMDMs differentiated in the presence of AdExos with authentic primary ATMs, we isolated resident and recruited ATMs and performed RNAseq. The primary ATMs were divided between long-lived resident macrophages, identifiable by high expression of the macrophage marker F4/80 macrophages and recruited/transient macrophages, that express F4/80 at low levels. F4/80lo and F4/80hi macrophages were isolated from both lean and high fat fed obese mice (*30*). PCA plots showed that BMDMs clustered separately from either population of primary ATMs (Figure 3.27), although a distinction was still clear between AdExo/PGAT BMDMs and untreated BMDMs. Hierarchical clustering of samples based on transcriptional profile yields similar results, with some distance between BMDM cells and primary ATMs (Figure 3.28).

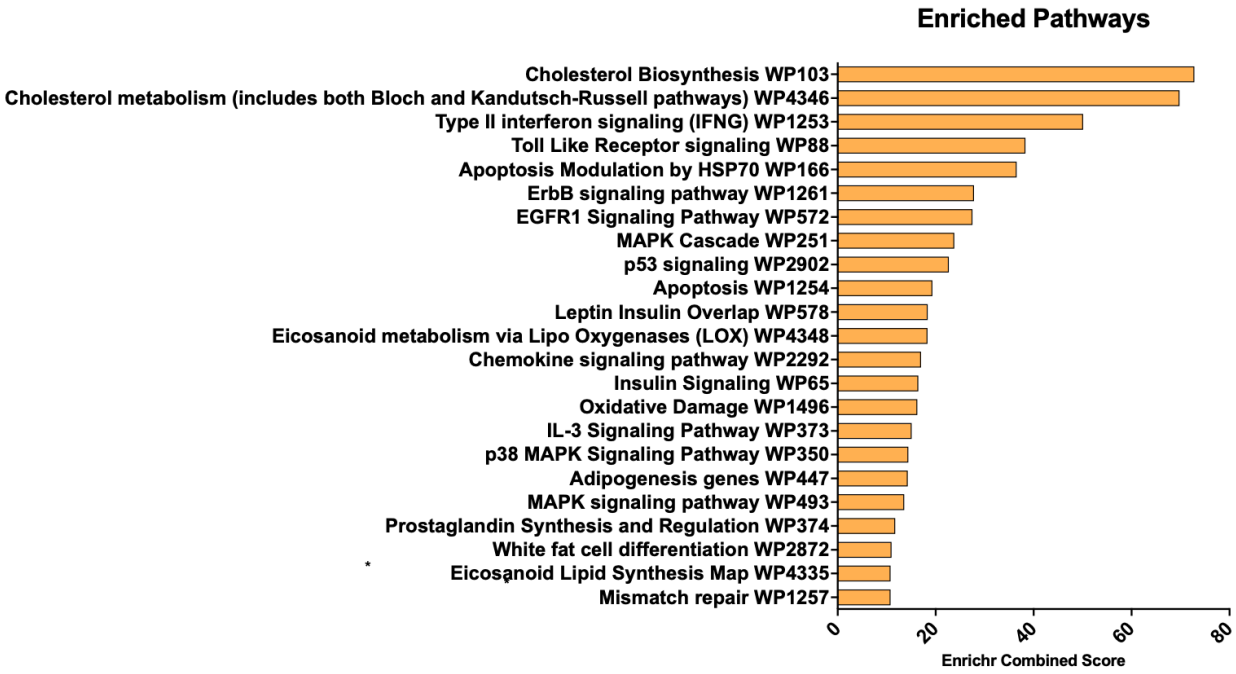


**Figure 3.24. AdExo-Induced BMDM Gene Pathways.** Common pathways associated with top 1000 differentially expressed genes in AdExo-treated BMDMs.

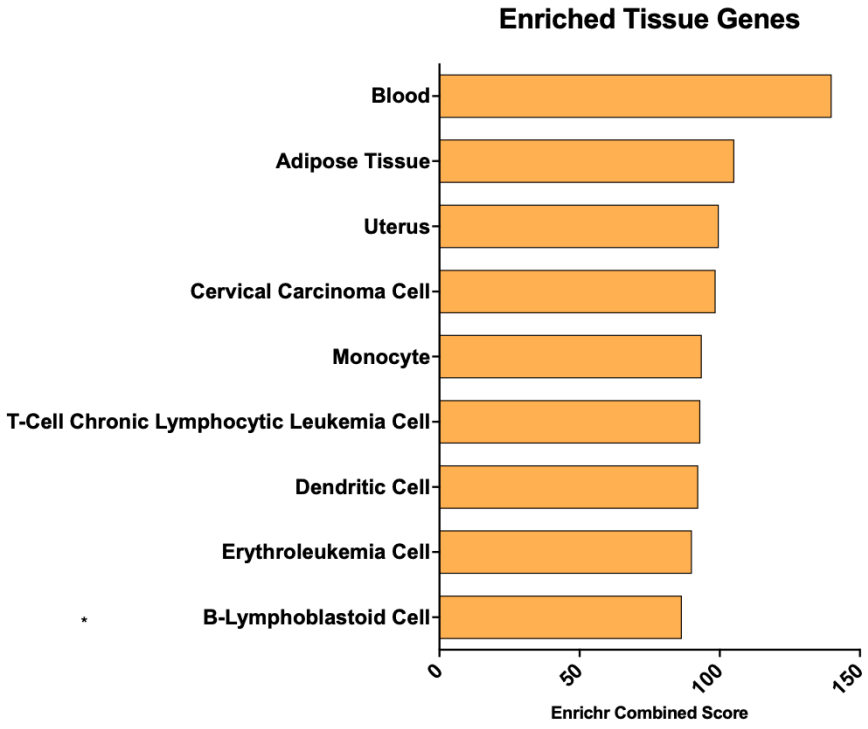


**Figure 3.25. AdExo-Induced BMDM Gene Tissues.** Tissues associated with top 1000 differentially expressed genes in AdExo-treated BMDMs.

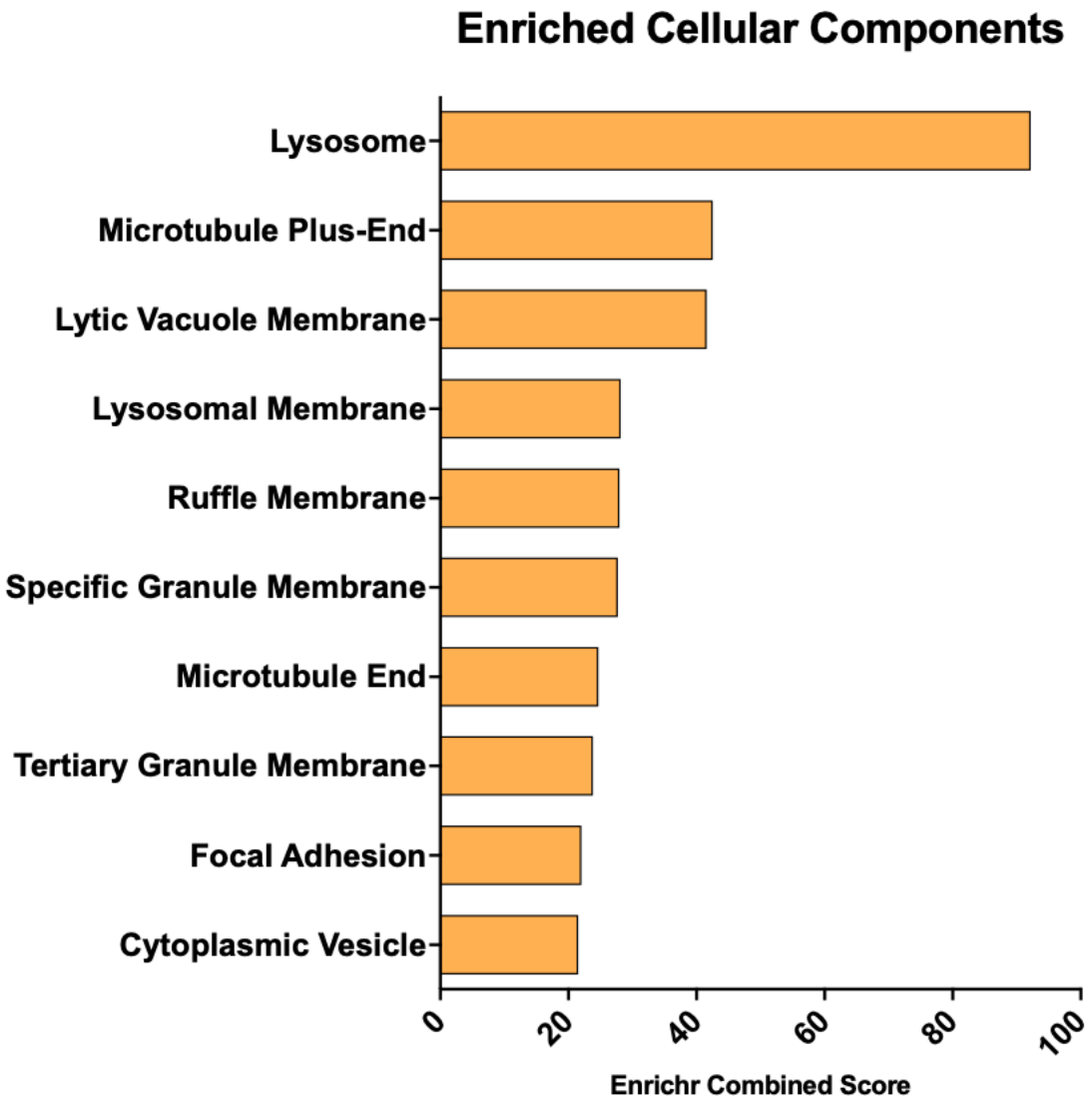


**Figure 3.26. AdExo-Induced BMDM Gene Subcellular Structures.** Cellular components associated with top 1000 differentially expressed genes in AdExo-treated BMDMs.

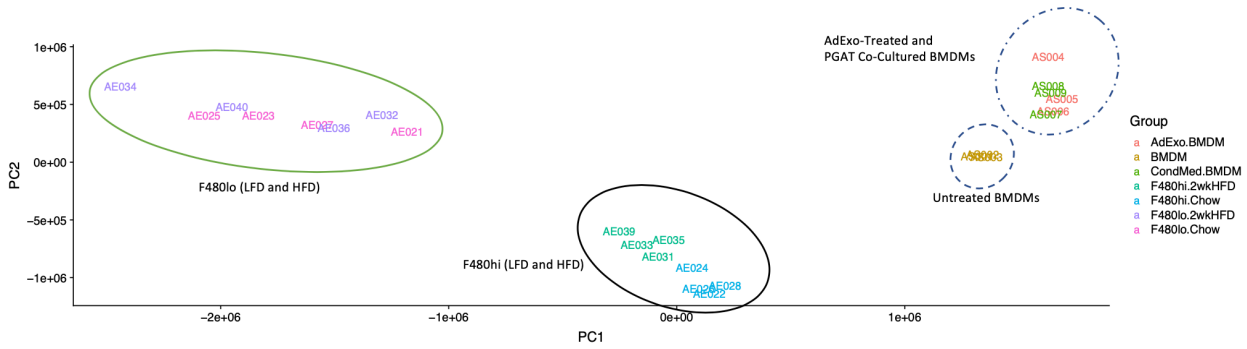


**Figure 3.27. BMDMs and Primary ATMs Cluster Separately.** Projection of samples onto two dimensions of principal components for untreated (BMDM), PGAT-co-cultured (CondMed.BMDM) and AdExo-treated (AdExo.BMDM) BMDMs along with primary f4/80hi ATMs from high fat diet- (F480hi.2wkHFD) and chow-fed (F480hi.Chow) animals and primary f4/80lo ATMs from high fat diet- (F480lo.2wkHFD) and chow-fed (F480lo.Chow) animals. A larger version of this figure is available at https://drive.google.com/open?id=1UtBP0DhqQLx4jf56UElS2vvGtvXFUlRI

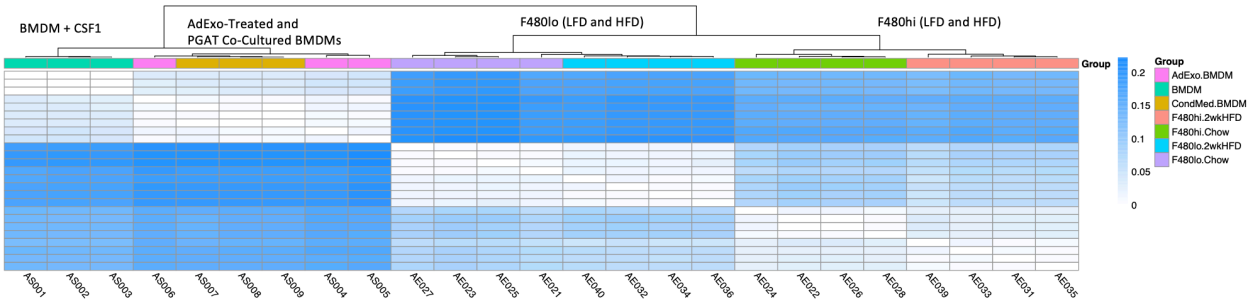


**Figure 3.28. BMDMs Treated with AdExos are More Similar to Primary ATMs than Untreated BMDMs.** Jensen-Shannon divergence hierarchy for untreated (BMDM), PGAT-co-cultured (CondMed.BMDM) and AdExo-treated (AdExo.BMDM) BMDMs along with primary f4/80hi ATMs from high fat diet- (F480hi.2wkHFD) and chow-fed (F480hi.Chow) animals and primary f4/80lo ATMs from high fat diet- (F480lo.2wkHFD) and chow-fed (F480lo.Chow) animals. A larger version of this figure is available at https://drive.google.com/open?id=1UtBP0DhqQLx4jf56UElS2vvGtvXFUlRI

Genes significantly upregulated in each population compared to untreated BMDMs were matched to establish pathways that define ATM-ness (Figure 3.29). In this analysis, AdExo treated BMDMs were more similar to F4/80lo than F4/80hi primary ATMs. A common set of 301 genes were significantly upregulated in AdExo and PGAT treated BMDMs, F4/80lo, and F4/80hi ATMs compared to untreated BMDMs. Pathway enrichment analysis found 43 programs upregulated in the in vitro and authentic ATMs, representing a wide variety of processes (Figure 3.30). Several programs associated with lipid metabolism and immune responses were in this group, but of note were pathways associated with angiogenesis and cell proliferation, programs that are consistent with the recently reported role of ATMs in adipose tissue expansion. Downregulated genes told a similar story, where 345 genes were significantly inhibited in all four “ATM-like” cell populations (Figure 3.31). These genes seem to be involved heavily in cholesterol synthesis, which would be an appropriate response given the high content of cholesterol in AdExos (Figure 3.32).

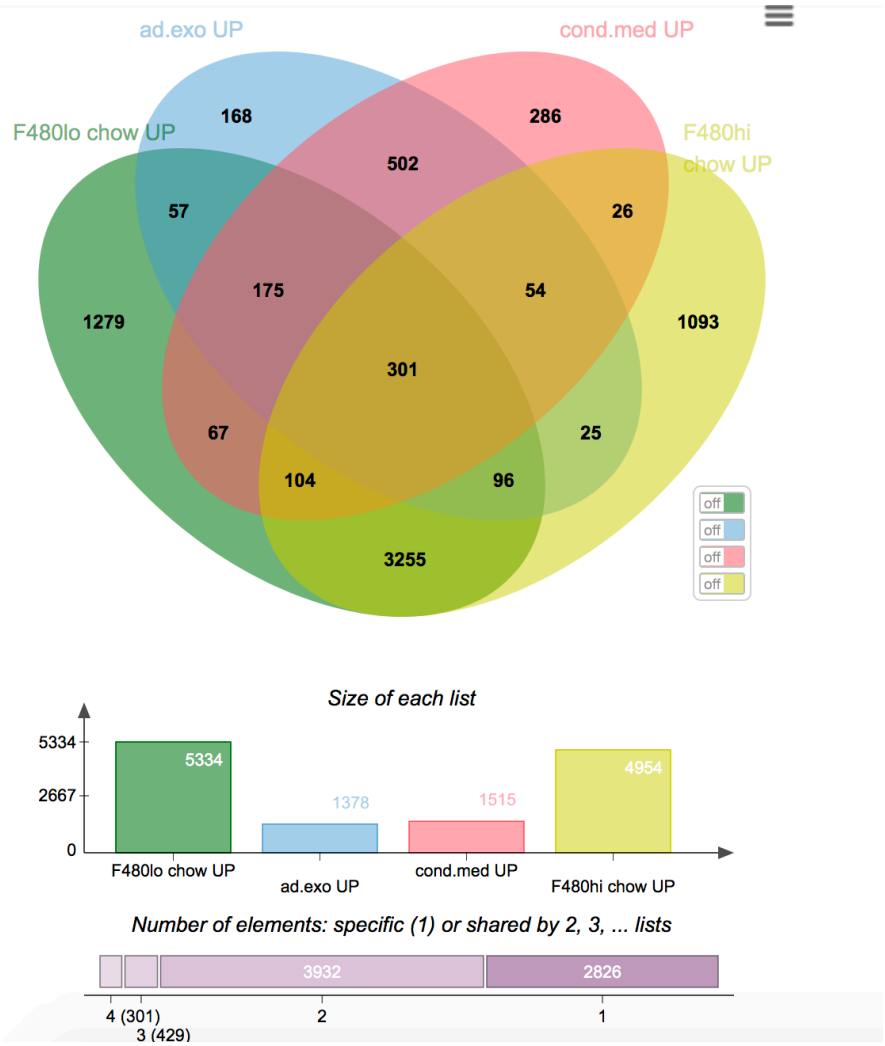


**Figure 3.29. Genes Upregulated Compared to Untreated BMDMs.** JVenn diagram displaying shared genes, significantly upregulated compared to BMDMs, in PGAT co-cultured (cond.med UP), AdExo-treated (ad.exo UP) BMDMs and primary f4/80lo ATMs (f480lo chow UP) and f480hi ATMs (f480hi chow UP) from chow-fed animals.

| |
|---|
| cytokine-mediated signaling pathway (GO:0019221) |
| cellular response to cytokine stimulus (GO:0071345) |
| response to lipid (GO:0033993) |
| response to lipopolysaccharide (GO:0032496) |
| response to molecule of bacterial origin (GO:0002237) |
| regulation of cell proliferation (GO:0042127) |
| positive regulation of leukocyte chemotaxis (GO:0002690) |
| positive regulation of angiogenesis (GO:0045766) |
| positive regulation of vasculature development (GO:1904018) |
| chemokine-mediated signaling pathway (GO:0070098) |
| negative regulation of STAT cascade (GO:1904893) |
| regulation of angiogenesis (GO:0045765) |
| cellular response to hormone stimulus (GO:0032870) |
| positive regulation of cellular process (GO:0048522) |
| negative regulation of apoptotic process (GO:0043066) |
| negative regulation of JAK-STAT cascade (GO:0046426) |
| inflammatory response (GO:0006954) |
| negative regulation of programmed cell death (GO:0043069) |
| positive regulation of transcription, DNA-templated (GO:0045893) |
| positive regulation of transcription from RNA polymerase II promoter (GO:0045944) |
| negative regulation of insulin receptor signaling pathway (GO:0046627) |
| positive regulation of cell differentiation (GO:0045597) |
| negative regulation of cellular response to insulin stimulus (GO:1900077) |
| regulation of transcription from RNA polymerase II promoter (GO:0006357) |
| regulation of JAK-STAT cascade (GO:0046425) |
| regulation of I-kappaB kinase/NF-kappaB signaling (GO:0043122) |
| positive regulation of cell proliferation (GO:0008284) |
| positive regulation of cell motility (GO:2000147) |
| cellular response to interleukin-1 (GO:0071347) |
| regulation of cell migration (GO:0030334) |
| regulation of natural killer cell chemotaxis (GO:2000501) |
| positive regulation of cell migration (GO:0030335) |
| cellular response to interleukin-7 (GO:0098761) |
| interleukin-7-mediated signaling pathway (GO:0038111) |
| regulation of insulin receptor signaling pathway (GO:0046626) |
| cellular response to hypoxia (GO:0071456) |
| cellular response to tumor necrosis factor (GO:0071356) |
| cellular response to organic substance (GO:0071310) |
| regulation of transcription, DNA-templated (GO:0006355) |
| STAT cascade (GO:0097696) |
| membrane lipid biosynthetic process (GO:0046467) |
| positive regulation of fat cell differentiation (GO:0045600) |

**Figure 3.30. Gene Pathways Upregulated in All ATM-Like Cells.** List of common pathways associated with genes, significantly upregulated compared to BMDMs, in PGAT co-cultured (cond.med UP), AdExo-treated (ad.exo UP) BMDMs and primary f4/80lo ATMs (f480lo chow UP) and f480hi ATMs (f480hi chow UP) from chow-fed animals.

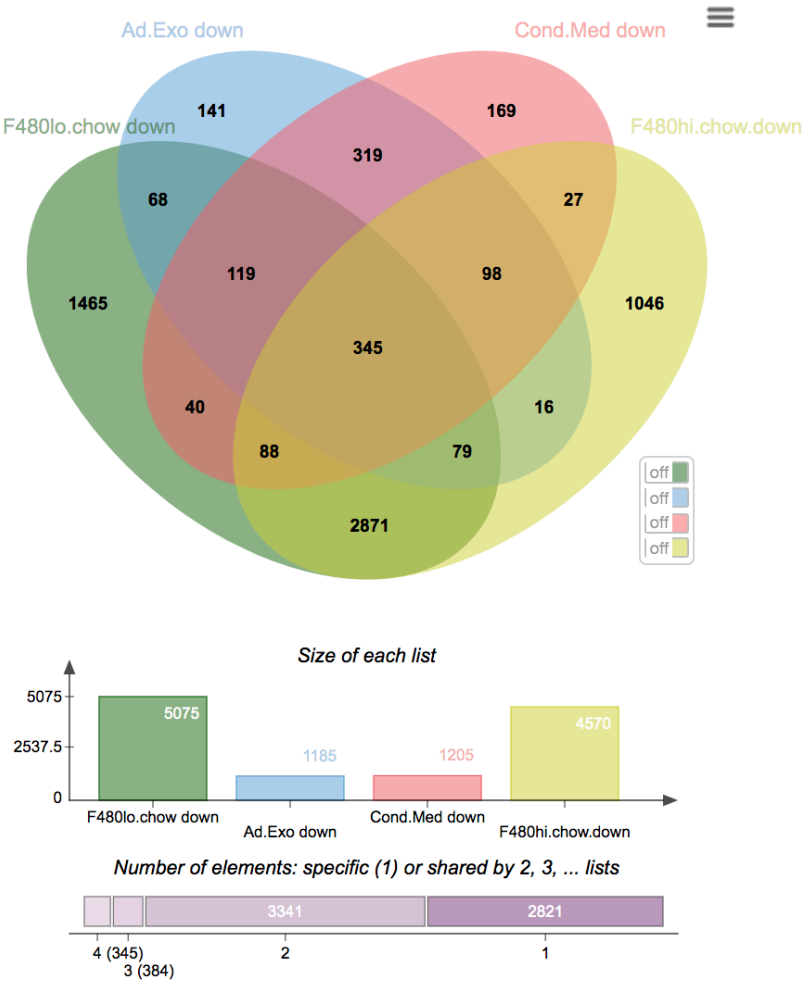


**Figure 3.31. Genes Downregulated in Comparison to Untreated BMDMs.** JVenn diagram displaying shared genes, significantly downregulated compared to BMDMs, in PGAT co-cultured (cond.med UP), AdExo-treated (ad.exo UP) BMDMs and primary f4/80lo ATMs (f480lo chow UP) and f480hi ATMs (f480hi chow UP) from chow-fed animals.

| |
|---|
| mitotic sister chromatid segregation (GO:0000070) |
| DNA metabolic process (GO:0006259) |
| mitotic cell cycle phase transition (GO:0044772) |
| DNA replication (GO:0006260) |
| cholesterol biosynthetic process (GO:0006695) |
| secondary alcohol biosynthetic process (GO:1902653) |
| sterol biosynthetic process (GO:0016126) |
| positive regulation of cell cycle process (GO:0090068) |
| G1/S transition of mitotic cell cycle (GO:0000082) |
| microtubule cytoskeleton organization involved in mitosis (GO:1902850) |
| cholesterol metabolic process (GO:0008203) |
| centromere complex assembly (GO:0034508) |
| DNA replication-independent nucleosome assembly (GO:0006336) |
| CENP-A containing nucleosome assembly (GO:0034080) |
| CENP-A containing chromatin organization (GO:0061641) |
| mitotic spindle organization (GO:0007052) |
| sister chromatid segregation (GO:0000819) |
| chromatin remodeling at centromere (GO:0031055) |
| cell cycle G1/S phase transition (GO:0044843) |
| histone exchange (GO:0043486) |
| cellular response to DNA damage stimulus (GO:0006974) |
| mitotic metaphase plate congression (GO:0007080) |
| metaphase plate congression (GO:0051310) |
| DNA repair (GO:0006281) |
| regulation of alcohol biosynthetic process (GO:1902930) |
| mitotic cytokinesis (GO:0000281) |
| mitotic nuclear division (GO:0140014) |
| regulation of cholesterol biosynthetic process (GO:0045540) |
| regulation of cholesterol metabolic process (GO:0090181) |
| regulation of steroid biosynthetic process (GO:0050810) |
| regulation of cell cycle process (GO:0010564) |
| DNA replication initiation (GO:0006270) |
| regulation of cytokinesis (GO:0032465) |
| regulation of mitotic cell cycle phase transition (GO:1901990) |
| regulation of mitotic nuclear division (GO:0007088) |
| regulation of mitotic cell cycle (GO:0007346) |
| cytoskeleton-dependent cytokinesis (GO:0061640) |
| G2/M transition of mitotic cell cycle (GO:0000086) |

**Figure 3.32. Gene Pathways Downregulated in All ATM-Like Cells.** List of common pathways associated with genes, significantly downregulated compared to BMDMs, in PGAT co-cultured (cond.med UP), AdExo-treated (ad.exo UP) BMDMs and primary f4/80lo ATMs (f480lo chow UP) and f480hi ATMs (f480hi chow UP) from chow-fed animals.

We found that AdExos were capable of inducing an ATM-like differentiation in naïve BMDMs *in vitro*. To test whether AdExos would be able to induce ATM-ness in mature cells *in vivo,* we treated peritoneal cells with AdExos. PKH26-labeled AdExos were injected into the peritoneal cavity of lean mice. After 24 hours, these mice were sacrificed and peritoneal cavity cells (PC cells) were isolated from the animals. These PC cells were then sorted using flow cytometry. Interestingly, the PKH26 exosomal marker was taken up almost exclusively by macrophages in this tissue as well, with >90% of PKH26+ cells also expressing F4/80 (Figure 3.33). Peritoneal macrophages from AdExo-injected animals and those from PBS-injected animals were sorted and RNA was collected. Quantitative PCR was performed to measure the same genes that were examined in the BMDM studies. The results revealed that several of the "ATM Genes" that were upregulated in BMDMs treated with AdExos, were also upregulated in PC macrophages injected with AdExos, but others were not (Figure 3.34). *Marco*, a "Kupffer Cell Gene" was strongly induced in PC macrophages from animals injected with AdExos. Interestingly, lipid-associated genes were not upregulated by AdExo injection, perhaps because the lipid takes some time to accumulate. AdExos were able to partially induce the ATM-like profile in *in vivo* cells, however they were not able to fully differentiate PC macrophages into ATMs. This does not provide definitive evidence about the ability of AdExo to alter the phenotype of other tissue macrophages.

Taken together the data in this chapter suggest that AdExos can help shape macrophage phenotype. We have found that AdExos are taken up primarily by macrophage populations in the PGAT and are sufficient to induce TAG accumulation, multinucleation, increased lysosomal content, and a gene expression profile consistent with primary ATMs. Thus, AdExos may be a critical signal in the differentiation and function of naïve macrophages as they become ATMs (Figure 3.35).

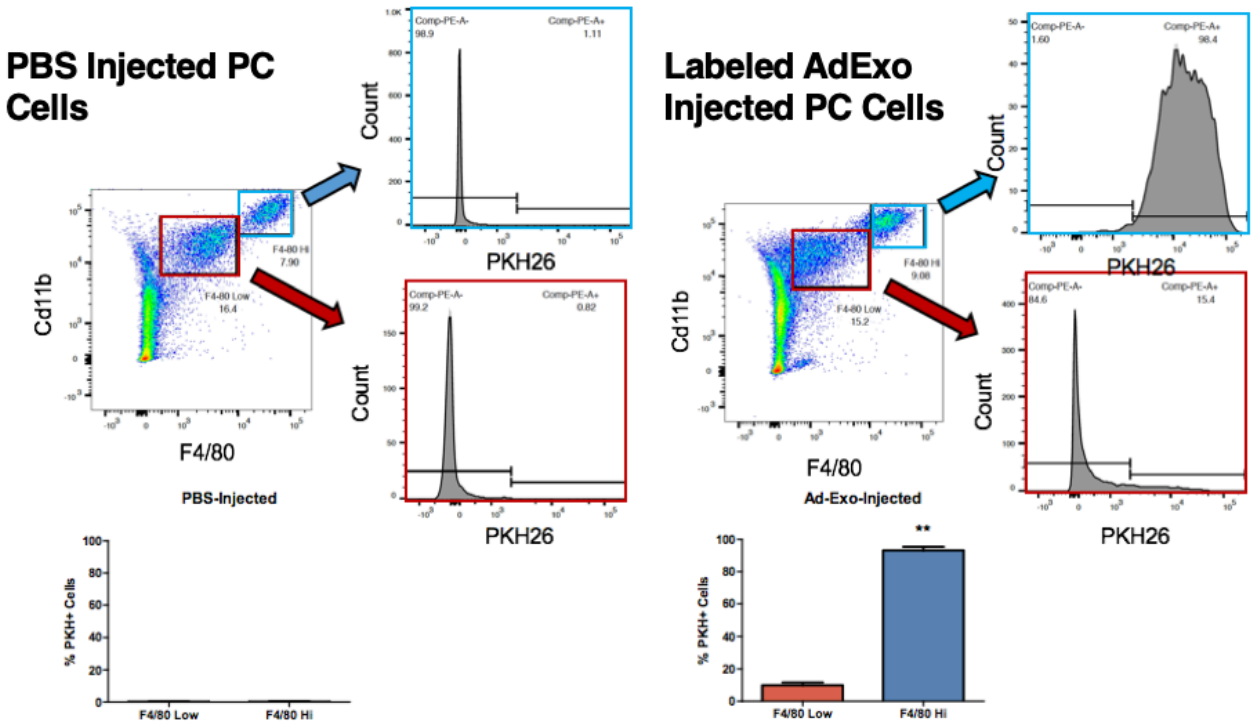


**Figure 3.33. AdExos Are Taken up by Peritoneal Cavity Macrophages.** Representative flow cytometry analysis of peritoneal cavity cells isolated from animals that were injected with either PKH26-labeled adipocyte-derived exosomes or PBS. Histograms show number of PKH26+ cells in CD45+, CD11b-hi, F4/80-hi (blue) and CD45+, CD11b-lo, F4/80-lo (red) cell populations. Data is summarized in bar graphs. **P < 0.01; error bars represent SD.

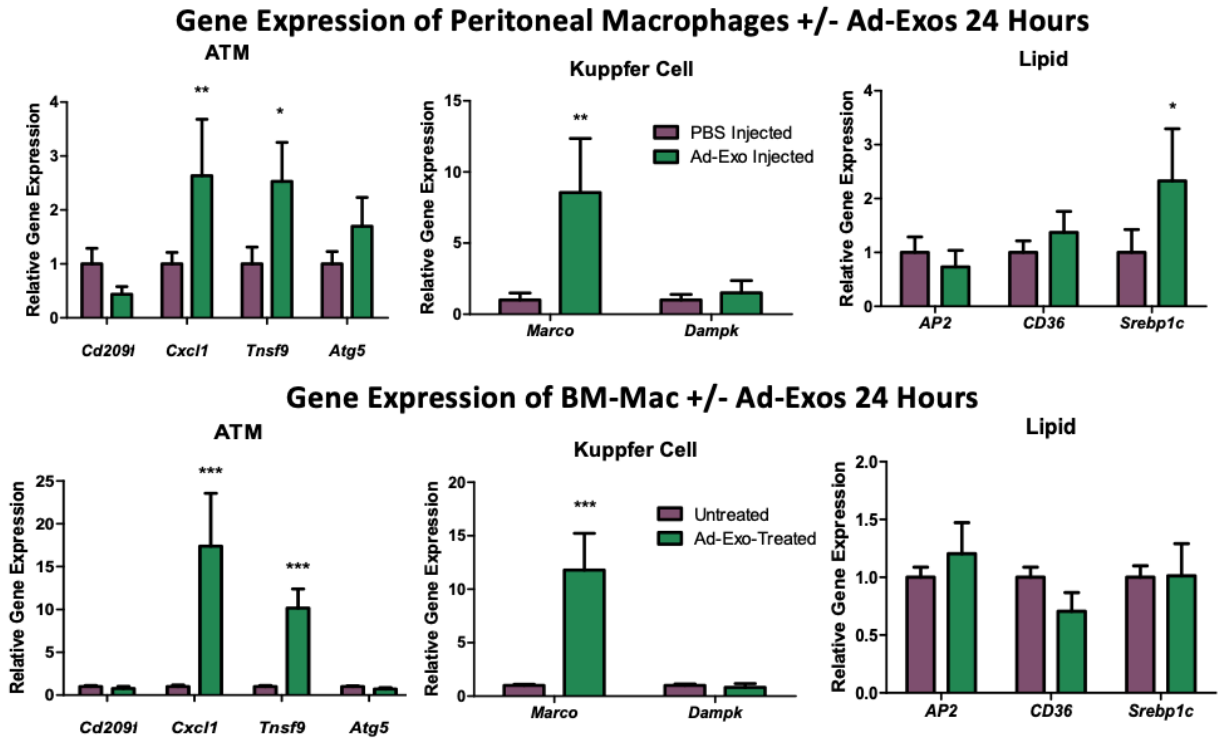


**Figure 3.34. AdExos Do Not Induce ATM-Like Differentiation in Peritoneal Cavity Macrophages.** Gene expression of peritoneal cavity cells isolated from animals that were injected with either PKH26-labeled adipocyte-derived exosomes or PBS. After 24 hours, cells were isolated from mice and sorted by flow cytometry, before isolating RNA and performing quantitative PCR (top) and BMDMs untreated or treated with AdExos for 25 hours before isolating RNA and performing quantitative PCR (bottom). Unpaired, two-tailed T-Test; n=4. *P < 0.05, **P < 0.01, ***P < 0.001; Error bars represent SD.

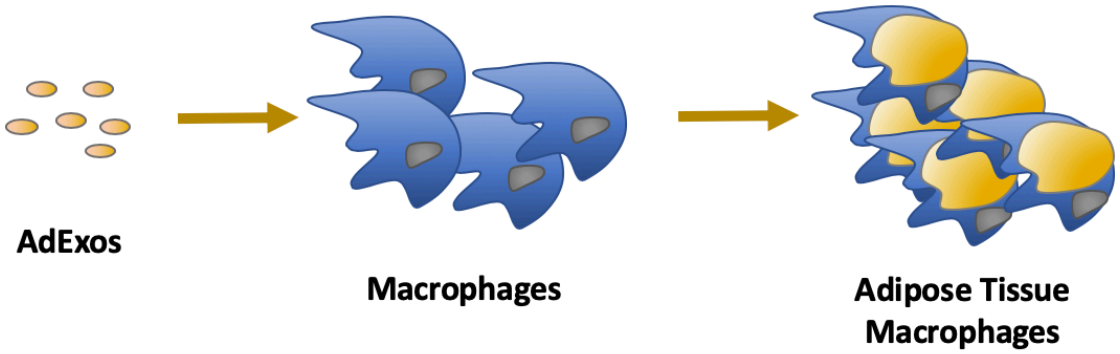


**Figure 3.35. Graphical summary of Chapter 3.**

### 3.2 References


1. Y. Lavin, A. Mortha, A. Rahman, M. Merad, Regulation of macrophage development and function in peripheral tissues. *Nat Rev Immunol* **15**, 731-744 (2015).
2. J. M. Cavaillon, Cytokines and macrophages. *Biomed Pharmacother* **48**, 445-453 (1994).
3. L. Peiser, S. Gordon, The function of scavenger receptors expressed by macrophages and their role in the regulation of inflammation. *Microbes Infect* **3**, 149-159 (2001).
4. G. Arango Duque, A. Descoteaux, Macrophage cytokines: involvement in immunity and infectious diseases. *Front Immunol* **5**, 491 (2014).
5. S. M. Jones, M. A. Moors, Q. Ryan, K. K. Klyczek, K. J. Blank, Altered macrophage antigen-presenting cell function following Friend leukemia virus infection. *Viral Immunol* **5**, 201-211 (1992).
6. E. R. Unanue, Antigen-presenting function of the macrophage. *Annu Rev Immunol* **2**, 395-428 (1984).
7. J. Cole, J. Aberdein, J. Jubrail, D. H. Dockrell, The role of macrophages in the innate immune response to Streptococcus pneumoniae and Staphylococcus aureus: mechanisms and contrasts. *Adv Microb Physiol* **65**, 125-202 (2014).
8. D. Hirayama, T. Iida, H. Nakase, The Phagocytic Function of Macrophage-Enforcing Innate Immunity and Tissue Homeostasis. *Int J Mol Sci* **19**, (2017).
9. C. Rosales, E. Uribe-Querol, Phagocytosis: A Fundamental Process in Immunity. *Biomed Res Int* **2017**, 9042851 (2017).
10. D. A. Ovchinnikov, Macrophages in the embryo and beyond: much more than just giant phagocytes. *Genesis* **46**, 447-462 (2008).
11. C. Varol, A. Mildner, S. Jung, Macrophages: development and tissue specialization. *Annu Rev Immunol* **33**, 643-675 (2015).
12. S. Hao, A. Dey, X. Yu, A. M. Stranahan, Dietary obesity reversibly induces synaptic stripping by microglia and impairs hippocampal plasticity. *Brain Behav Immun* **51**, 230-239 (2016).
13. H. Kettenmann, F. Kirchhoff, A. Verkhratsky, Microglia: new roles for the synaptic stripper. *Neuron* **77**, 10-18 (2013).
14. V. H. Perry, V. O'Connor, The role of microglia in synaptic stripping and synaptic degeneration: a revised perspective. *ASN Neuro* **2**, e00047 (2010).
15. B. D. Trapp *et al.*, Evidence for synaptic stripping by cortical microglia. *Glia* **55**, 360-368 (2007).
16. M. Katagiri *et al.*, Mechanism of stimulation of osteoclastic bone resorption through Gas6/Tyro 3, a receptor tyrosine kinase signaling, in mouse osteoclasts. *J Biol Chem* **276**, 7376-7382 (2001).
17. S. L. Teitelbaum, Bone resorption by osteoclasts. *Science* **289**, 1504-1508 (2000).
18. B. R. Coats *et al.*, Metabolically Activated Adipose Tissue Macrophages Perform Detrimental and Beneficial Functions during Diet-Induced Obesity. *Cell Rep* **20**, 3149-3161 (2017).
19. A. W. Ferrante, Jr., Macrophages, fat, and the emergence of immunometabolism. *J Clin Invest* **123**, 4992-4993 (2013).
20. A. W. Ferrante, Jr., The immune cells in adipose tissue. *Diabetes Obes Metab* **15 Suppl 3**, 34-38 (2013).
21. A. R. Nawrocki, P. E. Scherer, The delicate balance between fat and muscle: adipokines in metabolic disease and musculoskeletal inflammation. *Curr Opin Pharmacol* **4**, 281-289 (2004).
22. H. Shapiro *et al.*, Adipose tissue foam cells are present in human obesity. *J Clin Endocrinol Metab* **98**, 1173-1181 (2013).
23. N. K. Edens, R. L. Leibel, J. Hirsch, Mechanism of free fatty acid re-esterification in human adipocytes in vitro. *J Lipid Res* **31**, 1423-1431 (1990).
24. N. D. Roe, M. K. Handzlik, T. Li, R. Tian, The Role of Diacylglycerol Acyltransferase (DGAT) 1 and 2 in Cardiac Metabolism and Function. *Sci Rep* **8**, 4983 (2018).
25. C. L. Yen, S. J. Stone, S. Koliwad, C. Harris, R. V. Farese, Jr., Thematic review series: glycerolipids. DGAT enzymes and triacylglycerol biosynthesis. *J Lipid Res* **49**, 2283-2301 (2008).
26. K. J. McKelvey, K. L. Powell, A. W. Ashton, J. M. Morris, S. A. McCracken, Exosomes: Mechanisms of Uptake. *J Circ Biomark* **4**, 7 (2015).
27. Y. Lv, L. Fang, P. Ding, R. Liu, PI3K/Akt-Beclin1 signaling pathway positively regulates phagocytosis and negatively mediates NF-kappaB-dependent inflammation in Staphylococcus aureus-infected macrophages. *Biochem Biophys Res Commun* **510**, 284-289 (2019).

28. L. Boutens *et al.*, Unique metabolic activation of adipose tissue macrophages in obesity promotes inflammatory responses. *Diabetologia* **61**, 942-953 (2018).
29. E. L. Gautier *et al.*, Gene-expression profiles and transcriptional regulatory pathways that underlie the identity and diversity of mouse tissue macrophages. *Nat Immunol* **13**, 1118-1128 (2012).
30. D. A. Hill *et al.*, Distinct macrophage populations direct inflammatory versus physiological changes in adipose tissue. *Proc Natl Acad Sci U S A* **115**, E5096-E5105 (2018).
31. C. Benoist, L. Lanier, M. Merad, D. Mathis, P. Immunological Genome, Consortium biology in immunology: the perspective from the Immunological Genome Project. *Nat Rev Immunol* **12**, 734-740 (2012).
32. T. S. Heng, M. W. Painter, C. Immunological Genome Project, The Immunological Genome Project: networks of gene expression in immune cells. *Nat Immunol* **9**, 1091-1094 (2008).
33. T. Shay, J. Kang, Immunological Genome Project and systems immunology. *Trends Immunol* **34**, 602-609 (2013).

## CHAPTER 4: EXPLORING MECHANISMS THAT CONTROL ADIPOSE TISSUE-DERIVED EXOSOME RELEASE AND ESCAPE INTO CIRCULATION

### 4.1 Results

Obesity is a growing epidemic in the US and the world. Obesity is described as a state of excess body fat with expansion of adipose tissue. Roughly 40% of the US population is currently obese, and it is expected that 50% of the US population will be obese by 2030 (*1-3*). Obesity is associated with many complications, including atherosclerosis, type 2 diabetes mellitus (T2DM), and cancers, all contributing to premature death (*4-7*). The mechanism as to how obesity contributes to its complications is unknown. Although increasing BMI is correlated with one's risk for developing these diseases, there remain certain populations of extremely obese individuals with normal metabolic health and no indications of heart disease or cancer development (*8*). Understanding the how obesity increases morbidity and mortality would provide the opportunity to develop better therapies to treat obesity-associated disorders.

Some of the leading theories of the pathogenesis of obesity's co-morbidities include adipose tissue inflammation and ectopic lipid deposition (*9*). The former focuses on the finding that as obesity progresses, the number of macrophages in adipose tissue grows significantly (*10*). The amount of inflammation in adipose tissue correlates very strongly with one's risk for developing insulin resistance, a relationship that is even stronger than the relationship between insulin resistance risk and BMI (*11-15*). Several groups have found that inflammatory signaling is capable of inducing insulin resistance in energetic cells, however anti-inflammatory interventions for T2DM have been largely unsuccessful (*16-18*).

Another possible player in the pathogenesis of the co-morbidities of obesity is ectopic lipid deposition. Triglyceride storage in ectopic (non-adipose tissue) depots is a common symptom of obesity (*19*). The phenomenon has also been shown to correlate very strongly with risk for T2DM, atherosclerosis, and fatty liver disease (*9, 19-22*). The mechanism of action is thought to be carried out by lipid intermediate species that disrupt normal cell function (*23-25*). Effective therapies to resolve this

symptom in a targeted fashion have yet to be identified, however, exercise has been shown to clear ectopic depots of triglyceride and increase insulin sensitivity in those tissues (*26-28*).

Obesity is assuredly a very complex disorder and affects the homeostasis of many different organ systems, but seems to particularly center around the adipose tissue. Obesity can have dramatic effects in adipose tissue, including drastic changes in the compositions of cell-types contained within it and in the architecture of its parenchymal cells (*29, 30*). During obesity adipocytes can grow ~20-fold in diameter, increasing their lipid stores by several thousand-fold (*31*). Obesity has been shown to significantly alter much of the adipokine signaling from adipocytes (*32, 33*). Obesity is also known to increase baseline free fatty acid release from adipocytes and can induce insulin resistance in adipocytes, themselves (*20*).

Given that obesity induces adipose tissue macrophage accumulation, increased lipid release from adipocytes, and non-adipocyte triglyceride deposition, determining whether AdExos react to obesity is particularly relevant, having shown that AdExos are taken up by adipose tissue macrophages and can induce triglyceride accumulation in non-adipocytes.

To determine whether the triglyceride content of AdExos is increased in the state of obesity, PGAT was taken from WT and leptin-deficient *Lep*$^{ob/ob}$ mice and cultured for 16 hours. AdExos were isolated from the conditioned medium and analyzed using enzymatic assays. AdExos released from obese PGAT were determined to contain ~2.5 µmol of acylglyceride per gram of tissue, released every hour (Figure 4.1). This is equivalent to ~0.1% of the total acylglyceride content of the tissue and over twice the amount that is released from lean PGAT (Figure 4.2). The total mass of PGAT from the leptin-deficient mice is roughly six times as large (Figure 4.3). Acylglyceride measurements for AdExos are normalized by tissue mass and adipocytes are typically much more massive in the state of obesity, indicating that the amount of AdExo acylglyceride per adipocyte is likely increased even more than 2-fold in obese PGAT.

To determine how AdExo lipid composition is altered in the obese state, targeted lipidomics was performed on AdExos from lean and obese PGAT. Surprisingly, the lipid profiles of obese AdExos were very similar to lean AdExos, with some minor differences in sphingomyelin and free cholesterol concentrations (Figure 4.4). The relative molar amounts of lipids in the AdExos, largely did not change, even the relative amounts of tri- and mono-acylglycerides (Figure 4.4). This was particularly interesting, considering the increased total acylglyceride being released from obese PGAT (Figure 4.2). Thus, we decided to investigate the number of exosomes being released from PGAT in each condition.

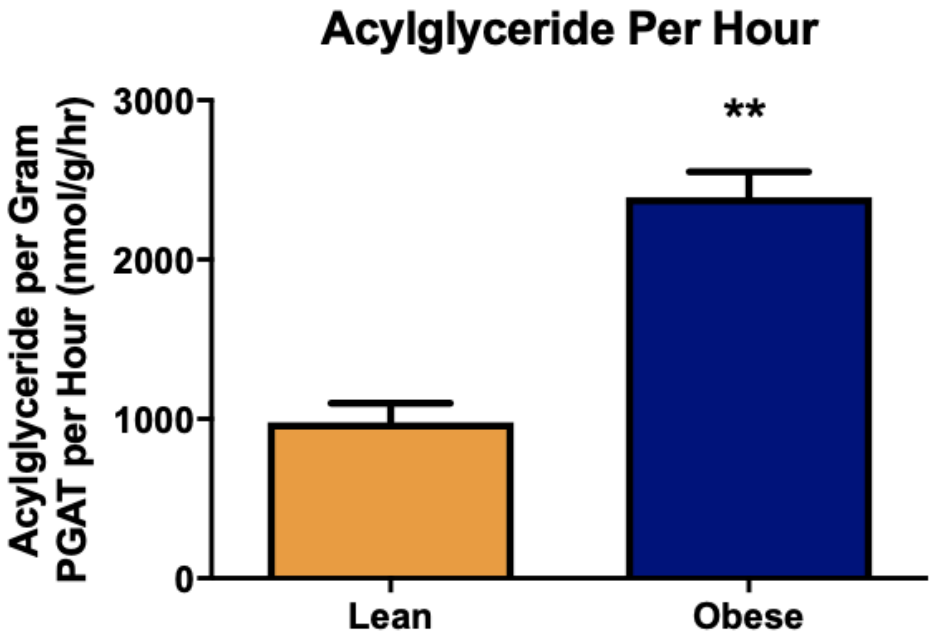


**Figure 4.1. Obesity increases the amount of acylglyceride released in AdExos from PGAT by two-fold.** Acylglyceride content of exosomes isolated from the PGAT of WT or *Lep*$^{ob/ob}$ mice, expressed per g of tissue per hour. Unpaired two-tailed t test; n = 8; **P < 0.005. Error bars represent SD.

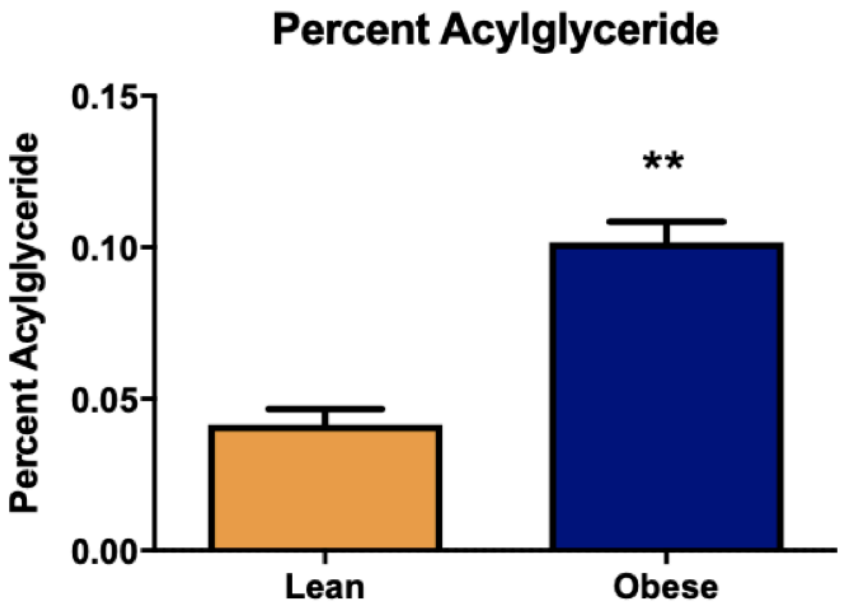


**Figure 4.2. Obese PGAT releases 0.1% of total acylglyceride content in AdExos.** Acylglyceride content of purified adipocyte-derived exosomes from WT or *Lep*$^{ob/ob}$ PGAT, expressed as a percentage of the acylglyceride content of the tissue itself. Unpaired two-tailed t test; n = 8; **P < 0.005. Error bars represent SD.

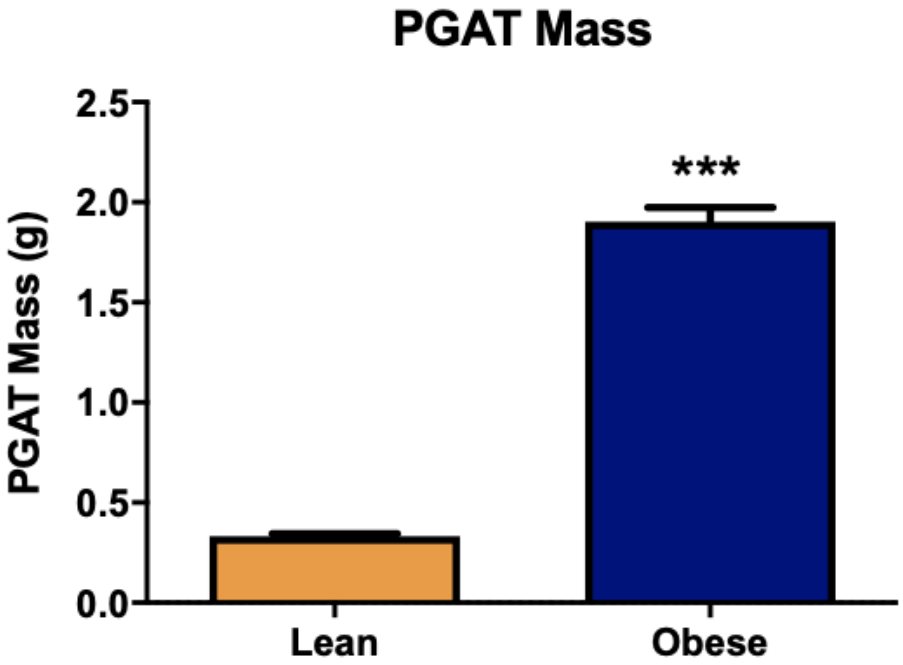


**Figure 4.3. Obese PGAT is more massive than lean PGAT.** Mass of total PGAT removed from WT and *Lep*$^{ob/ob}$ mice. Unpaired two-tailed t test; n = 8; ***P < 0.001. Error bars represent SD

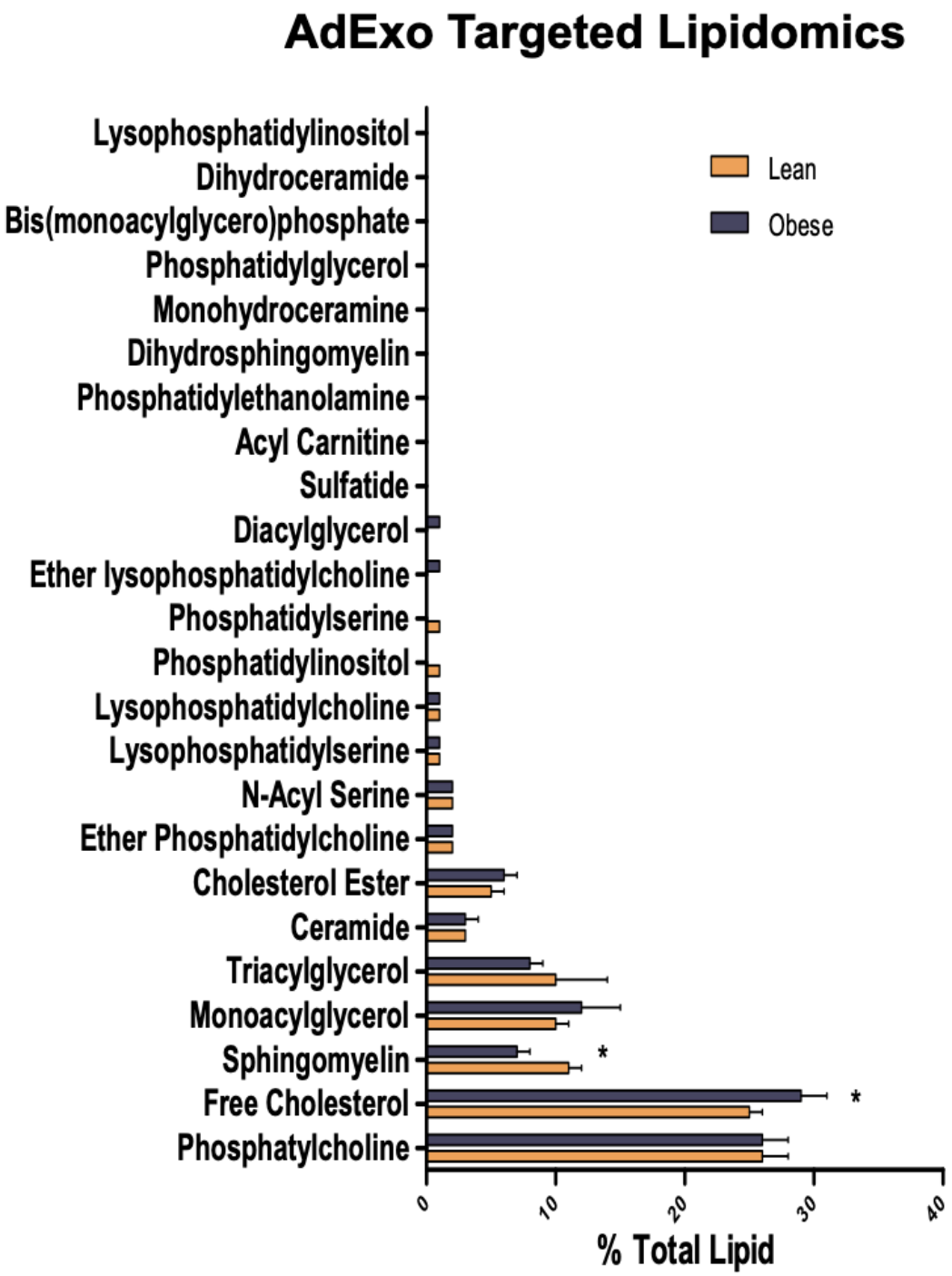


**Figure 4.4. Obese AdExos have similar lipid content profile to lean AdExos.** Targeted lipidomics of adipocyte-derived exosomes isolated from WT and *Lep*$^{ob/ob}$ mouse PGAT. Unpaired, two-tailed T-Test; n=3; * p-value < 0.05.

Obese PGAT was found to release ~$3.5x10^{11}$ exosomes per gram of tissue per hour (Figure 4.5). This number, again, was more than twice the amount released from lean PGAT and seems sufficient to explain the discrepancy in total acylglyceride released. On the macro-scale, the relative amounts of lipids within a single AdExo doesn't change from lean state to obese state, however, the number of particles released doubles, and therefore so does the total amount of acylglyceride contained within AdExos. The size distribution of AdExo particles from obese PGAT also looks very similar to those from lean tissue (Figure 4.6). There is perhaps a small rightward shift in the distribution, indicating slightly more particles with larger diameters in the obese AdExo samples, however the mean diameter of obese AdExos (115 +/- 54nm) was smaller than mean diameter of lean AdExos (118 +/- 57nm). The median of the obese AdExo distribution was 104nm, whereas the median diameter for lean AdExos was 102nm. Overall, obese AdExos and lean AdExos were strikingly similar (Supplemental Figure 4.1).

If obesity can be considered as the state of energy overabundance, fasting can be considered the state of energy underabundance. To determine whether fasting would have any effect on AdExo release rates, mice were fasted for 16 hours overnight. PGAT was harvested from these animals and cultured for 16 hours. AdExos were isolated and investigated using enzymatic assays and nanoparticle tracking analysis. AdExo acylglyceride content was significantly increased in fasted animals, even more so than obese animals (Figure 4.7). This was once again accompanied by a proportional increase in AdExo number (Figure 4.8). The size distribution of AdExos from fasted PGAT was very similar to those from lean fed PGAT, with a mean diameter of 112 +/- 60 nm and a median diameter of 101 nm (Figure 4.9). These data seem to indicate that in the fasting and obese states, the structure of exosomes being released appear to be very similar, however, the release rates of exosomes are greatly affected.

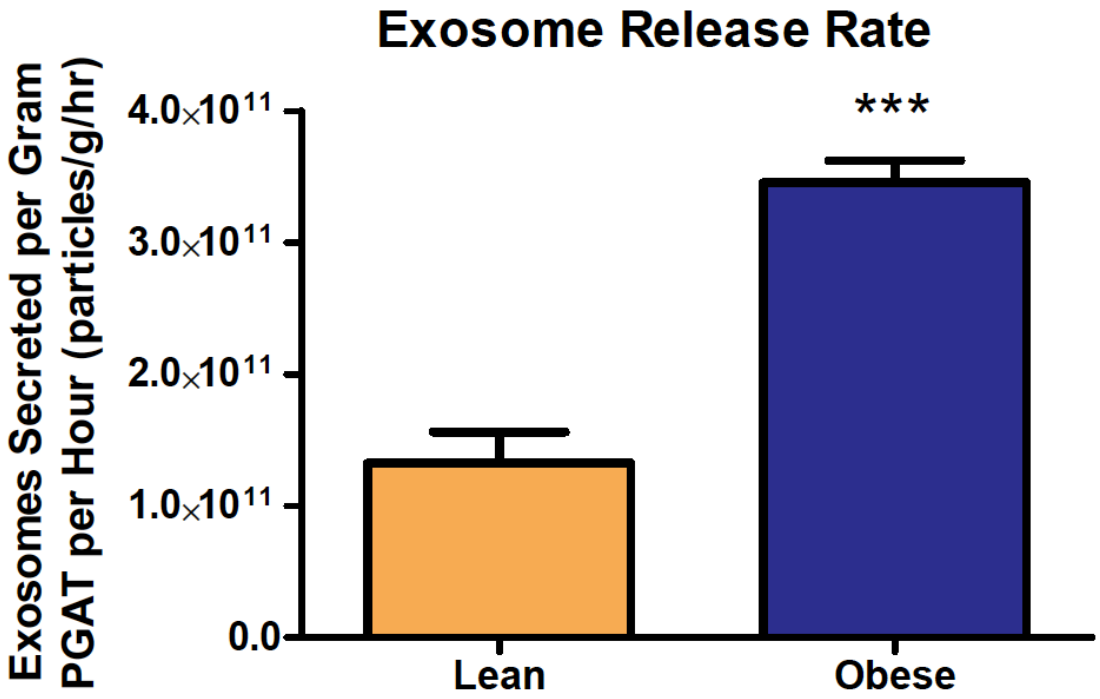


**Figure 4.5. Obese PGAT secretes more AdExos.** Quantification of exosomes released by adipose tissue per gram per hour from adipose tissue from lean and *Lep*$^{ob/ob}$ mice, as measured by Nanoparticle Tracking Analysis. Unpaired two-tailed t test; n = 8; ***P < 0.001. Error bars represent SD.

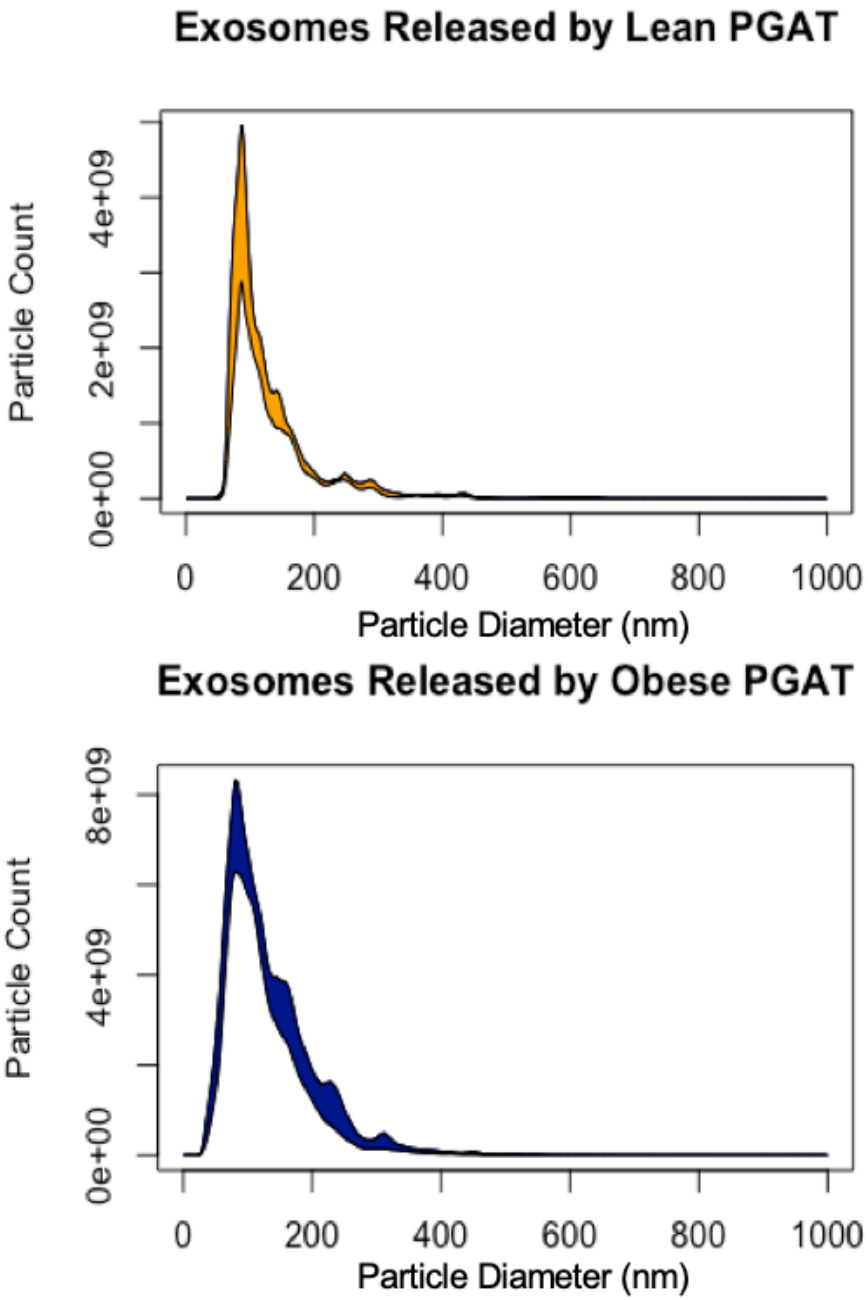


**Figure 4.6. Obese AdExo size distribution.** Nanoparticle tracking analysis histogram of purified adipose tissue-derived exosomes, depicting particle diameter and the number of particles at each diameter released by 1 g of lean (top, orange) or leptin-deficient obese (*Lep*$^{ob/ob}$) (bottom, blue) adipose tissue per hour.

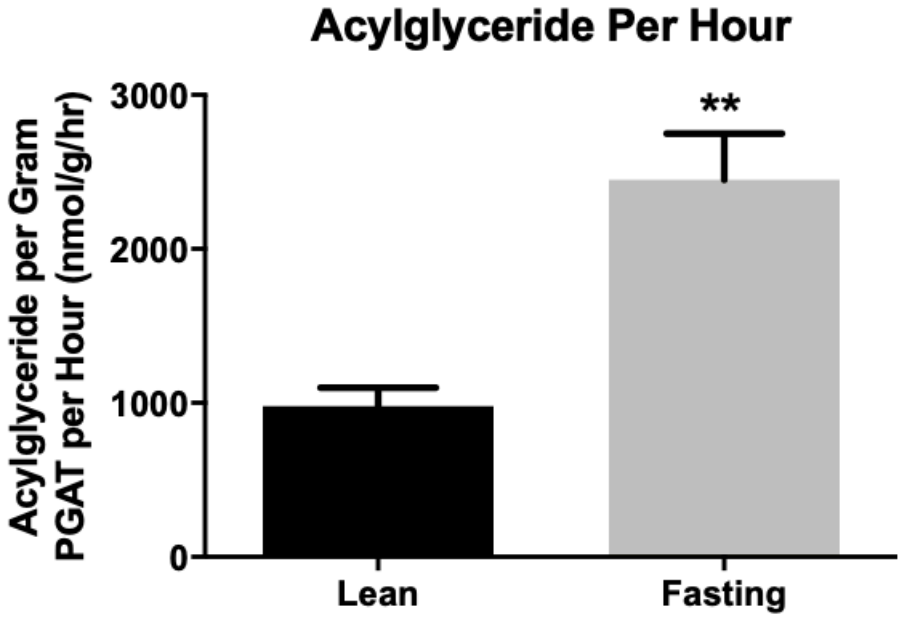


**Figure 4.7. Fasting increases acylglyceride released in AdExos.** Acylglyceride content of exosomes isolated from PGAT of lean mice fed *ad lib* or fasted for 16 hours, expressed per g of tissue per hour. Unpaired two-tailed t test; n = 8; **P < 0.005. Error bars represent SD.

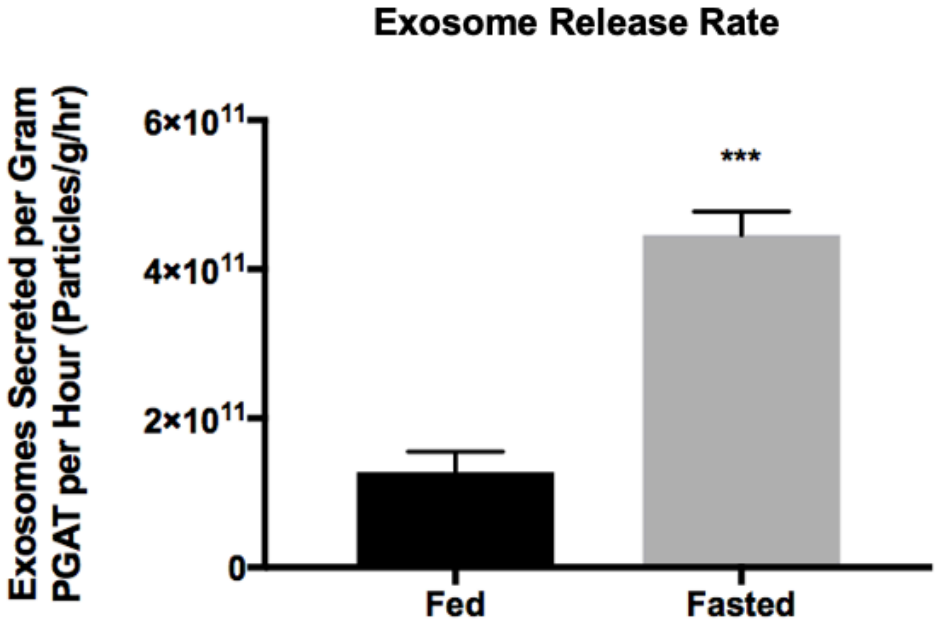


**Figure 4.8. Fasting increases AdExo release rate.** Quantification of exosomes released by adipose tissue per gram per hour from PGAT of WT fed and fasted mice, as measured by Nanoparticle Tracking Analysis. Unpaired two-tailed t test; n = 8; ***P < 0.001. Error bars represent SD.

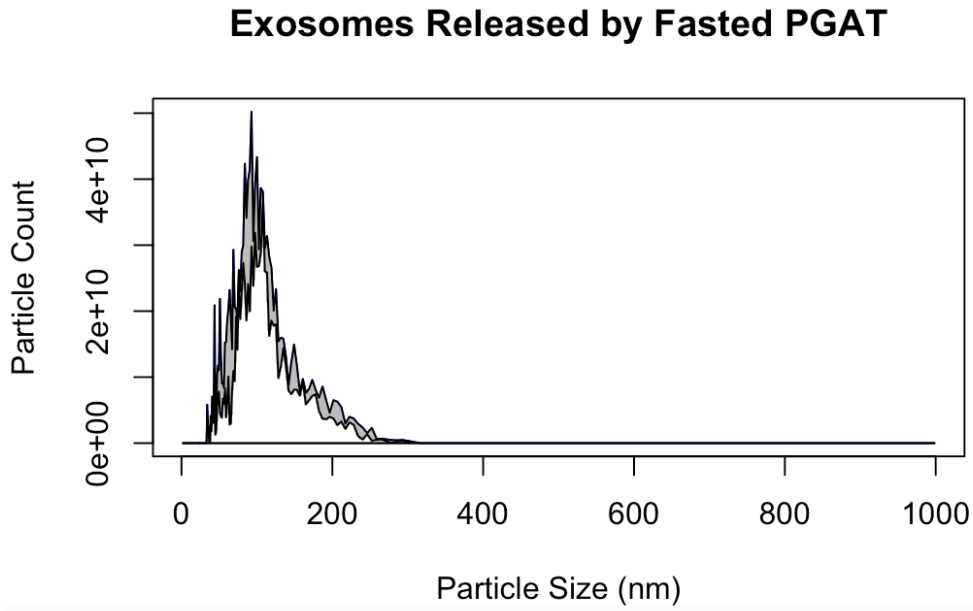


**Figure 4.9. Fasting Viewsizer Profile.** Viewsizer 3000 Nanoparticle Tracking Analysis histogram of purified adipose tissue-derived exosomes from WT fasted mice, depicting particle diameter and the number of particles at each diameter released by 1 g of lean adipose tissue per hour.

The fact that AdExo release is increased by both fasting and obesity is fairly interesting. In terms of understanding the mechanisms that control release, these two findings alone would indicate that AdExo release rate is not defined by energetic need, at least not solely, nor is it set by cell size. Interestingly, in both fasting and obesity, adipocyte lipolysis is known to increase, so it is possible that AdExo release is controlled by the same or similar signaling pathways that control lipid release as free fatty acids (*34*-*38*).

To identify potential physiological mechanisms of AdExo release, PGAT explants were treated with various pharmacological compounds. These compounds included common metabolic signaling hormones, such as insulin and glucagon, which has been previously shown to impact exosome release from adipose tissue (*39*). Drugs for the treatment of T2DM, like Rosiglitazone were used, as well as adrenergic stimulators, like CL 243,316. Surprisingly, no treatments to PGAT explants have induced any changes in the number of AdExos released from the tissue (Figure 4.10). CL 243,316 treatment was capable of increasing lipolysis in the PGAT explants, but had no effect on AdExo release, indicating that AdExo release rate is not determined by adrenergic stimulation (Figure 4.11, Figure 4.12).

We have seen that both obesity and fasting can lead to increased release of acylglyceride in AdExos (Figure 4.1, Figure 4.7). We have also seen that AdExos are taken up primarily by F4/80+ macrophages in the adipose tissue (Figure 3.4), and that they are capable of inducing neutral lipid accumulation in naïve BMDMs (Figure 3.5). To identify the effects of fasting and obesity on ATMs *in* vivo, primary stromal vascular cells were isolated from obese PGAT, and lean PGAT fed *ad lib* or fasted for 16 hours. These SVCs were investigated using confocal microscopy and ATMs from obese or fasted mice were found to contain increased neutral lipid (Figure 4.13). This finding is consistent with previous data in supporting the hypothesis that AdExos are capable of transporting triglyceride to local macrophages and inducing lipid accumulation in those cells.

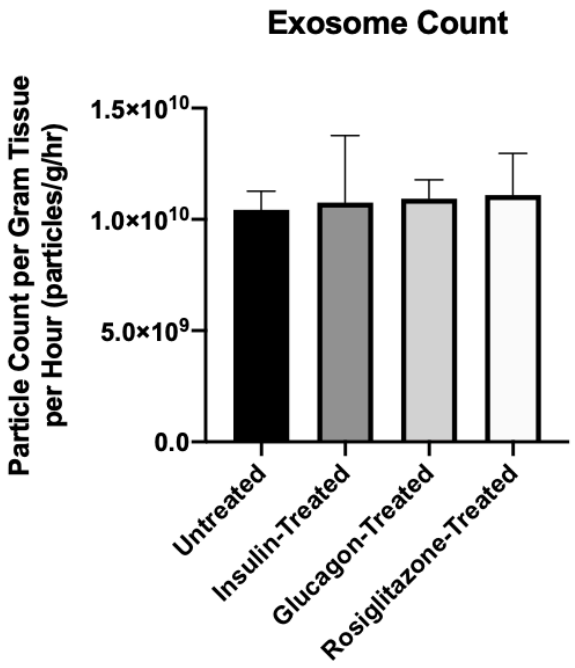


**Figure 4.10. AdExo release rate not affected by metabolic hormones.** Quantification of exosomes released by adipose tissue per gram per hour from WT PGAT explants. Explants were untreated or treated with insulin, glucagon, or rosiglitazone. Measurements were made by Viewsizer 3000 Nanoparticle Tracking Analysis. Error bars represent SD.

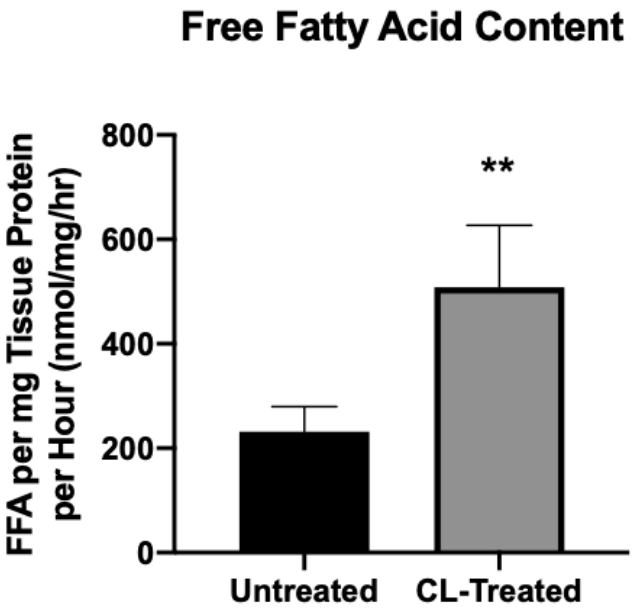


**Figure 4.11. CL-Treatment increases PGAT FFA release.** Free fatty acid content of PGAT conditioned medium cultured untreated or with CL-243,316 for 16 hours per gram per hour. Unpaired two-tailed t test; n = 6; **, P < 0.005.

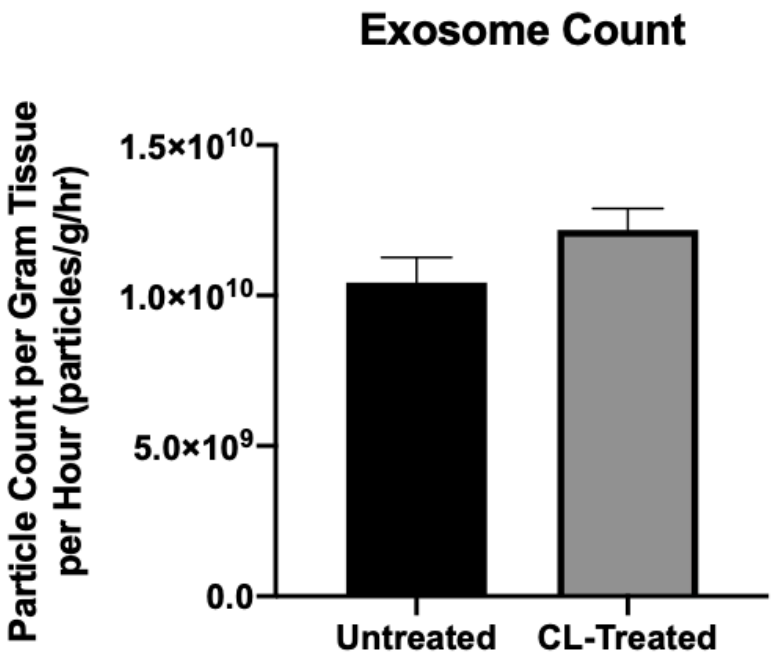


**Figure 4.12. CL-Treatment does not affect AdExo release from PGAT.** Quantification of exosomes released by adipose tissue per gram per hour from WT PGAT explants. Explants were untreated or treated with CL-243,316. Measurements were made by Viewsizer 3000 Nanoparticle Tracking Analysis. Error bars represent SD.

This raises the question of whether endogenous AdExos are capable of escaping the adipose tissue and being taken up by cells in other tissues. To begin answering these questions, we made a transgenic mouse that expresses the fluorescent marker protein tdTomato specifically in adipocytes (Figure 4.14). TdTomato protein was detectably expressed in adipocyte-tomato-expressing (AdTom) PGAT, and undetectable in WT (Figure 4.15). TdTomato protein was not present in the adiponectin-lacking stromal vascular cells of AdTom PGAT (Figure 4.15). And tdTomato was present in AdExos derived from AdTom PGAT (Figure 4.15). The fluorescence of the tdTomato was also detectable in AdTom AdExos using fluorescent spectrophotometry, whereas WT AdExos contained no such fluorescence, again confirming that some portion of the AdExos are derived from adipocytes (Figure 4.16).

To determine the rough proportion of exosomes released by adipose tissue that are derived from adipocytes, AdExos were isolated from AdTom PGAT and measured via fluorescent spectrophotometry and nanoparticle tracking analysis to establish a ratio of fluorescence per exosome. AdTom PGAT was then separated into its adipocyte and non-adipocyte (SVC) fractions. These cells were cultured, AdExos were isolated from the conditioned media, and the AdExos were analyzed in the same way to determine the ratio between tdTomato fluorescence and exosome count. As was expected exosomes released from AdTom SVCs had nearly no detectable fluorescence per exosome (Figure 4.17). AdTom adipocyte cultures released exosomes with roughly similar amounts of fluorescence per exosome as whole AdTom PGAT released (Figure 4.17), seeming to indicate that a majority of the AdExos being released by PGAT are adipocyte-derived.

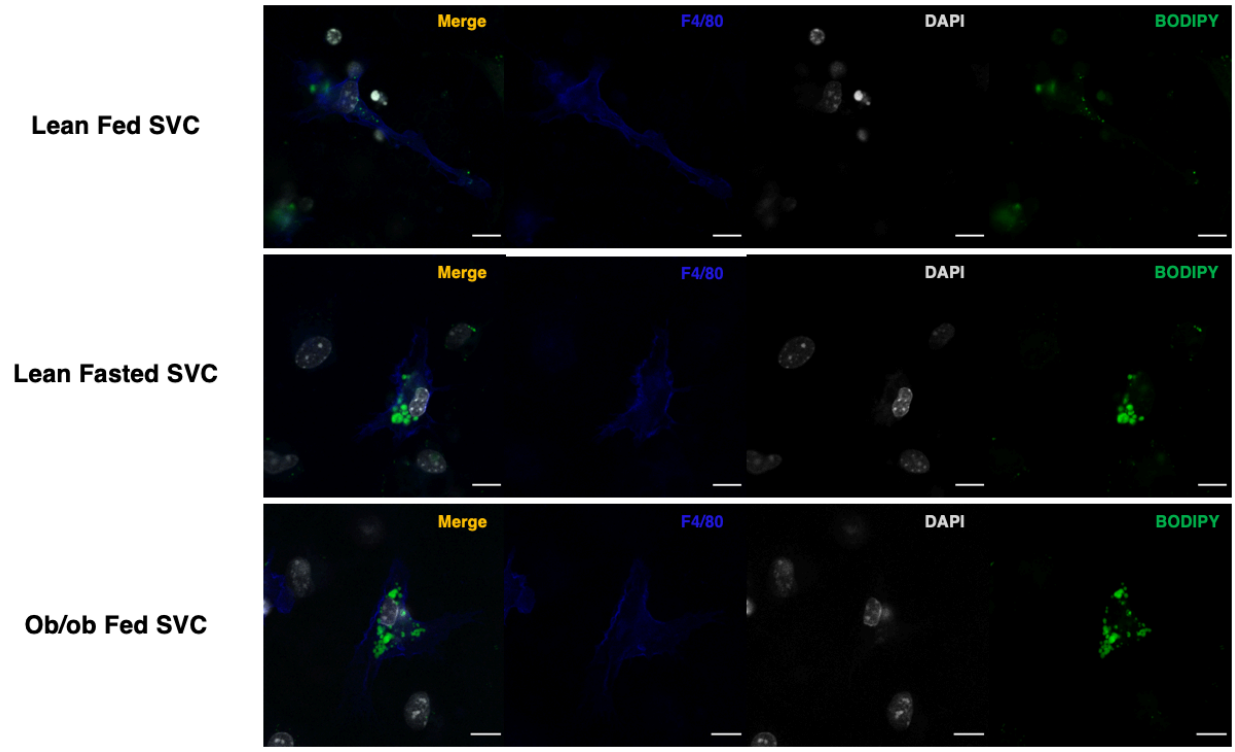


**Figure 4.13. Obesity and fasting increases ATM neutral lipid content.** Confocal microscopy images of primary stromal vascular cells that were isolated from *Lep*$^{ob/ob}$ (bottom), or WT fed (top) and fasted (middle) mice. SVCs were plated and immunostained with antibodies against F4/80 (blue), as well as DNA fluorescent stain DAPI (white) and neutral lipid fluorescent stain BODIPY (green). Scale bars, 10 μm.

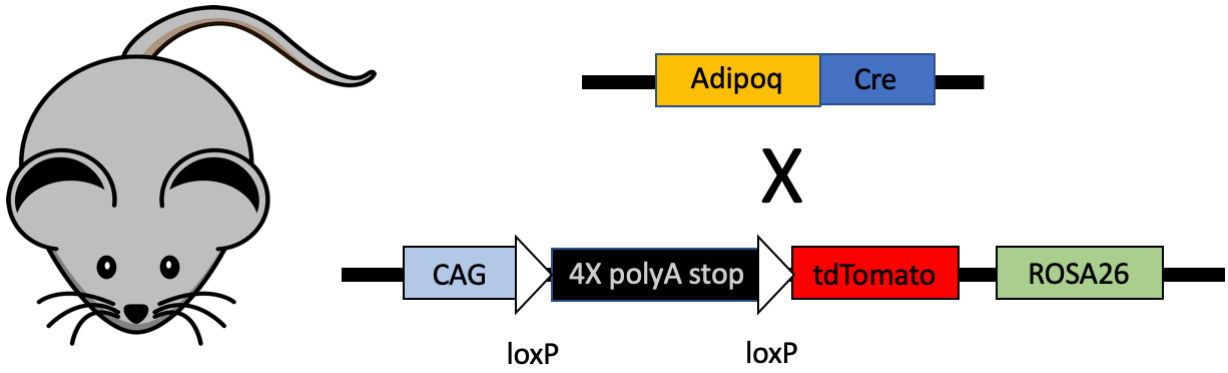


**Figure 4.14. Scheme describing the generation of the AdTom reporter mouse.**

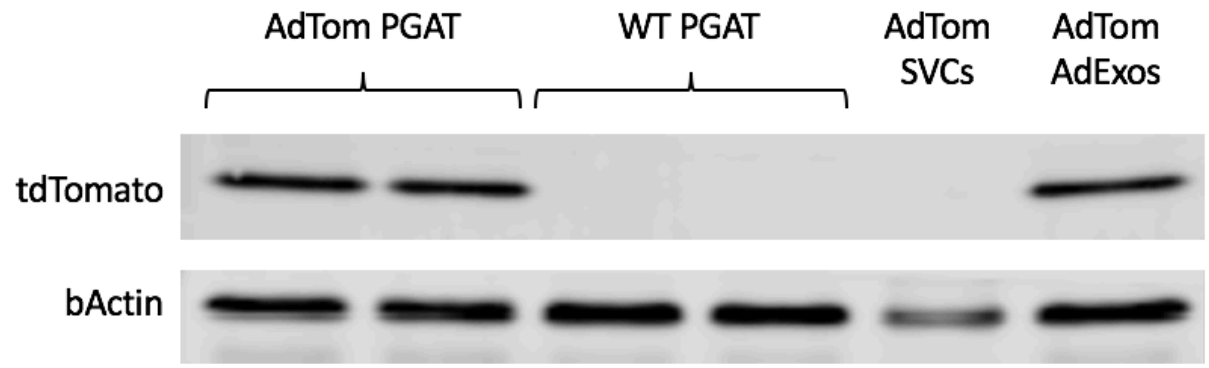


**Figure 4.15. TdTomato protein is contained within AdTom AdExos.** Western blot of total protein from whole AdTom PGAT, WT PGAT, SVCs isolated from AdTom PGAT, and AdExos isolated from AdTom PGAT. Blots were probed using antibodies against tdTomato and bActin.

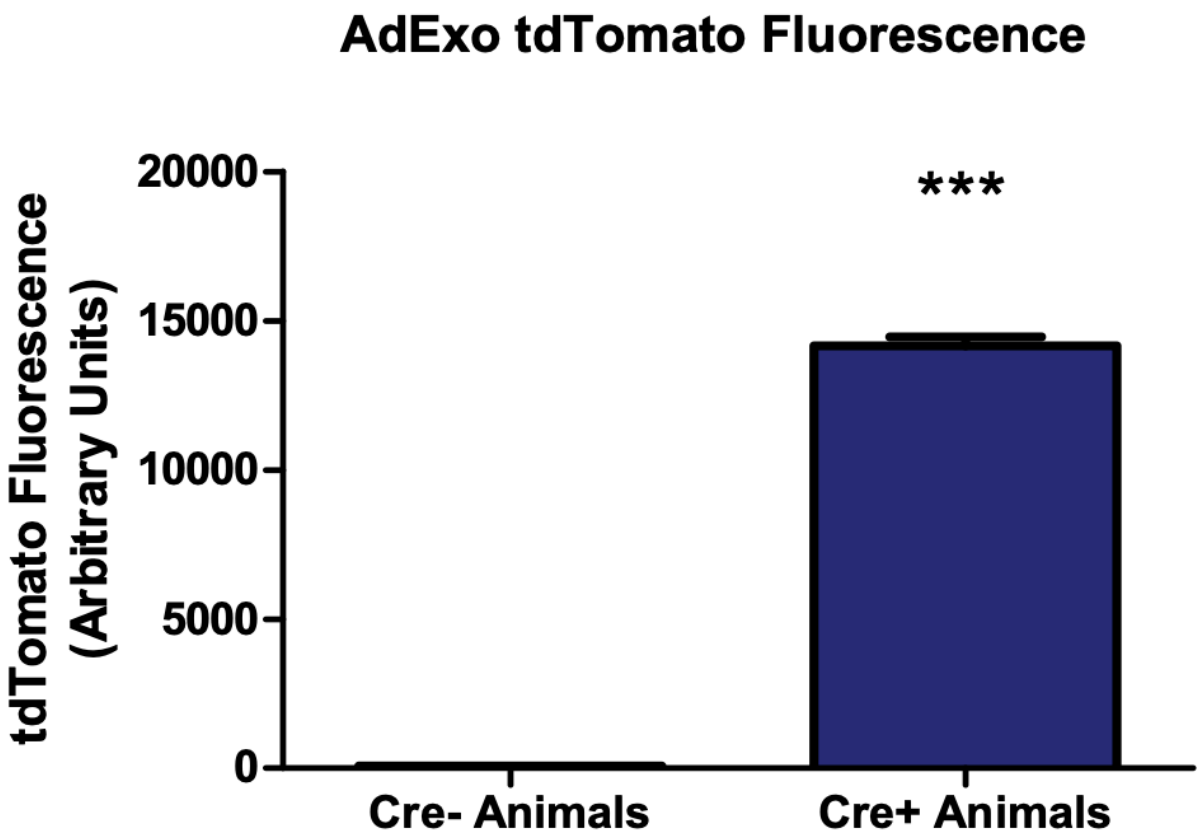


**Figure 4.16. AdTom AdExos contain tdTomato fluorescence.** Relative tdTomato fluorescence of AdExos isolated from control (Cre-) or AdTom (Cre+) PGAT in which the fluorescent protein was either not expressed (Cre-) or expressed specifically in adipocytes (Cre+). Unpaired two-tailed t test; n = 4; *** p-value < 0.001, Error bars represent SD.

Serum samples were taken from AdTom mice to establish whether AdExos are escaping into circulation. Circulating exosomes were isolated from AdTom serum samples and western blotting revealed the presence of tdTomato protein within the exosome fraction (Figure 4.18). This confirmed that AdExos were escaping adipose tissue and contributing to the circulating exosome population. As a rough quantitative measure, the ratio of CD63 (canonical exosomal marker) to tdTomato protein content was calculated for exosomes from PGAT explants vs exosomes from circulation. Explant-derived AdExos contained an ~11-fold higher tdTomato/CD63 ratio compared to those from circulation (Figure 4.19), indicating that they represent a minority of the lipid species in circulation.

Efforts to detect tdTomato outside of adipose tissue have been fruitless. As mentioned above, even SVCs within AdTom PGAT, which are known to take up AdExos, contained no detectable signal (Figure 4.15). If AdTom AdExos are also labeled with PKH67 fluorescence before they are added to BMDMs, PKH67 can be easily identified within the cells, whereas no tdTomato fluorescence or protein signal can be detected in the cells (Figure 4.20). Our best hypothesis to explain this phenomenon is that the tdTomato protein is being degraded. AdExos have been shown to be taken up via macropinocytosis (Figure 3.10), which means they likely go through an endosomal/lysosomal pathway. It is possible that certain cytosolic proteins in the AdExos are degraded, while membrane-bound dyes, like PKH67 are protected from macrophage degradation. This investigation is ongoing and efforts to overcome this obstacle are discussed in the next chapter.

Taken together these data seem to suggest that AdExo release is controlled by energy status. Both obesity and fasting can increase the number and total acylglyceride content of exosomes released from PGAT. The physiological mechanism through which this control take place remains unknown. And we have seen that AdExos can be taken up locally by macrophages, but also escape the tissue and enter circulation (Figure 4.21).

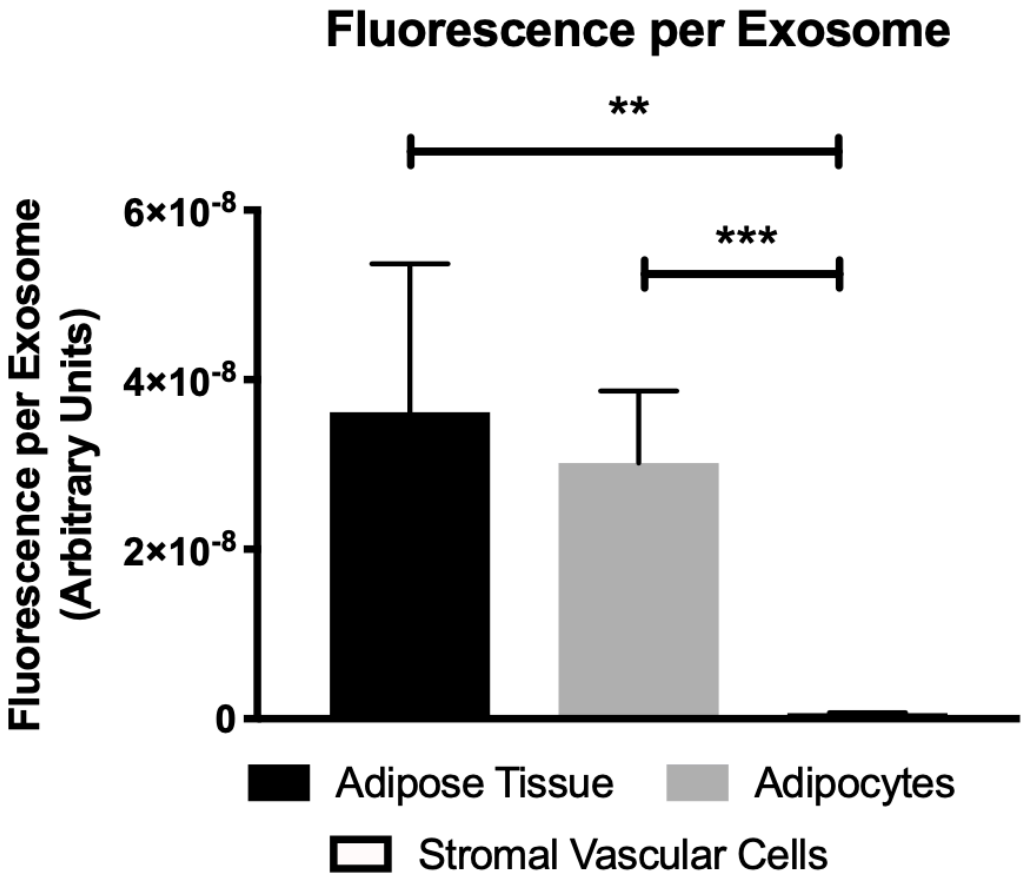


**Figure 4.17. Majority of AdExos are adipocyte-derived.** TdTomato fluorescence per exosome, as measured by nanoparticle tracking analysis, for AdExos purified from whole AdTom PGAT, adipocytes isolated from AdTom PGAT, and SVCs isolated from AdTom PGAT. One-way ANOVA; n = 4, **P < 0.01, ***P < 0.001.

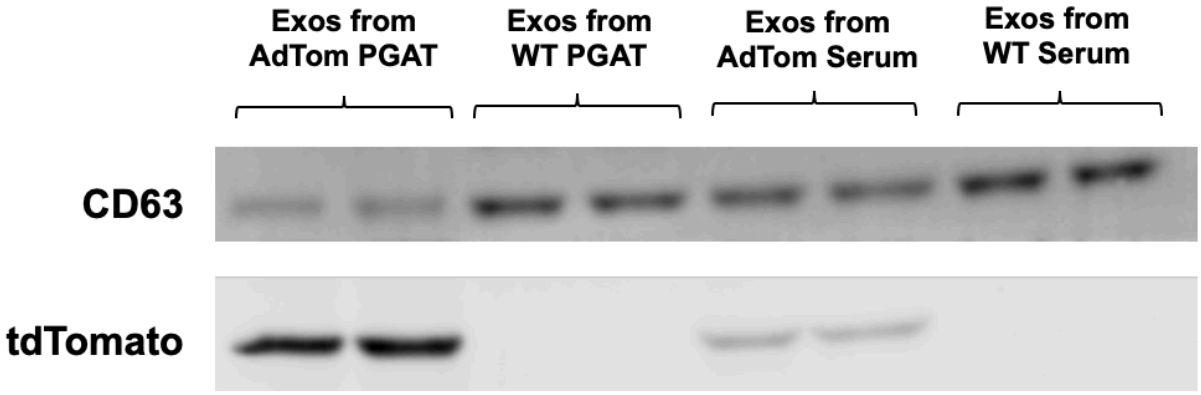


**Figure 4.18. TdTomato protein contained within AdTom circulating exosomes.** Western blot of total protein from AdExos isolated from AdTom PGAT, AdExos isolated from WT PGAT, exosomes isolated from AdTom serum, and exosomes isolated from WT serum. Blots were probed using antibodies against CD63 and tdTomato.

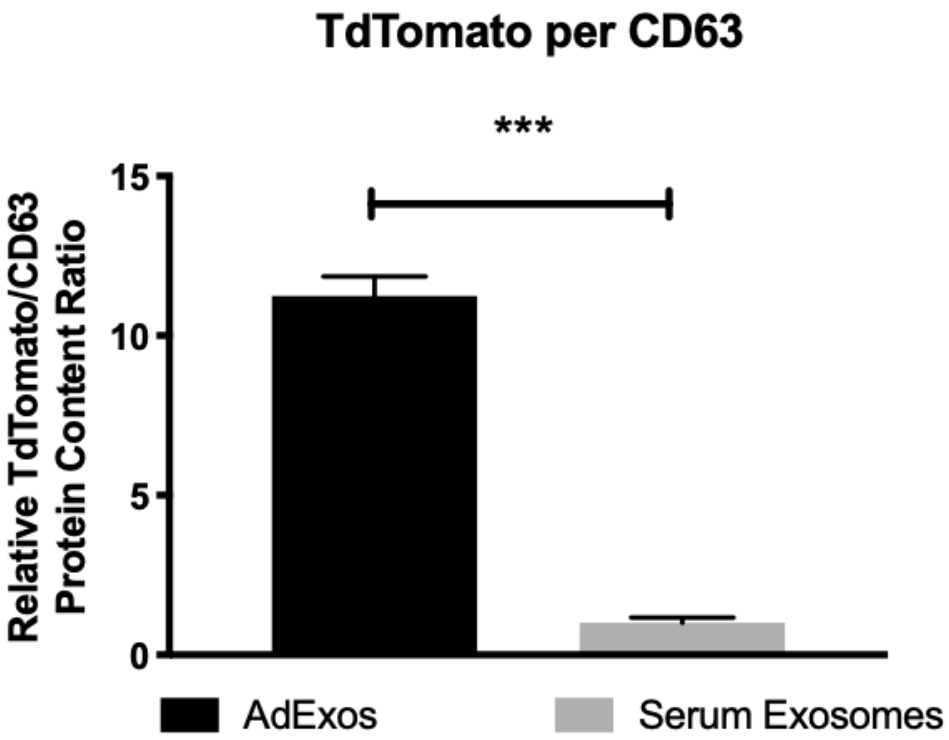


**Figure 4.19. AdExos represent minority of circulating exosomes.** Quantification of protein content of AdExos isolated from AdTom PGAT explants and serum samples, as determined by Western blot. Values are expressed as a relative ratio of tdTomato protein to CD63 protein. Unpaired two-tailed t test; n = 2; *** p-value < 0.001, Error bars represent SD.

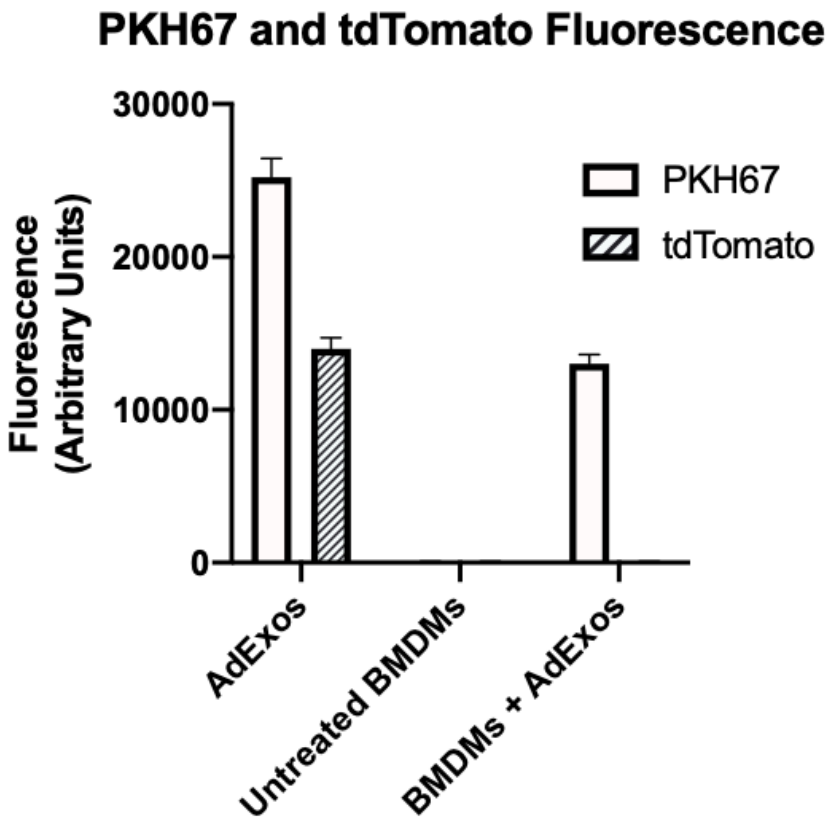


**Figure 4.20. BMDMs do not contain tdTomato fluorescence after taking up AdTom AdExos.** PKH67 and tdTomato fluorescence of AdExos and BMDMs, as measured by fluorescence spectrophotometer. AdExos were isolate from AdTom PGAT explants and labeled with PKH67, before being measured for PKH67 and tdTomato fluorescence. Naïve BMDMs untreated or treated with these labeled AdExos and then measured for PKH67 and tdTomato fluorescence.

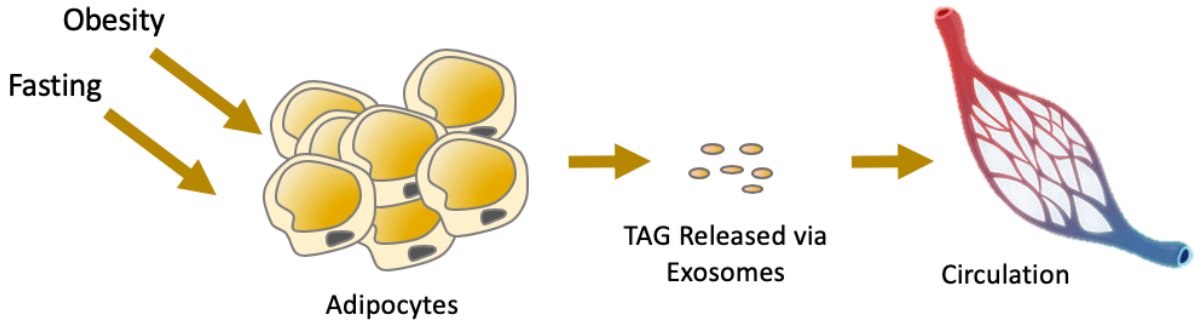


**Figure 4.21. Graphical summary of Chapter 4.**

### 4.2 References


1. L. Zamosky, Obesity's growing threat. While the adult obesity rate went up again in 2013, associated health problems could explode in the next 10 years unless patients and physicians take action. *Med Econ* **91**, 36, 38-41 (2014).
2. T. Zhang *et al.*, Rate of change in body mass index at different ages during childhood and adult obesity risk. *Pediatr Obes* **14**, e12513 (2019).
3. E. A. Finkelstein *et al.*, Obesity and severe obesity forecasts through 2030. *Am J Prev Med* **42**, 563-570 (2012).
4. F. X. Pi-Sunyer, Medical hazards of obesity. *Ann Intern Med* **119**, 655-660 (1993).
5. Long-term pharmacotherapy in the management of obesity. National Task Force on the Prevention and Treatment of Obesity. *JAMA* **276**, 1907-1915 (1996).
6. A. E. Field *et al.*, Impact of overweight on the risk of developing common chronic diseases during a 10-year period. *Arch Intern Med* **161**, 1581-1586 (2001).
7. W. C. Willett, W. H. Dietz, G. A. Colditz, Guidelines for healthy weight. *N Engl J Med* **341**, 427-434 (1999).
8. R. P. Wildman *et al.*, The obese without cardiometabolic risk factor clustering and the normal weight with cardiometabolic risk factor clustering: prevalence and correlates of 2 phenotypes among the US population (NHANES 1999-2004). *Arch Intern Med* **168**, 1617-1624 (2008).
9. J. Boren, M. R. Taskinen, S. O. Olofsson, M. Levin, Ectopic lipid storage and insulin resistance: a harmful relationship. *J Intern Med* **274**, 25-40 (2013).
10. S. P. Weisberg *et al.*, Obesity is associated with macrophage accumulation in adipose tissue. *J Clin Invest* **112**, 1796-1808 (2003).
11. M. Bluher, Adipose tissue inflammation: a cause or consequence of obesity-related insulin resistance? *Clin Sci (Lond)* **130**, 1603-1614 (2016).
12. L. Boutens, R. Stienstra, Adipose tissue macrophages: going off track during obesity. *Diabetologia* **59**, 879-894 (2016).
13. A. W. Ferrante, Jr., Macrophages, fat, and the emergence of immunometabolism. *J Clin Invest* **123**, 4992-4993 (2013).
14. C. N. Lumeng, S. M. Deyoung, J. L. Bodzin, A. R. Saltiel, Increased inflammatory properties of adipose tissue macrophages recruited during diet-induced obesity. *Diabetes* **56**, 16-23 (2007).
15. L. Russo, C. N. Lumeng, Properties and functions of adipose tissue macrophages in obesity. *Immunology* **155**, 407-417 (2018).
16. M. C. Arkan *et al.*, IKK-beta links inflammation to obesity-induced insulin resistance. *Nat Med* **11**, 191-198 (2005).
17. J. M. Olefsky, C. K. Glass, Macrophages, inflammation, and insulin resistance. *Annu Rev Physiol* **72**, 219-246 (2010).
18. Z. G. Gao, J. P. Ye, Why do anti-inflammatory therapies fail to improve insulin sensitivity? *Acta Pharmacol Sin* **33**, 182-188 (2012).
19. H. Yki-Jarvinen, Ectopic fat accumulation: an important cause of insulin resistance in humans. *J R Soc Med* **95 Suppl 42**, 39-45 (2002).
20. P. Morigny, M. Houssier, E. Mouisel, D. Langin, Adipocyte lipolysis and insulin resistance. *Biochimie* **125**, 259-266 (2016).
21. G. I. Shulman, Ectopic fat in insulin resistance, dyslipidemia, and cardiometabolic disease. *N Engl J Med* **371**, 2237-2238 (2014).
22. M. Snel *et al.*, Ectopic fat and insulin resistance: pathophysiology and effect of diet and lifestyle interventions. *Int J Endocrinol* **2012**, 983814 (2012).
23. J. E. Schaffer, Lipotoxicity: when tissues overeat. *Curr Opin Lipidol* **14**, 281-287 (2003).
24. A. C. Sletten, L. R. Peterson, J. E. Schaffer, Manifestations and mechanisms of myocardial lipotoxicity in obesity. *J Intern Med* **284**, 478-491 (2018).
25. R. Zechner, F. Madeo, D. Kratky, Cytosolic lipolysis and lipophagy: two sides of the same coin. *Nat Rev Mol Cell Biol* **18**, 671-684 (2017).
26. S. Lee *et al.*, Effects of Exercise Modality on Insulin Resistance and Ectopic Fat in Adolescents with Overweight and Obesity: A Randomized Clinical Trial. *J Pediatr* **206**, 91-98 e91 (2019).

27. D. E. Larson-Meyer *et al.*, Effect of calorie restriction with or without exercise on insulin sensitivity, beta-cell function, fat cell size, and ectopic lipid in overweight subjects. *Diabetes Care* **29**, 1337-1344 (2006).
28. Y. Tamura *et al.*, Effects of diet and exercise on muscle and liver intracellular lipid contents and insulin sensitivity in type 2 diabetic patients. *J Clin Endocrinol Metab* **90**, 3191-3196 (2005).
29. J. J. Fuster, N. Ouchi, N. Gokce, K. Walsh, Obesity-Induced Changes in Adipose Tissue Microenvironment and Their Impact on Cardiovascular Disease. *Circ Res* **118**, 1786-1807 (2016).
30. S. Sam, T. Mazzone, Adipose tissue changes in obesity and the impact on metabolic function. *Transl Res* **164**, 284-292 (2014).
31. M. Jernas *et al.*, Separation of human adipocytes by size: hypertrophic fat cells display distinct gene expression. *FASEB J* **20**, 1540-1542 (2006).
32. I. M. Jazet, H. Pijl, A. E. Meinders, Adipose tissue as an endocrine organ: impact on insulin resistance. *Neth J Med* **61**, 194-212 (2003).
33. L. Bozkurt *et al.*, The Cross-Link between Adipokines, Insulin Resistance and Obesity in Offspring of Diabetic Pregnancies. *Horm Res Paediatr* **86**, 300-308 (2016).
34. M. D. Jensen, M. W. Haymond, J. E. Gerich, P. E. Cryer, J. M. Miles, Lipolysis during fasting. Decreased suppression by insulin and increased stimulation by epinephrine. *J Clin Invest* **79**, 207-213 (1987).
35. T. S. Nielsen, N. Jessen, J. O. Jorgensen, N. Moller, S. Lund, Dissecting adipose tissue lipolysis: molecular regulation and implications for metabolic disease. *J Mol Endocrinol* **52**, R199-222 (2014).
36. P. Arner, Human fat cell lipolysis: biochemistry, regulation and clinical role. *Best Pract Res Clin Endocrinol Metab* **19**, 471-482 (2005).
37. P. Arner, D. Langin, Lipolysis in lipid turnover, cancer cachexia, and obesity-induced insulin resistance. *Trends Endocrinol Metab* **25**, 255-262 (2014).
38. J. Laurencikiene *et al.*, Regulation of lipolysis in small and large fat cells of the same subject. *J Clin Endocrinol Metab* **96**, E2045-2049 (2011).
39. C. Crewe *et al.*, An Endothelial-to-Adipocyte Extracellular Vesicle Axis Governed by Metabolic State. *Cell* **175**, 695-708 e613 (2018).

# CHAPTER 5:DISCUSSION, CONCLUSIONS, AND FUTURE DIRECTIONS

## 5.1 Results

We have seen that, in addition to the FFA released during normal lipolysis, adipocytes are also capable of releasing whole TAG in exosomes (AdExos). This pathway of release is controlled, in some way, by obesity and fasting, but occurs independently from adipocyte lipase activity. AdExos are taken up at high rates by local macrophages in the PGAT. AdExos are sufficient to induce neutral lipid accumulation and an ATM-like gene expression profile in naïve macrophages. We have also seen that AdExos can leave PGAT and enter the circulation, though, whether they are picked up by or interact with cells outside of adipose tissue remains unknown (Figure 5.1).

Adipose tissue-derived exosomes in the circulation are not new. Many studies have reported adipocyte proteins and miRNA contained within circulating exosomes (*1-3*). The key questions, regarding our findings, are whether or not circulating AdExos contain neutral lipid, and whether they contribute to circulating triglyceride in any meaningful way. There have been some difficulties in getting to the bottom of these questions. Because of the high lipid content of AdExos, traditional, density-based purification strategies for exosomes proved inefficient. We were able to develop a size-fractionation strategy to effectively isolate AdExos from PGAT explant cultures. This purification process, however, presents problems when faced with isolating exosomes from serum, as circulating particles of similar size are isolated along with exosomes. Indeed, we have found that ApoB-containing particles are contained within exosome fractions from serum (Figure 5.2), contaminating potential acylglyceride quantifications.

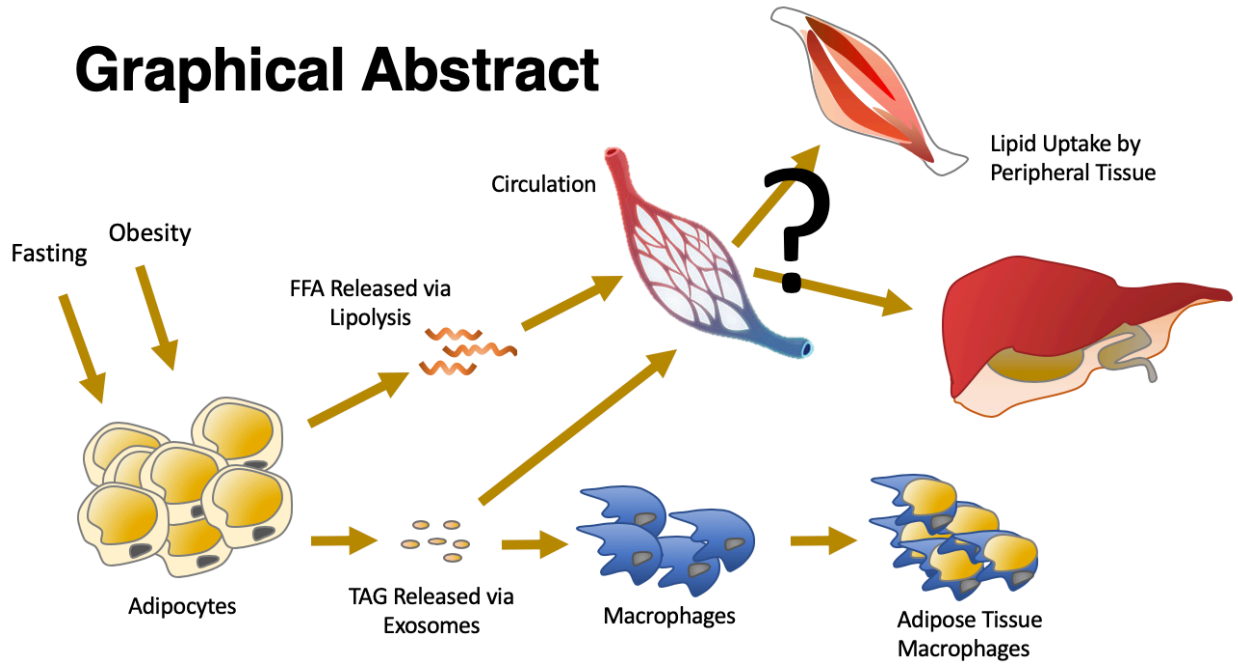


**Figure 5.1. Graphical summary of AdExo actions.**

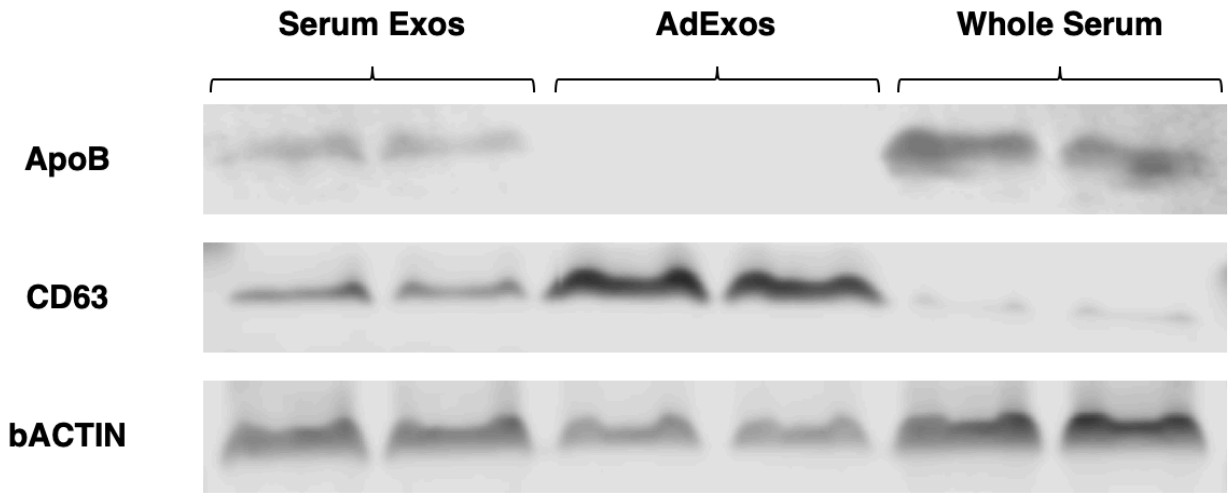


**Figure 5.2. Serum AdExo fractions contain ApoB protein.** Western blots of protein from exosomal fractions isolated from mouse serum (Serum Exos) or PGAT explants (AdExos), and protein isolated whole mouse serum. Blots were probed using antibodies against ApoB, CD63, and bActin.

We are presently working on alternate methods of purification to answer the circulating AdExo-TG question. Magnetic bead pulldowns with antibodies against adipocyte membrane proteins have proved inefficient, possibly because of low concentrations of adipocyte membrane proteins expressed on each exosome. Current efforts are focused on using a genetic mouse model, called the MetRS* mouse to robustly label AdExos, specifically. These mice have a floxed mutant Methionyl tRNA Synthetase gene. When expressed under an adipocyte-specific Cre recombinase, this mutant tRNA synthetase allows for Azidonorleucine (ANL) to be incorporated into proteins any time a methionine residue would be added to the protein (*4*-*6*). This amino acid substitution has no effect on protein function, but effectively incorporates a label onto all proteins translated in adipocytes (Figure 5.3, [figure modified from Hazenpichler et al.]). Azide groups in ANL are capable of undergoing a CLICK reaction with alkyne groups, producing a sturdy covalent bond. In these animals every protein on AdExos should contain ANL, while exosomes derived from other cells will not. Serum samples can be incubated with alkyne-biotin molecules to bind ANL-containing proteins and pull intact AdExos, specifically, out of solution (Figure 5.4). This would allow for a whole host of investigations to be conducted on *in vivo* isolated, circulating AdExos, including deciphering TAG content.

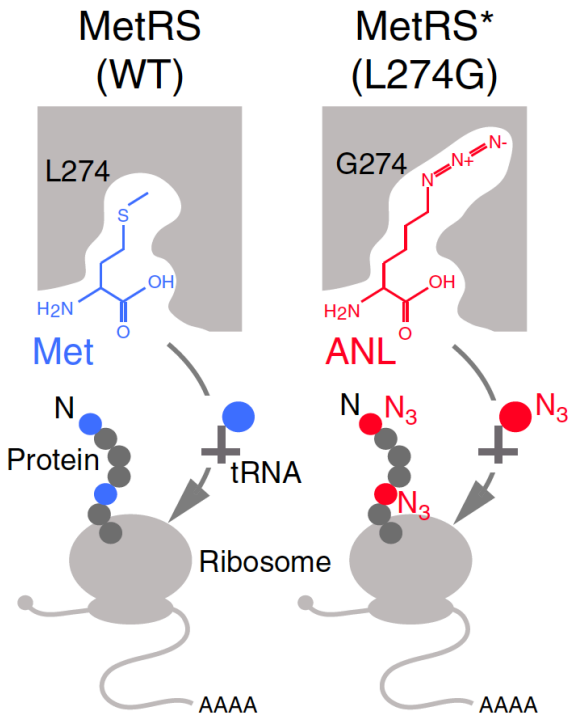


**Figure 5.3. MetRS* mouse allows for ANL to be incorporated into proteins.**

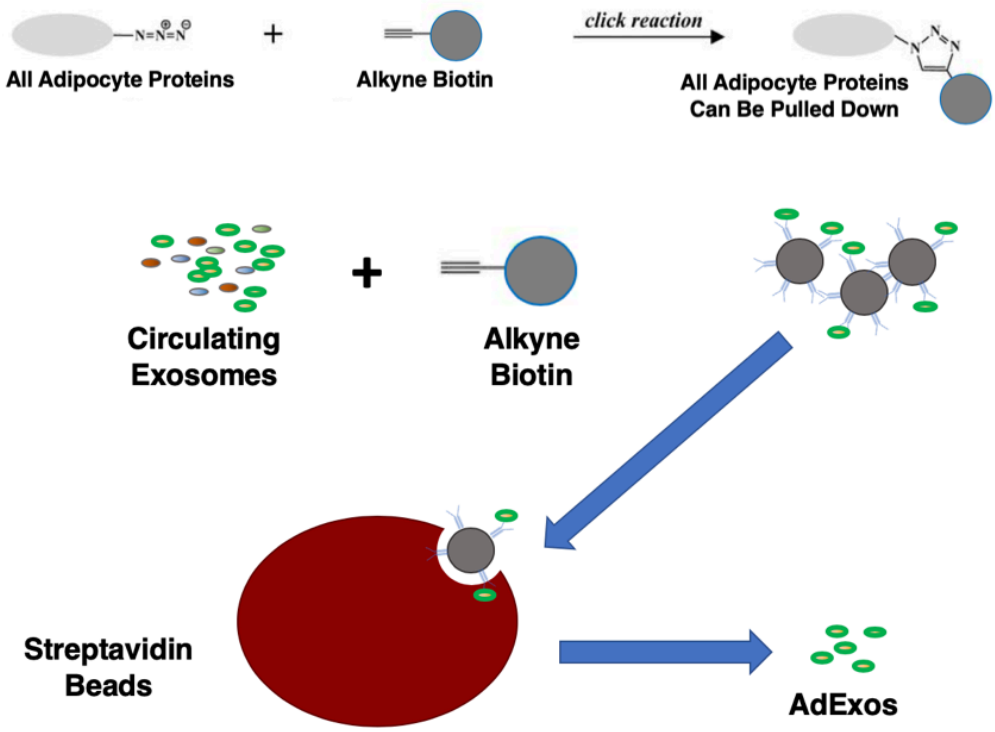


**Figure 5.4. MetRS* mice will allow specific pulldown of AdExos from circulation.**

The physiological mechanism controlling AdExo release is a subject of significant interest. As mentioned before, both obesity and fasting lead to increased AdExo secretion from PGAT. This indicates that AdExo release is not responding specifically to systemic energy need or energy oversaturation. Both fasting and obesity are known to induce increased lipolysis in adipocytes, however, reducing lipolysis, using genetic models or pharmacological inhibitors, has no effect on AdExos, neither increasing nor decreasing the amount released. Furthermore, systemic metabolic signals, such as insulin and glucagon, that are known to have dramatic effects on lipolysis rates, have no effect on AdExo release (*7-9*). These data suggest that AdExo release is not a response to systemic metabolic status and further distance this lipid release pathway from canonical lipolysis.

Some data that could potentially shed light on potential mechanisms are the preliminary data on AdExos released from different adipose tissue depots. Perigonadal (PGAT) and subcutaneous (SubQ) adipose tissues are both white fat depots that play a similar role in the body, though they differ in several important factors: PGAT is more innervated, and contains more immune cells than SubQ, and SubQ depots have a lesser capacity for pre-adipocyte differentiation, and adipocytes are typically larger than in PGAT (*10*). The intrascapular brown adipose tissue depot (BAT), however has very distinct roles compared to white adipose tissues. BAT's main role is thermogenic. It achieves this goal by burning fatty acids through beta-oxidation, but instead of producing ATP, mitochondrial membrane leak through the action of uncoupling protein 1 (UCP1), produces heat (*11-13*). Using NTA, we find that BAT explants release the most AdExos per gram of tissue, 1.5-fold more than PGAT, and 3-fold more than SubQ depots (Figure 5.5). BAT AdExos and SubQ AdExos are smaller than those released from PGAT (Figure 5.6). Interestingly, however, BAT AdExos contain, by far, the least amount of TAG, with SubQ AdExos also containing less TAG than PGAT AdExos (Figure 5.7). These data require more in-depth exploration, to fully understand.

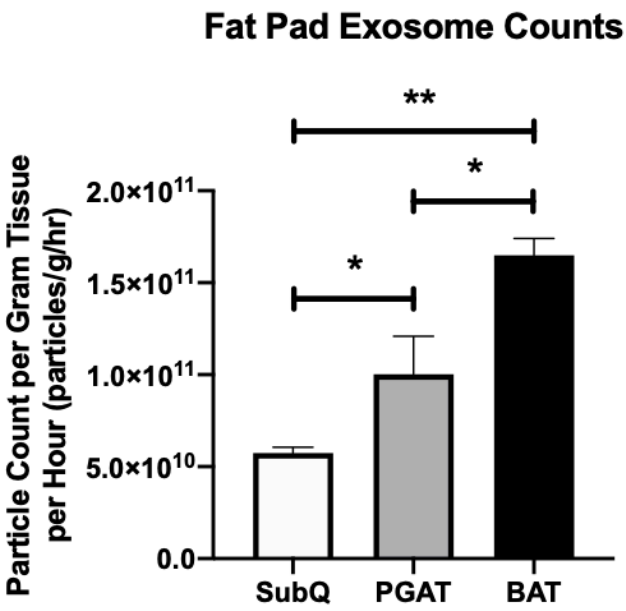


**Figure 5.5. BAT releases more AdExos per gram than PGAT.** Quantification of exosomes released by subcutaneous (SubQ), perigonadal (PGAT) and brown (BAT) adipose tissue explants, per gram of tissue per hour. Measurements were made by Viewsizer 3000 Nanoparticle Tracking Analysis. One-way ANOVA; *P < 0.05, **P < 0.01. n = 2. Error bars represent SD.

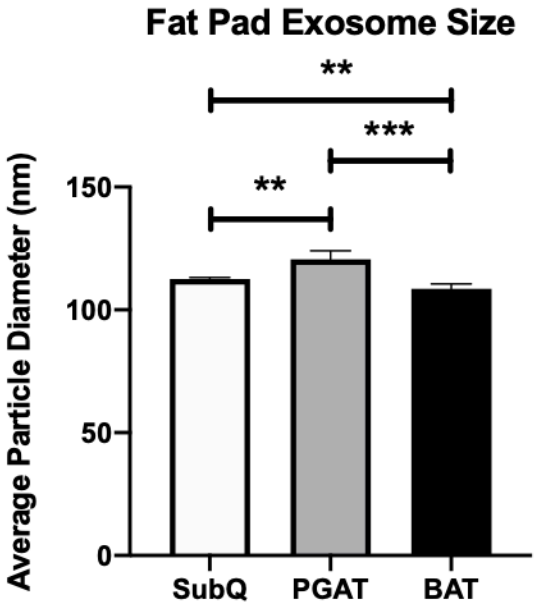


**Figure 5.6. PGAT AdExos have the largest diameter.** Average diameter of exosomes released by subcutaneous (SubQ), perigonadal (PGAT) and brown (BAT) adipose tissue explants. Measurements were made by Viewsizer 3000 Nanoparticle Tracking Analysis. One-way ANOVA; **P < 0.01, ***P < 0.001. n = 2. Error bars represent SD.

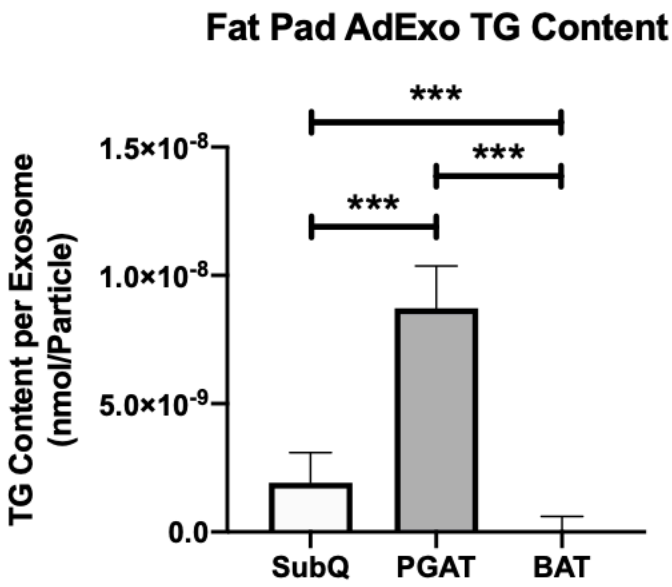


**Figure 5.7. BAT AdExos contain very little TAG.** Acylglyceride content of exosomes released by subcutaneous (SubQ), perigonadal (PGAT) and brown (BAT) adipose tissue explants, per exosome. One-way ANOVA; ***P < 0.001. n = 2. Error bars represent SD.

One possible explanation for AdExo release rates reacting to obesity and fasting is that AdExos are released as an adipocyte stress response. Chronic obesity and long-term fasting are both known to induce a significant amount of stress in adipocytes (*14-16*). It is possible that AdExos could be released as signaling structures to communicate that stress or as a mechanism to off-load unwanted material. Exosomes have been shown to be used by cells as a means of offloading misfolded protein (*17-19*). To test this theory, we could induce adipocyte ER stress with pharmacological molecules such as thapsigargin or EGTA, and then measure AdExo release in response to those stress stimuli (*20, 21*).

All of this says nothing about the cell biology of AdExo release, which remains a black box. How lipid droplet structure would come to be contained within exosomal vesicles is completely unknown. It is possible that pieces of lipid droplet bud off from the central droplet of the adipocyte, creating a structure with all of the necessary neutral lipid, phospholipid, and protein components. This process however, would be extremely energetically costly, and would likely require cellular machinery that is heretofore unknown. Another scenario could involve smaller lipid droplets that eventually fuse with the central lipid droplet that are captured before fusion. Lipid droplet materials are trafficked to developing exosomes and constructed within the vesicle. There are ways to disrupt exosome secretion, such as using Rab GTPase inhibitors, however, almost all of the known proteins involved in exosome secretion also have functions in the general endosomal pathway (*22, 23*). Disrupting these proteins pharmacologically or genetically also leads to disruption in cell trafficking, causing cellular dysfunction (*24*). These methods are therefore not ideal in physiological studies; however, they may prove useful tools in unraveling the cell biology of AdExo release.

The cell biology of AdExo uptake is also incompletely understood. BMDM neutral lipid uptake from AdExos occurs through PI3K-dependent macropinocytosis or phagocytosis. However, there remain many questions about the fate of AdExo contents in recipient cells. For example, what happens to the non-TAG lipid species in AdExos when added to BMDMs? The lipidomic contents of AdExos are not fully represented in the cells that take them up. AdExos, if they are taken up via macropinocytosis or phagocytosis are likely to eventually fuse with the lysosome. Many of the membrane-associated AdExo

lipids may be recycled to the plasma membrane or degraded. The TAG content of AdExos is translated very clearly to TAG content in BMDMs, however the AdExo MAG is completely absent in BMDMs. It is unlikely that the MAG content of AdExos is re-esterified such that it contributes to TAG accumulation in BMDMs as this process would require DGAT, and DGAT inhibition has no effect on the magnitude of TAG accumulation in BMDMs. The most likely explanation is that the MAG is hydrolyzed and used for energy to fuel the actions of the macrophage. Likewise, AdExos contain very high levels of cholesterol, and many of the gene pathways activated in AdExo-treated BMDMs involve response to cholesterol, however, BMDM cholesterol content, relative to other lipid species as determined by mass spectrometry, remains unchanged compared to untreated BMDMs.

AdExo uptake is capable of inducing ATM-like gene expression profiles in naïve macrophages. The mechanism through which AdExos are able to induce these changes is unknown. Specific mRNA or protein contained within AdExos could be having direct effects on BMDM signaling and gene expression. The signal could be transduced through lysosome-associated machinery that sample lysosomal degradation products to inform the cell. Or the reaction could simply be a response to increased lipid content in these cells. Depleting the AdExos of their neutral lipid content, could help distinguish between these possibilities. We have seen that AdExos contain PNPLA2/ATGL, whether this lipase is functional is also unknown. However, perhaps it would be possible to activate lipolysis in AdExos, depleting the vesicles of TAG, before adding them to BMDMs, to see if their reaction changes.

Whatever the mechanism, the evidence is clear that AdExos appear to educate naïve macrophages to become more like ATMs. This, of course, raises the question as to whether this is a tool utilized by other tissues. Almost all mammalian cell types have been found to secrete exosomes (*25*). Large proportions of circulating exosomes have been shown to be taken up by macrophages, in general (*26, 27*). Is it possible that parenchymal cells throughout the body release exosomes which are taken up by newly-replicated or newly-arrived macrophages to inform them of their tissue location? Could these parenchymal-derived exosomes promote tissue-specific adaptive functions that could help the tissue (Figure 5.8)? We have started to investigate this question by treating naïve BMDMs with exosomes from

primary osteoblasts, to see if they become more osteoclast-like. The gene expression response to OsbExos in “Osteoclast Genes” were mixed. However, the developmental pathway of osteoclasts is actually very well studied, and has been found to require RANK-ligand in order to fully differentiate (*28, 29*). How tissue resident macrophages elsewhere in the body develop is not well-understood, and exosomal education could be a potential pathway. The effectiveness of the pathway in other tissues would be relatively straightforward to investigate by treating naïve BMDMs with exosomes isolated from parenchymal cells (hepatocytes, neurons, etc…) and comparing gene expression profiles with those expected from their corresponding tissue resident macrophage population.

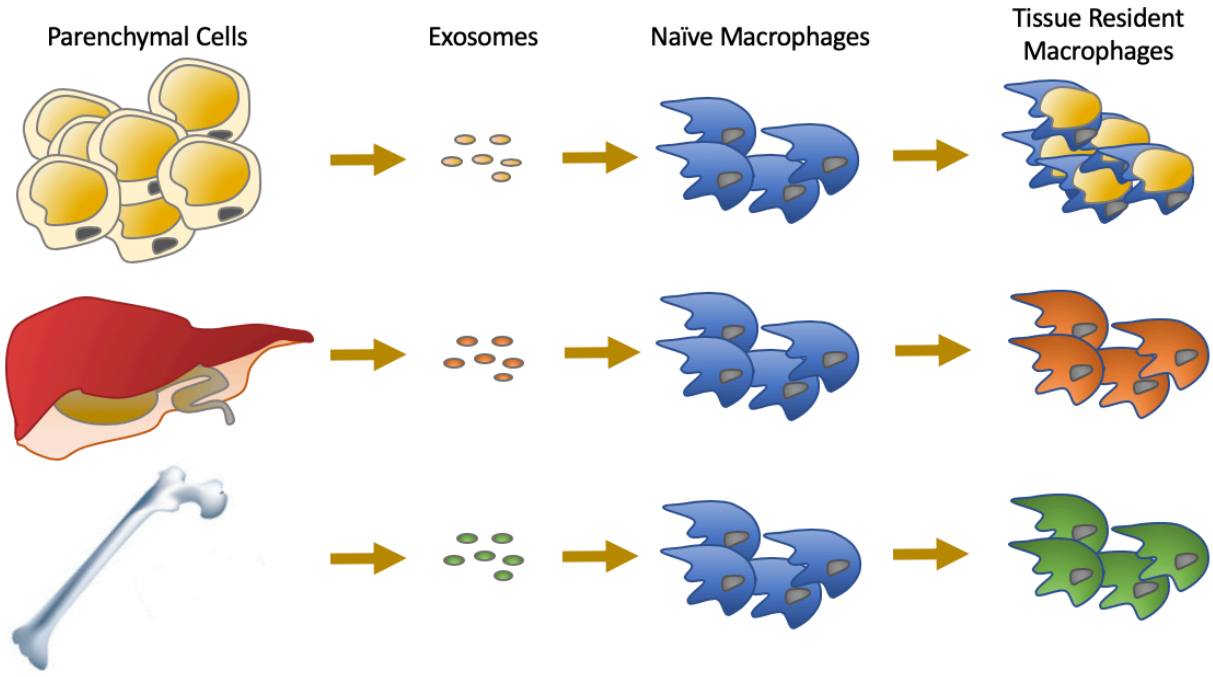


**Figure 5.8. Parenchymal cell-derived exosomes may induce tissue-resident-like macrophage differentiation.**

Altogether, it remains unclear what purpose this pathway of TAG release in AdExos serves. It would seem counterproductive to imagine that AdExos are a means to distribute energy to peripheral cells, as the energy required to transport necessary materials and produce the exosomes would likely vastly outweigh the cost of canonical lipolysis as a means of distribution. There is a possible advantage to the long-lived nature of exosomes, such that they are able to travel great distances through circulation. In addition, the extensive membrane and associated proteins could allow for more specific cellular targeting than can be generally achieved by FFA release. Perhaps, AdExos are used to transport TAG to specific cells to be used for energetic needs. The role of TAG in AdExos could also be purely in signaling.

Another potential hypothesis relates back to the adipocyte stress response discussed earlier. Adipocytes are long-lived (~10 years in human) cells that can change size and shape (>20-fold increase to cell diameter) dramatically based on lipid content. They need to be able to change size with some speed in order to respond to large influxes of lipid, or outfluxes of lipid during fasting. It is likely that adipocytes require some amount of maintenance and remodeling, especially during these high-stress periods. We also know that the ability of macrophages to hydrolyze lipid is necessary for adipose tissue homeostasis, as in LIPA-deficient mice, adipocytes slowly shrink as TAG storage is moved from adipose tissue to ectopic depots (*30, 31*). The adipose tissue lipid cycle hypothesis postulates that adipocytes unload TAG and membrane lipids to local macrophages via exosomes, which is then degraded and released back to adipocytes to allow for remodeling (Figure 5.9). This process would be upregulated when adipocytes need to significantly increase or decrease their size, which results in increased AdExo release during obesity and fasting. This proposed cycle is mirrored in the bone, another long-lived tissue that requires re-modeling. Osteoclasts, the tissue resident macrophage of the bone degrades mineralized bone, releasing bone-building materials that are taken up and remodeled by osteoblasts, the parenchymal cell of the bone (Figure 5.10). This process is known to be upregulated in times of high remodeling needs, such as bone growth in development, or during physical activity when bone can be damaged (*32, 33*).

Whatever their biological function, AdExos may also take part in the development of pathologies. Obesity is associated with increased inflammation in the adipose tissue, increased circulating TAG, and increased ectopic TAG deposition. Each of those obesity symptoms are, in turn, associated with insulin resistance, atherosclerosis, and stroke, many of the main causes of morbidity and mortality in obesity. There is a potential role for AdExos in connecting obesity to these co-morbidities. AdExos are largely taken up by immune cells in the adipose tissue and are capable of inducing significant changes in those cells. AdExos have also been shown to enter circulation. And if AdExos are taken up by non-adipose tissue cells, they have already been shown to induce TAG accumulation in cells that take them up.

Much more work needs to be done to understand how AdExos operate biologically. However, if AdExos turn out to be involved in these pathological processes, targeting AdExos could be a useful therapeutic in preventing obesity-related disease.

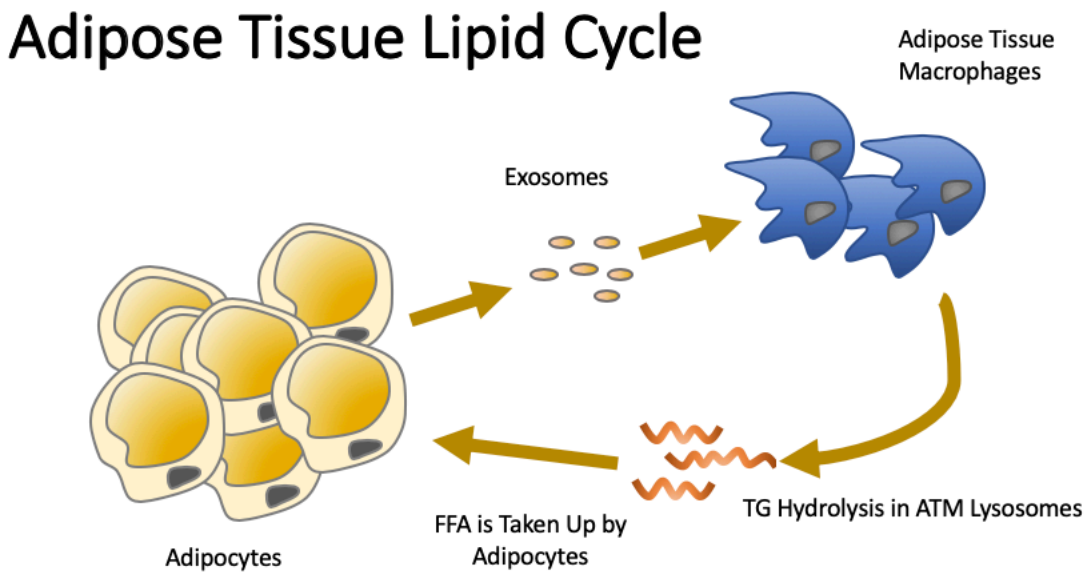


**Figure 5.9. Graphical representation of adipocyte remodeling.**

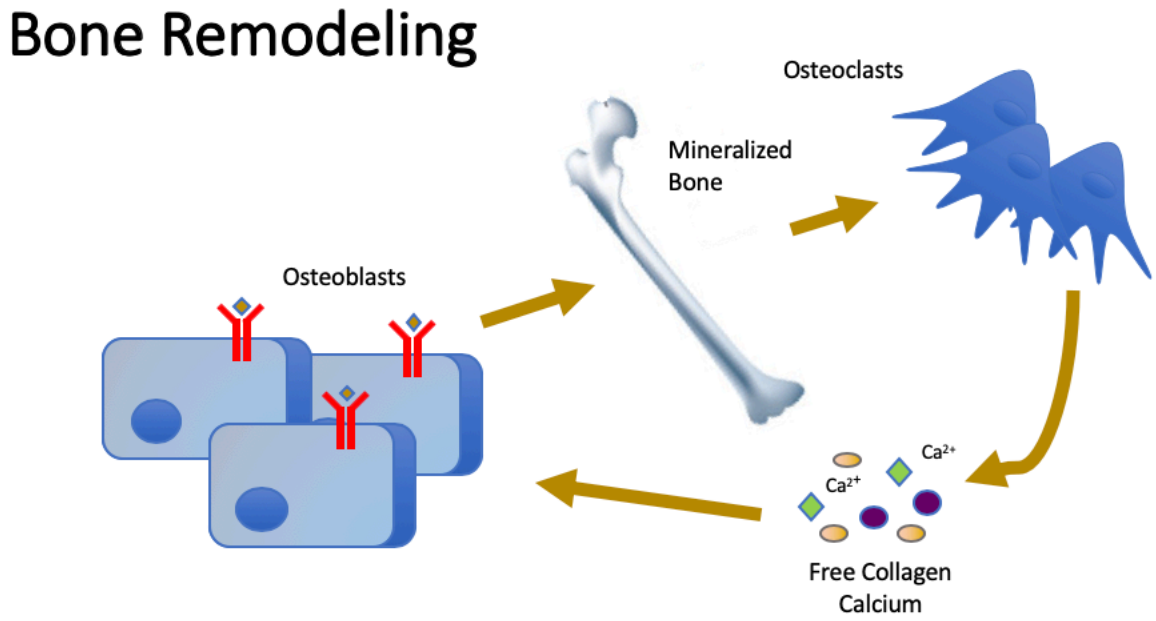


**Figure 5.10. Graphical representation of bone remodeling.**

### 5.2 References


1. T. Thomou *et al.*, Adipose-derived circulating miRNAs regulate gene expression in other tissues. *Nature* **542**, 450-455 (2017).
2. S. Kita, N. Maeda, I. Shimomura, Interorgan communication by exosomes, adipose tissue, and adiponectin in metabolic syndrome. *J Clin Invest* **129**, 4041-4049 (2019).
3. X. Gao, C. Salomon, D. J. Freeman, Extracellular Vesicles from Adipose Tissue-A Potential Role in Obesity and Type 2 Diabetes? *Front Endocrinol (Lausanne)* **8**, 202 (2017).
4. R. Hatzenpichler *et al.*, In situ visualization of newly synthesized proteins in environmental microbes using amino acid tagging and click chemistry. *Environ Microbiol* **16**, 2568-2590 (2014).
5. B. Alvarez-Castelao *et al.*, Cell-type-specific metabolic labeling of nascent proteomes in vivo. *Nat Biotechnol* **35**, 1196-1201 (2017).
6. B. Alvarez-Castelao, C. T. Schanzenbacher, J. D. Langer, E. M. Schuman, Cell-type-specific metabolic labeling, detection and identification of nascent proteomes in vivo. *Nat Protoc* **14**, 556-575 (2019).
7. T. Scherer *et al.*, Brain insulin controls adipose tissue lipolysis and lipogenesis. *Cell Metab* **13**, 183-194 (2011).
8. J. E. Liljenquist *et al.*, Effects of glucagon on lipolysis and ketogenesis in normal and diabetic men. *J Clin Invest* **53**, 190-197 (1974).
9. R. E. Duncan, M. Ahmadian, K. Jaworski, E. Sarkadi-Nagy, H. S. Sul, Regulation of lipolysis in adipocytes. *Annu Rev Nutr* **27**, 79-101 (2007).
10. M. M. Ibrahim, Subcutaneous and visceral adipose tissue: structural and functional differences. *Obes Rev* **11**, 11-18 (2010).
11. A. Fedorenko, P. V. Lishko, Y. Kirichok, Mechanism of fatty-acid-dependent UCP1 uncoupling in brown fat mitochondria. *Cell* **151**, 400-413 (2012).
12. J. Nedergaard, T. Bengtsson, B. Cannon, Unexpected evidence for active brown adipose tissue in adult humans. *Am J Physiol Endocrinol Metab* **293**, E444-452 (2007).
13. P. Trayhurn, Origins and early development of the concept that brown adipose tissue thermogenesis is linked to energy balance and obesity. *Biochimie* **134**, 62-70 (2017).
14. D. J. Espiritu, T. Mazzone, Oxidative stress regulates adipocyte apolipoprotein e and suppresses its expression in obesity. *Diabetes* **57**, 2992-2998 (2008).
15. M. F. Gregor, G. S. Hotamisligil, Thematic review series: Adipocyte Biology. Adipocyte stress: the endoplasmic reticulum and metabolic disease. *J Lipid Res* **48**, 1905-1914 (2007).
16. A. N. Rouble, S. N. Tessier, K. B. Storey, Characterization of adipocyte stress response pathways during hibernation in thirteen-lined ground squirrels. *Mol Cell Biochem* **393**, 271-282 (2014).
17. N. Fussi *et al.*, Exosomal secretion of alpha-synuclein as protective mechanism after upstream blockage of macroautophagy. *Cell Death Dis* **9**, 757 (2018).
18. M. Simons, G. Raposo, Exosomes--vesicular carriers for intercellular communication. *Curr Opin Cell Biol* **21**, 575-581 (2009).
19. Y. J. Lim, S. J. Lee, Are exosomes the vehicle for protein aggregate propagation in neurodegenerative diseases? *Acta Neuropathol Commun* **5**, 64 (2017).
20. P. Sehgal *et al.*, Inhibition of the sarco/endoplasmic reticulum (ER) Ca(2+)-ATPase by thapsigargin analogs induces cell death via ER Ca(2+) depletion and the unfolded protein response. *J Biol Chem* **292**, 19656-19673 (2017).
21. T. Takadera, M. Ohtsuka, H. Aoki, Chelation of extracellular calcium-induced cell death was prevented by glycogen synthase kinase-3 inhibitors in PC12 cells. *Cell Mol Neurobiol* **30**, 193-198 (2010).
22. K. Menck *et al.*, Neutral sphingomyelinases control extracellular vesicles budding from the plasma membrane. *J Extracell Vesicles* **6**, 1378056 (2017).
23. M. Ostrowski *et al.*, Rab27a and Rab27b control different steps of the exosome secretion pathway. *Nat Cell Biol* **12**, 19-30; sup pp 11-13 (2010).
24. K. Essandoh *et al.*, Blockade of exosome generation with GW4869 dampens the sepsis-induced inflammation and cardiac dysfunction. *Biochim Biophys Acta* **1852**, 2362-2371 (2015).
25. D. M. Pegtel, S. J. Gould, Exosomes. *Annu Rev Biochem* **88**, 487-514 (2019).

26. D. Feng *et al.*, Cellular internalization of exosomes occurs through phagocytosis. *Traffic* **11**, 675-687 (2010).
27. T. Imai *et al.*, Macrophage-dependent clearance of systemically administered B16BL6-derived exosomes from the blood circulation in mice. *J Extracell Vesicles* **4**, 26238 (2015).
28. B. F. Boyce, L. Xing, Functions of RANKL/RANK/OPG in bone modeling and remodeling. *Arch Biochem Biophys* **473**, 139-146 (2008).
29. J. H. Park, N. K. Lee, S. Y. Lee, Current Understanding of RANK Signaling in Osteoclast Differentiation and Maturation. *Mol Cells* **40**, 706-713 (2017).
30. H. Du, G. A. Grabowski, Lysosomal acid lipase and atherosclerosis. *Curr Opin Lipidol* **15**, 539-544 (2004).
31. H. Du *et al.*, Lysosomal acid lipase-deficient mice: depletion of white and brown fat, severe hepatosplenomegaly, and shortened life span. *J Lipid Res* **42**, 489-500 (2001).
32. Z. Li *et al.*, Mechanical regulation of bone formation and resorption around implants in a mouse model of osteopenic bone. *J R Soc Interface* **16**, 20180667 (2019).
33. M. M. Pechet, E. Bobadilla, E. L. Carroll, R. H. Hesse, Regulation of bone resorption and formation. Influences of thyrocalcitonin, parathyroid hormone, neutral phosphate and vitamin D3. *Am J Med* **43**, 696-710 (1967).

## CHAPTER 6: MATERIALS AND METHODS

Animals and Animal Care

Male C57BL/6J, B6.FVB-Tg(Adipoq-cre)1Evdr/J and B6.V-Lep/obJ mice were obtained from The Jackson Laboratory (Bar Harbor, ME) at ages ranging from 4 to 12 weeks old. Mice harboring a floxed allele of *Pnpla2/Atgl* (C57BL/6NTac) were kindly provided by Erin Kershaw (University of Pittsburgh). Mice with adipocyte-specific deletion of *Pnpla2/Atgl* were generated in the F2 generation of animals from the intercrossing of B6.FVB-Tg(Adipoq-cre)1Evdr/J and C57BL/6NTac-Tg(*Pnpla2*$^{fl/fl}$) mice. To genotype animals, DNA was isolated from tail lysate and PCR was performed using PCR primers as previously described (*6*). Mice were housed in pathogen-free barrier facility, in ventilated cages with free access to autoclaved water and low-fat pellet diet (5% calories from fat, PicoLab Rodent Diet 20; Purina Mills Inc). Mice were maintained on a 12-hour light/dark cycle and housed with 3-5 male mice per cage. Animal procedures were approved by Columbia University Institutional Animal Care and Use Committee.

Isolation and Culturing of Adipose Tissue Stromal Vascular Cells (SVCs)

Following $CO_2$ asphyxiation and cervical dislocation, mice were dissected and perigonadal adipose tissue (PGAT) isolated. PGAT was placed in FACS buffer (PBS (GIBCO), 0.2% bovine serum albumin (BSA, Sigma-Aldrich), and 5mM Ethylenediaminetetracetic acid (EDTA, Sigma-Aldrich)), minced into fine (<10 mg) pieces. Samples were centrifuged at 500*g* for 5 minutes at room temperature to pellet debris. Floating adipose tissue (AT) fragments were transferred into Dulbecco's Modified Eagle Medium (DMEM, Invitrogen) with 10 mg/mL BSA and digestive enzymes (0.14 units/mL of Liberase TM (Roche Applied Science) and 50U/mL of DNase I (Sigma-Aldrich)) and digested in a 37°C orbital shaker at 185 rpm for 30 minutes. Following digestion, the solution was passed through a sterile 250-μm nylon mesh (Sefar Filtration Inc). The suspension was centrifuged for 5 minutes at 500 *g* at room temperature. The stromal vascular cells (SVCs) pellet was washed by resuspending in FACS buffer and centrifuging once more at 500*g* for 5 minutes at room temperature. For immunostaining, SVCs were first plated by resuspending them in culture medium (DMEM, 20% L929 cell-conditioned media, 10% fetal bovine serum (FBS, Invitrogen), and 1% Penicillin-Streptomycin (P/S, Invitrogen) at a concentration of 500,000 cells/mL. SVCs were cultured overnight at 37°C in 4 well chamber slides (LabTek) in 5% $CO_2$ and fresh DMEM was added.

In Vitro Preparation of BMDMs, BM-ATMs, AdExo-induced differentiated cells and Foam Cells

Bone marrow (BM) cells were collected from femurs of 4-5-week-old wild-type C57BL/6J mice. BM cells were plated 50-60x$10^6$ cells in a tissue culture flask (175 mL size) at 37°C and 5% $CO_2$ for two days in 100 ml of BM culture medium (Minimum Essential Medium Alpha (MEM-α, Invitrogen), 10% FBS, 1% Non-essential amino acids (NEAA, Invitrogen), 1% P/S). After two days, non-adherent cells were collected, centrifuged at 500*g* for 5 minutes, counted, and seeded on cell culture plates (BD Bioscience) or 4 well coated chamber slides (LabTek) at a concentration of 1.5x$10^6$ cells/ 2 mL/well in BM culture medium

supplemented with 30 ng/mL of colony stimulating factor-1 (CSF-1/M-CSF, R&D systems). After three days of differentiation in the presence CSF-1 most cells were adherent and the medium was removed. These cells were used for DGAT inhibitor and macropinocytosis inhibitor studies. The cells were further differentiated into bone marrow-derived adipose tissue macrophages (BM-ATMs) or AdExo-induced differentiated cells. For differentiation of cells into BM-ATMs, 100 mg of PGAT was isolated from 12-week-old male C57BL/6J male mice and placed in porous tissue inserts (BD Bioscience) with BM-culture medium and CSF-1 (30 ng/ml). For AdExo-induced differentiated cells, fresh ad-exos purified from conditioned medium of 100 mg of PGAT cultured overnight were added to BM-culture medium every day. EM and confocal experiments were carried out after 6 days of PGAT co-culture or AdExo treatment. Gene expression data was gathered from macrophages following 10 days of PGAT co-culture, AdExo, or OsbExo treatment. Culture medium containing fresh CSF-1 was changed every 3 days. Foam cells were generated as previously described (*8*).

For each experiment, control bone marrow-derived macrophages (BMDMs) were differentiated using the same condition and medium except the medium was not supplemented with AdExo, OsbExo or conditioned medium from PGAT.

EM Imaging

*Macrophages* - BM-ATMs and BM-foam cells pellets were fixed with 2% paraformaldehyde. Cells were embedded, sectioned, stained with Osmium tetroxide and uranyl acetate using standard protocols (REF). *AdExos* -After collecting the exosome fraction from lean or obese adipose tissue conditioned medium, paraformaldehyde was added to each sample (2% vol/vol). Samples were air dried on Formvar-carbon-coated grids, negative stained with uranyl acetate, and washed. Grids were examined under a JEOL JEM-1200 EXII electron microscope. Images were captured with an ORCA-HR digital camera and recorded with image capturing software (AMT Image Capture Engine, Advanced Microscopy Techniques, Corp).

Atglistatin Treatment

PGAT was cultured for 16 hours in Dulbecco's Modified Eagle Medium supplemented with 50μM Atglistatin (Sigma-Aldrich). Conditioned medium was collected to measure free fatty acid content, or added to BMDMs. BMDM lipid content was visualized using confocal microscopy and BODIPY staining after 24 hours or triglyceride concentration was measured using the method described below after 3 hours of incubation.

Free Fatty Acid Treatment

BMDMs were differentiated for 3 days before being switched to BM Medium (+CSF-1) with 100μM Palmitate, 400μM Oleate, and 10mM glycerol. Confocal images were taken after 6 days of free fatty acid treatment, medium being changed every 3 days.

Ad-Exo Isolation and Labeling

Perigonadal Adipose Tissue was taken from 10 - 12-week-old male C57BL/6J, minced to 2mm, and cultured in Minimum Essential Medium Alpha (MEM-a, Invitrogen) for a 1-hour pre-culture. Tissue was then washed and centrifuged with MEM-a before being cultured in MEM-a for 16 hours. Adipose Tissue was passed through a 70μm filter (Greiner Bio-One EASYstrainer) and conditioned medium was collected. The medium was then passed through a 0.8μm syringe filter (Sartorius Minisart) and then concentrated via 100kD centrifuge filters (Millipore Amicon Ultra – 2mL Centrifuge Filters). Filtrate samples were taken from the flow-through of this stage of purification. The concentrated conditioned medium was then either labeled with PKH26 (Sigma PKH Red Fluorescent Cell Linker Kit) according to manufacturer's instructions, or left unlabeled. The medium was added to a gel filtration column (Thermo Scientific Disposible 5mL Polypropelyne Columns), packed with Illustra Sephacryl S-1000 Superfine Silica Gel (GE Healthcare), using PBS as the mobile phase. Fractions containing 30 – 200nm objects (by diameter) were collected and once again concentrated using centrifuge filters. Filtrate samples were concentrated via Vacufuge (Eppendorf) and matched to exosome samples by volume. After isolation, the fluorescent emission of labeled exosomes was measured using a FLUOstar Optima fluorescence spectrophotometer plate reader (BMG-Labtech). For BMDM treatment, $1x10^{10}$ exosomes were administered per mL culture medium.

Fasting Experiments

Animals were fasted for 16 hours overnight (5PM – 9AM). At completion of 16hrs tissue was collected and cultured for 16 hours before AdExo isolation.

DGAT1/2 Inhibitor Treatment

BMDMs were pre-incubated with 30μM AZD7679 (AstraZeneca), 10μM PF-06424439 (Tocris) for 1 hour in DMEM. BMDMs were then treated with AdExos for 24 hours, for confocal microscopy, or 3 hours, for triglyceride assay.

Macropinocytosis Inhibitor Treatment

BMDMs were pre-incubated with 100μM LY294002 (Sigma-Aldrich) for 1 hour in DMEM. BMDMs were then treated with AdExos for 3 hours, and analyzed using triglyceride assay.

Metabolic Signaling Molecule Treatment

WT PGAT explants were treated with 5 μg/mL insulin, 20 nM glucagon, 1 μM rosiglitazone, or 15 μM CL-316,243 (Sigma). Exosome number was assessed using Viewsizer 3000 nanoparticle tracking analysis after AdExo isolation. For CL-316,243, whole conditioned medium was measured for FFA content using the Abcam FFA Assay kit.

Fluorescent Microscopy

For whole tissue visualization, perigonadal adipose tissue was removed from 12-week-old obese (*Lep ob/ob)* mice. The tissue was minced and incubated with 1:1000 v/v anti-F4/80 Rat mAb (Invitrogen), and 1:1000 v/v Perilipin 2 (D1D8) XP Rabbit mAb (Cell Signaling) overnight at 4$^{o}$C, and then incubated in secondary 1:500 v/v Novex™ Goat anti-Rabbit IgG (H+L) Secondary Antibody, Cy5® conjugate (Invitrogen) and 1:500 v/v Goat Anti-Rat IgG (H+L) Secondary Antibody, Cy3 conjugate (Invitrogen) antibodies for two hours. The tissue was then stained with 1:300 v/v BODIPY 493/503 (4,4-Difluoro-1,3,5,7,8-Pentamethyl-4-Bora-3a,4a-Diaza-s-Indacene, Thermofisher Scientific) and 1:4000 v/v DAPI (Thermofisher Scientific) fluorescent stains for 5 minutes, before washing and visualizing on Nikon A1R MP confocal microscope. Bone-marrow-derived cells were cultured on chamber well slides, fixed in 2% paraformaldehyde, before primary and secondary antibody staining. The cells were washed and then stained with fluorescent stains 1:300 v/v BODIPY, 1:4000 v/v DAPI, and 5mM Lysotracker (Invitrogen) at 37$^{o}$C for 30 minutes.

Triglyceride Assay

Measuring of triglyceride content in isolated exosomes, tissue, and BMDMs was done using Abcam's Triglyceride Quantification Kit, according to the manufacturer's protocol.

Nanoparticle Tracking Analysis

Purified exosome samples were analyzed for particle concentration and size distribution using nanoparticle tracking analysis method by Malvern NanoSight NS300 (Malvern Instruments Ltd, Malvern, United Kingdom), or ViewSizer 3000 (MANTA Instruments, Horiba Scientific). The assays were performed according to the recommended protocols of each manufacturer. Briefly, for the NanoSight, three independent replicates of diluted exosome preparations in PBS were injected at a constant rate into the tracking chamber by the provided syringe pump. The specimens were tracked at room temperature for 60s. Shutter and gain were manually adjusted for optimal detection and were kept at optimized settings for all samples. The data were captured and analyzed with NTA Build 127 software (version 2.2, Malvern Instruments Ltd, Malvern, UK). For the Viewsizer 3000, 50 15s tracking measurements were captured at room temperature for each sample. The measurements were then analyzed using in-built Viewsizer™ software.

Western Blots

After isolation, PGAT, BM-derived cells, and exosomes samples were resuspended in tissue extraction reagent I (Invitrogen) with protease inhibitor cocktail (Sigma-Aldrich). Samples were homogenized using a stainless-steel bead homogenizer. Protein concentrations were measured using a BIO-RAD Protein Assay (BIO-RAD) and 20-50 µg of protein were denatured at 96°C for 5 minutes in 4x protein sample buffer (200 mM Tris 6.8, 8% sodium dodecyl sulfate, 0.4% Bromophenol blue, 40% glycerol, and 5% β-mercaptoethanol). Protein was loaded on 10-15% SDS-polyacrylamide gels and ran at 100-140 volts for 2-3 hours. Proteins were transferred on nitrocellulose (Thermo) or polyvinylidene difluoride (PVDF, Fisher

Scientific) with a wet transfer system (BIO-RAD) for 45 minutes. Membranes were blocked with 5% non-fat milk solution and incubated with primary antibodies overnight at 4°C: anti-CD63 (System Biosciences), anti-HSP70 (System Biosciences), anti-CD9 (System Biosciences), anti-CAV1 (Cell Signaling), anti-FABP4 (Abcam), anti-COXIV (Cell signaling), anti-Lamin B1 (Abcam), anti-β-actin (Sigma-Aldrich), anti-PNPLA2/ATGL (Cell signaling), anti-LAMP2 (Abcam). Membranes were washed with Tri-Buffered Saline Tween-20 (TBST) and incubated with secondary antibodies either HRP conjugated (Abcam) for ECL chemiluminescence detection system (G&E science) development or fluorescent antibodies for LICOR odyssey system (LICOR) development.

Proteinase Treatment

Purified ad-exos were isolated from WT PGAT conditioned medium. These exosomes were exposed in suspension to either 100µg/mL of recombinant, PCR grade, Proteinase K (Sigma), 0.5% v/v Triton-X100, or both for 15 minutes on ice. After exposure, all samples were incubated with 1mM PMSF proteinase inhibitor (Sigma) for 15 minutes, before undergoing normal Western blotting protocol as described above.

Lipidomics Studies

Purified AdExos or BMDMs were treated with 2:1(v/v) chloroform:methanol, 1mM butylated hydroxytoluene, and 500 nmol of deuterium-labeled lipid standard with stainless steel beads. The sample was sonicated for 30 min at room temperature before being centrifuged at 13000rpm for 10min at 4$^{o}$C. The sample was dried completely under nitrogen and then reconstituted with DMSO. Sample was analyzed via LC-MS/MS. Lipid extracts were spiked with appropriate internal standards, and analyzed using an Agilent 1200 HPLC system coupled with an Applied Biosystem Triple Quadrupole/Ion Trap mass spectrometer (3200Qtrap). The protocols were described previously (*24*).

Quantitative PCR

Total RNA was extracted from tissues, cells, and exosomes using RNeasy mini-kits (Qiagen). First-strand cDNA was synthesized using Superscript III reverse transcriptase and random hexamers (Invitrogen). Quantitative RT-PCR assays were carried out using DNA Engine Opticon 2 system instruments (BIORAD) and PCR SYBR Green I QuantiTect Master Mix (Qiagen). Data were normalized to *Rps3* using the ΔΔC(t) method, when presented as relative transcript levels. All primers used are listed in Table S1.

RNAseq Analysis

Primary ATMs were sorted using flow cytometry. Total RNA was isolated from untreated BMDMs, AdExo-treated BMDMs, BMDMs co-cultured with PGAT, F4/80hi primary ATMs from chow-fed animals, F4/80hi primary ATMs from high fat diet-fed animals, F4/8lo primary ATMs from chow-fed animals, and F4/80lo primary ATMs from high fat diet-fed animals using RNeasy mini-kits (Qiagen). RNA quality was determined

using Bioanalyzer. Sequencing of isolated RNA was performed by the Columbia Genome Center, using the Illumina HiSeq 2500.

Primary Osteoblast Culture

Calvaria from newborn mice (P2-P5) were collected, washed in PBS, and pre-digested in collagenase digestion solution (58 U/mL Collagenase Type 2 (Worthington), 2.5% Trypsin-EDTA, in MEMa) at 37oC, shaking, for 20 min. Medium was removed and re-incubated with collagenase digestion solution at 37oC, shaking, for 60 min. Cells were washed and cultured in Osb Culture Medium (MEMa, 10% FBS, 1% P/S, 4mM L-Glutamine). After 2 days, the cells were trypsinized and passed through a 70μm strainer. Cells were then cultured with Osb Culture Medium + 5mM Glycerol 2 Phosphate and 0.1mg/mL Ascorbic Acid. Osteoblasts were fully differentiated after 10 days. Conditioned medium was then collected daily for exosome isolation.

PGAT Injections

Whole perigonadal adipose tissue from 16-week ob/ob animals was injected with 30μL and roughly $1x10^{10}$ PKH26-labeled exosomes, immediately following removal from the animal. After a one-hour incubation in MEMa, the tissue was then digested with Liberase and centrifuged to separate adipocyte and SVC fractions. Both fractions were lysed and their PKH26 fluorescence measured using a fluorescent spectrophotometer. SVCs were also utilized for FACS analysis.

Peritoneal Cavity Macrophage Isolation

30μL of PKH26-labeled ad-exos or PBS were injected into the peritoneal cavity of 8-week old WT C57BL/6J mice. 24 hours later, the mice were sacrificed. The skin on the ventral side of the animal was opened and 5 mL ice-cold FACS Buffer was injected into the peritoneal cavity. The peritoneum of the animal was massaged, before the injected buffer was re-collected using a syringe. The collected buffer was spun for 8 min at 1500rpm to pellet cells. The peritoneal cavity cells were then washed and resuspended in FACS buffer for flow cytometry or cell sorting.

FACS Analysis

SVCs were pelleted and resuspended in FACS buffer with 2% Fc Block (BD Bioscience) and placed on rotator for 30 minutes at 4°C in dark. Fluorophore-conjugated antibodies were added for 30 minutes at 4°C on rotator: 1:100 v/v eFluor 660-F4/80 antibody (AbD Serotec), 1:100 v/v anti-CD11b-FITC antibody (Invitrogen), and 1:100 v/v anti-CD45.2-PerCP-Cy5.5 antibody (Invitrogen). Cells were washed twice with FACS buffer centrifuged at 1600 *rcf* for 3 minutes and resuspended in FACS buffer with (4',6-Diamidino-2-Phenylindole, Dihydrochloride) (DAPI, Invitrogen). Cells were analyzed using a Fortessa Flow Cytometer (BD Biosciences) or sorted using a BD Aria II Cell Sorter (BD Biosciences). Data analysis was done on FlowJo software.

Statistical analysis

Statistical analyses were performed as described in the figure legend for each experiment. Data is presented as mean ± standard deviation. The indicated sample size (n) represents biological replicates. Statistical significance was determined by Student's t test, one- and two-way ANOVA with post-hoc X tests using Graphpad Prism 7 and R. Significance was set at *:$P < 0.05$.